EPA-650/2-73-044
September 1973

Final Report to the Control Systems Laboratory of the U.S. Environmental Protection Agency under Contract Number 68-02-0212, September 1973

Petrographic Characteristics and Physical Properties of Marls, Chalks, Shells, and Their Calcines Related to Desulfurization of Flue Gases

Richard D. Harvey
Robert R. Frost
Josephus Thomas, Jr.

ILLINOIS STATE GEOLOGICAL SURVEY, Urbana, Illinois

Petrographic Characteristics and Physical Properties of Marls, Chalks, Shells, and Their Calcines Related to Desulfurization of Flue Gases

Richard D. Harvey, Robert R. Frost, and Josephus Thomas, Jr.

Final Report to the Control Systems Laboratory of the U.S. Environmental Protection Agency under Contract Number 68-02-0212
September 1973

ILLINOIS STATE GEOLOGICAL SURVEY, Urbana, Illinois

PETROGRAPHIC CHARACTERISTICS AND PHYSICAL PROPERTIES OF MARLS, CHALKS, SHELLS, AND THEIR CALCINES RELATED TO DESULFURIZATION OF FLUE GASES

CONTENTS

TABLES

APPENDIXES

ILLUSTRATIONS

Page

Figure

Page

Figure

Plate

PETROGRAPHIC CHARACTERISTICS AND PHYSICAL PROPERTIES OF MARLS, CHALKS, SHELLS, AND THEIR CALCINES RELATED TO DESULFURIZATION OF FLUE GASES

Richard D. Harvey, Robert R. Frost, and Josephus Thomas, Jr.

ABSTRACT

Thirty-seven operating and other pits in fresh-water marl in the northeastern quarter of the United States and twenty-four deposits of chalk in chalky limestone, four deposits of shell and coquina, two deposits of caliche, and a large carbonate sludge refuse pile, all in the eastern part of the United States, were sampled and studied in relation to their potential use in limestone ($CaCO_3$) processes for control of SO_2 emission from fossil fuel combustion. Earlier studies had suggested the superiority of these materials over denser limestones in these processes. Each sample and its calcined product (lime) were investigated for their petrography, mineralogy, chemistry, pore structure, and surface area.

The occurrence of marl containing 80 percent or more $CaCO_3$ is restricted largely to Pleistocene age sediments that occur in the states around the Great Lakes and in Virginia. Annual production of marl in recent years has been approximately 2 million tons; it is at present used entirely as agricultural limestone and for related soil-conditioning. Production could be vastly increased if demand increased. Chalk and chalky limestone are generally restricted to the sedimentary rocks of Upper Cretaceous and Tertiary age in the Kansas-Nebraska-Colorado area and in the southeastern states from Texas to Florida. Currently chalks and chalky limestones in most of these states are used primarily in the manufacturing of cement.

Marls are composed principally of equant calcite grains, most of which are less than 4μ in diameter, that are weakly agglomerated and also of mollusk shells, which consist of aragonite. Together these minerals provide a $CaCO_3$ content that is most frequently between 80 and 90 percent. Impurities are mainly quartz silt and organic matter. The pore volume of marls averages about 0.50 cc/g, which corresponds to a porosity of about 57 percent. Calcination of marl at 850° C for 5 to 10 minutes under high gas flow increases the pore volume about 0.2 cc/g marl——slightly more than the theoretical increase calculated from the $CaCO_3$ content because of the presence of organic matter. The physical characteristics of high pore volume and fine grain size in marls and their calcines indicate that they should have high reactivities with SO_2. Such characteristics of solids are of major importance in most gas-solid interactions. Because of the ease of their production and disaggregation, marls should be given important consideration for use in limestone scrubbing of flue gases at power plants in areas near marl deposits.

The grain size and grain shape of chalks are essentially the same as those of marls. Chalks generally have a higher clay content than marls but contain less quartz and organic matter. Their pore volume varies, mainly from one chalk formation to another (0.043 to 0.302 cc/g), and frequently it is 0.3 cc/g less than that of marls. The calcines of chalks have pore volumes slightly less than theoretical (pore volume of the chalk plus 0.2 times the $CaCO_3$ content of the chalk). Judging from pore-volume data, chalks and some chalky limestones also should have higher reactivities with SO_2 gases than would dense limestones.

On the basis of petrographic and pore-structure analyses, it is recommended that carbonate shell materials not be crushed and used in SO_2 scrubbing; however, their calcines are probably as reactive as those of other carbonates.

Carbonate waste sludge resembles marl in many properties and is potentially very reactive with SO_2, especially for use in wet scrubbing processes.

INTRODUCTION

Air pollution caused by emission of sulfur oxides from power plants is a major environmental problem, especially in highly industrialized areas. Current research on this problem includes the use of limestone or lime to react with sulfur dioxide (SO_2) to prevent its emission. Several processes based on this chemical reaction have been proposed and are being tested at a number of plants (Raben, 1973). If one of these processes can be proved technically feasible and reliable, it will be of considerable importance, because these processes generally require the lowest capital and operating costs of any prospective process of SO_2 control. Of the various processes being considered by power companies and others, the wet lime-limestone scrubbing process is favored as the short-range solution for removal of SO_2 from stack gases (Dibbs, 1971), especially if cost for waste sludge disposal can be held below $3 per ton of wet sludge (Rochelle, 1973).

Tests of Borgwardt (1970), Attig and Sedor (1970), and Coutant et al. (1971) of a sample of calcareous marl from Michigan and subsequent tests of two other samples of similar marl (Harvey and Steinmetz, 1971) have shown that these incoherent (soft) types of carbonate rocks have a relatively high capacity for reaction with SO_2 at elevated temperatures such as those that occur in coal-fired boilers. Other relatively incoherent types, illustrated by two samples of chalk and a sample of oolitic aragonite sand, also showed high SO_2 absorption capacities (Harvey and Steinmetz, 1971). It is thought that these types of carbonates, upon heating, yield calcines having large pore volumes and large surface areas. These properties of the calcines are considered the major factors affecting the relative SO_2 sorption capacities of samples of carbonate rocks. In addition, a marl and a chalk showed high reactivity with SO_2 in a laboratory wet scrubbing system (Drehmel, 1971). Since so few samples have been tested, detailed examination and testing of a number of these highly reactive rock types are needed for efficient selection of carbonate materials for maximum desulfurization by limestone processes.

The purposes of this study are to locate and sample a number of deposits of marls, chalks, and sea shells; to characterize the samples petrographically and chemically; to determine the grain-size and pore-volume distribution of the samples; and to relate these properties to the pore-volume distribution and the surface area of the calcined products.

Samples of sea shells are included in this study because of their similarities to the oolitic aragonite sand, which was determined to have high absorption capacity in previous tests. Both the oolitic sand and the sea shells originate in nearshore marine environments; both consist of very fine grained fibrous carbonate crystallites; and many sea shells consist of aragonite.

Definitions of Sample Types and Other Terms

It will be useful to clarify and define the types of carbonate materials studied. Marl is not a precise petrologic term, and geologists from various parts of the world use this term to describe a variety of rocks. The

term marl as used in this report is restricted to a soft, incoherent, and very fine grained material that is composed largely of calcite and is found in some fresh-water lakes and bogs. A lake marl occurs beneath a considerable body of water (larger than 25 acres), and a bog marl occurs beneath a tract of wet land covered with dense vegetation and, in many places, with peat. In this report, the classification of a sample of marl as a lake or bog marl is based on the presence or absence of a natural lake at the sample locality. If such a lake does not occur in the specific locality of a sample, the sample is classified as a bog marl. It is recognized that most bogs evolved from a lake by overgrowth of vegetation. However, this classification of marl was made in the field at the time of sample collection and was considered the most useful for descriptive purposes. Some marls have a pronounced sandy texture, or "feel," due to the presence of abundant particles in the size range of 100μ to 2000μ (microns). These marls are referred to as tufaceous marls. Some calcareous shales, calcareous siltstones, and very clayey or silty limestones, many phosphatic, that occur in the southeastern part of the United States are described in older geologic literature as marls. These rocks, marine in origin, are unlike the lake marls in composition and texture and are not classified as marls in this study.

Coquina is a type of carbonate rock that is composed mainly (> 75 percent) of shells and shell fragments and calcareous tests of invertebrates that are partly lithified, or cemented, into a rock material. Geologic literature contains references to shell marls and marls that formed under marine environments and contain abundant shells and shell fragments with various amounts of sand, silt, and clay. These do not resemble the fresh-water marls in texture. For clarity, the so-called shell marls, when they contain abundant calcareous shells, are classified in this report as coquinas.

Shell is a type of carbonate material that consists of hard rigid coverings of a variety of invertebrates that accumulate in large quantities in certain localities under shallow water. A single shell is hard and consists of calcite or aragonite crystallites. The shells are not cemented together. They are dredged for commercial purposes from nearshore deposits, mainly along the Gulf Coast in this country.

Chalk, as used in this report, is a variety of limestone consisting of very fine grained, porous, and partly incoherent carbonate rock composed of 50 percent or more $CaCO_3$ and containing abundant minute marine fossils. Geologic literature contains references to chalks that are actually calcareous siltstones, containing as little as 30 percent $CaCO_3$. These rocks should not be considered chalks and are excluded from this study.

Calcine refers to a piece of chalk, marl, or other carbonate rock that has been calcined, that is, heated sufficiently to convert $CaCO_3$ in the rock to grains of lime (CaO).

Pore structure is used in the broadest sense to include the properties of pore volume, pore-volume distribution, and mean pore size in particles.

Grain is a single crystalline unit or crystallite. Microscopic observation with polarized light permits analysis of the shape and size of grains within rock materials.

A particle may be a single grain, but more frequently consists of several coherent grains. For particles of colloidal dimensions, the sedimentation method of size analysis is particularly useful for obtaining particle-size data.

General Sample Processing and Methods of Analyses

Samples were taken from selected deposits of marls, chalks, and other carbonate rock types. In some cases, samples were taken from stockpiles by digging a shallow hole at several different places on the stockpile and removing about half a liter of sample from the bottom of each hole. About 30 pounds of sample was taken. Many samples of marl were taken by hand-augering the upper 15 feet of the deposit. In deposits of chalk and marl with observed differences in lithology between various strata or beds, separate samples, distinguished by alphabetic letter, were taken and the thickness recorded. Specific localities of the deposits, together with brief remarks concerning the deposits and samples, are given in numerical order in appendix 2.

A comprehensive series of laboratory tests and analyses were made on the samples. To provide small samples for the tests, the larger field samples were dried, crushed, thoroughly mixed, and quartered. Each sample was split until approximately 400 grams remained. One quarter of this material was sieved to obtain the 16x18, 18x40, 40x50, 50x170, and the 170x200 mesh fractions. The 16x18, 40x50, and 170x200 mesh fractions were separated for pore-structure measurements and calcination tests. Thin sections were prepared from two size fractions for petrographic analyses with a Quantimet image-analyzing computer. Another quarter was further reduced to pass a 100-mesh screen. This sample was subjected to particle-size, mineralogical, and chemical analyses. The particles larger than 16 mesh were examined with the scanning electron microscope (SEM) equipped with an X-ray analyzer. Lastly, half of the 400-gram sample of marls was subjected to Harvard miniature compaction tests (Wilson, 1970); and in the case of chalks, bulk density determinations were made on pieces cut uniformly from the block samples.

Grain Size by Image Analysis

Microscopic measurements were made of the grain sizes of samples in the 16x18- and 170x200-mesh fractions. Several hundred particles of each fraction were embedded in epoxy, and thin sections approximately 10μ thick were prepared. Fifty or more different fields of view in these sections were analyzed with a Quantimet under cross-polarized light at a total magnification of x 1950. Resolution was approximately 0.7μ. Thus, many grains less than 1μ in size were not detected by the Quantimet. However, the data obtained give representative and relative measures of the grain sizes of the samples.

Grain size as measured with the Quantimet for each field of view is expressed in terms of the mean chord length in microns. The mean grain chord length ($\bar{C}$) was computed from Quantimet output readings of grain area (A) and the grain area projection (P), according to:

$$\bar{C} = \frac{A}{P}\frac{L}{M}$$

where L is the length of the magnified field of view scanned by the Quantimet and M is the magnification. The results of analysis of 50 or more fields of view are averaged to give a mean grain chord length representative of the sample. The mean grain chord length is related to the maximum diameter (D) of spheres according to:

$$D = 1.274\ \bar{C}.$$

Another parameter of the grain texture in rocks from Quantimet analysis is a measure of the total length of grain boundaries. Since the circumference (or boundary) of a circle is πD, the grain boundary length per unit area (B), expressed in mm/mm^2, can be computed from P for each field of view according to:

$$B = \pi \frac{M}{L} P.$$

For two samples with the same size of grains, differences in observed (B) reflect differences in the mean shape or roundness of the grains in the samples.

Quantimet analyses of electron micrographs can be determined in the same way as the optical microscope fields of view.

Particle-Size Analysis by Sedimentation

Most samples of marl and chalk were subjected to particle-size analyses by the sedimentation method. The marl and chalk sample was crushed to pass 100 mesh (0.15 mm), mixed with distilled water, vigorously stirred for 15 minutes, and allowed to settle undisturbed for particle-size analyses. The weight percentage of solids in a constant volume of aliquot removed at certain periods of time by pipette from a constant depth in the slurry gave the data to calculate the distribution of particle sizes in the sample. The data were plotted as a cumulative percentage versus particle size curve. Interpolation of the curve at the 50 percent point gave the median particle size.

Methods of Mineral and Chemical Analyses

Samples were analyzed for their mineral composition by X-ray diffraction of whole rock powders and by optical microscopic determinations. The

percentage of insoluble residue was measured in warm 1N HCl acid and the residue was analyzed by X-ray diffraction to determine the types of clay and other less abundant minerals present in the samples.

Analyses of the chemical oxides were determined by the Analytical Chemistry Section of the Illinois State Geological Survey. The sodium oxide (Na_2O) content was determined by neutron activation; K_2O by flame photometry; CO_2, total S (computed and listed as SO_3), H_2O (weight loss at 110° C), and organic carbon by gravimetric analysis; and the remaining oxides by X-ray fluorescence spectrometry. The loss on ignition can be figured from the data presented for each sample by finding the sum of the CO_2, H_2O, organic C, and SO_3 values.

Experimental Methods of Calcination and Determination of Pore Structure and Surface Area

Pore Structure by Mercury Porosimetry

The mercury porosimeter used in these studies was a 15,000 psi Model 5-7121 from American Instrument Company. The 15,000 psi pressure limit corresponds to penetration of mercury into pores 0.012μ (1.2×10^{-6} cm) in diameter or greater. The instrument measures the volume of mercury that penetrates voids between particles and pores within particles as a function of pressure. With this instrument the total penetration volume, equal to the total pore and void volume, must be less than 0.2 cc. The instrument has proved satisfactory for use in the present studies.

The translation of penetration volume versus pressure data into penetration volume versus pore and void diameter data requires that two important parameters be known. These are: (1) the shape of the pores and voids and (2) the contact angle between the mercury-material interface. In most mercury porosimeter measurements it is assumed that the pores and voids are cylindrical and that, on the basis of experimental evidence, the contact angle is 130 degrees. The pressure readings are converted into the corresponding pore (or void) diameter, which is then plotted against the measured penetration volume. The resulting plot is a penetration-volume curve that can be used to evaluate the void volume, the total pore volume, and the mean size of the true pores.

The interpretation of a penetration-volume curve obtained for a single particle of material (fig. 1a) is usually simple. Because no voids can be associated with the single particle of material, the penetration-volume curve is the pore-volume curve and, provided that all pores have been reached, the measured total penetration volume is equal to the total pore volume of the material. However, the observed pore-volume curve may not be the true pore-volume curve. If the material contains rather large interior cavities connected to the surface by narrow pores (usually called "ink bottle" pores), the cavities will not be filled until the narrow pores can be penetrated and, hence, the true pore-volume curve will not be observed. The comparison of the pore-volume curve for the single particle with the penetration-volume curves for other particle-size fractions of the material can indicate whether or not "ink bottle" pores are present.

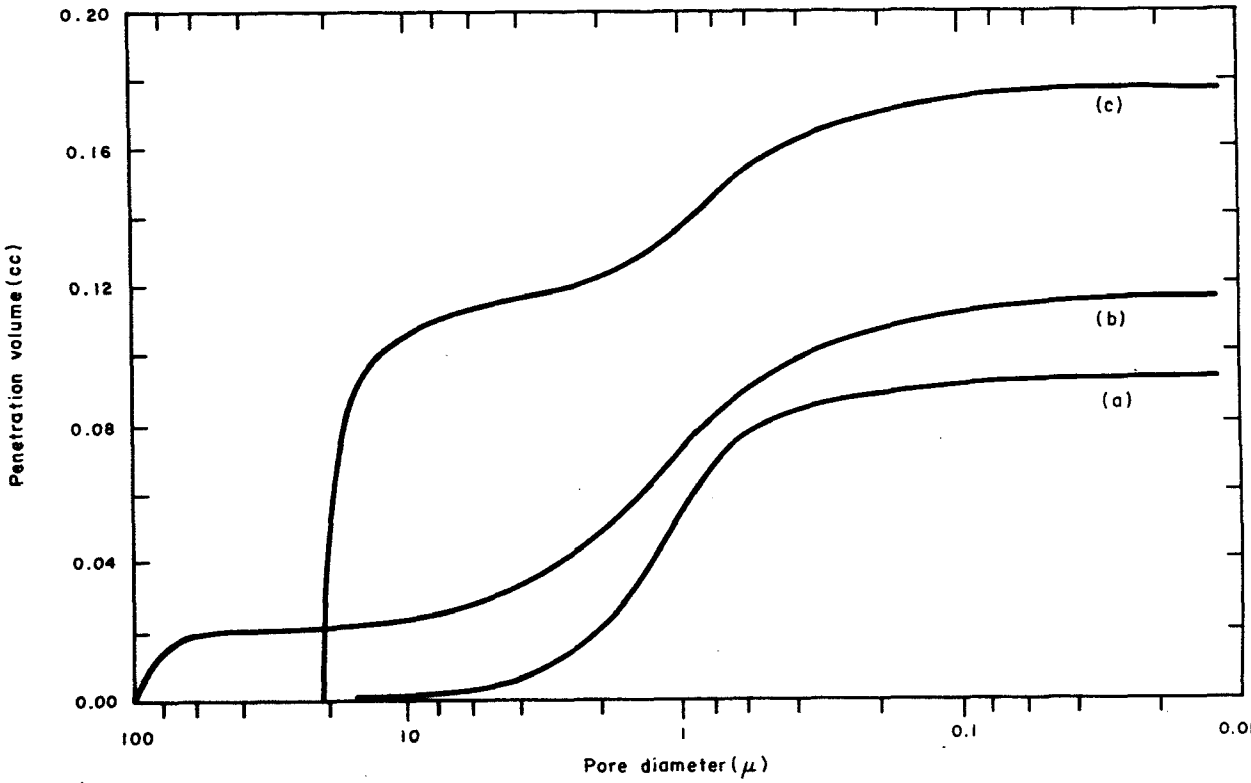

Fig. 1 - Examples of penetration-volume curves for (a) a single particle, (b) 16x18 mesh particles, and (c) 170x200 mesh particles of marl.

In the present study, as in most studies, it was more desirable to use a large number of particles rather than a single particle in the pore-structure measurements. The mesh sizes of particles chosen were 16x18 (1200μ to 1000μ), 40x50 (420μ to 300μ), and 170x200 (98μ to 74μ). All mesh sizes are U.S. Standard. Most of the measurements were made on the 16x18 mesh fraction. Although actual use of the marls, chalks, and shells now being studied would probably require the material to be ground to minus 170 mesh (88μ) in the "limestone-injection" process for SO_2 removal, it will be seen that the pore structure created by calcination is nearly the same for 170x200-mesh particles as for 16x18-mesh particles. However, it should be pointed out that the total pore volume obtained for the 16x18-mesh fraction of a marl or chalk cannot be used simply to represent the total pore volume available in any smaller size fraction of the same material. Because of the polygranular nature of these particles, subdivision of a large particle will take place principally along pores, thereby reducing the total pore volume within the resulting particles. The lost pore volume would be converted into additional void volume between particles.

A major problem in correct interpretation of porosimetry data is to distinguish between void volume and actual pore volume. Any agglomeration of small particles will create a considerable number of interparticle voids, and unless the amount of mercury intrusion into the voids can be determined, the pore-volume measurement will be erroneously high. The penetration of mercury into the voids between packed spheres is characterized by a rather abrupt breakthrough pressure corresponding to the apparent pore diameter of the voids and by subsequent gradual filling of the toroidal voids around the contacting particles.

At the beginning of the present study, penetration-volume measurements were made on nonporous Iceland spar (pure calcite, density 2.71 g/cc) to enable corrections to be made on the observed penetration values of marls and other samples for interparticle void space and other factors such as mercury compressibility. These data showed that 90+ percent of the void space for 16x18-mesh spar was filled at the initial pressure of 1.8 psia (pounds per square inch absolute) and that the remaining void space was filled in the 1.8 to 12 psia range, corresponding to the 100μ to 15μ pore-size range. A small amount of additional penetration volume was measured in the 12 to 15,015 psia range (15μ to 0.012μ pore-size range). The penetration-volume data for Iceland spar were used to correct other penetration-volume data. A typical penetration-volume curve for 16x18-mesh particles of marl is shown in figure 1b. The first step in the curve represents the filling of voids, and the second step represents the filling of pores within the particles.

For 170x200-mesh particles of nonporous calcite most of the voids are filled at 12 psia (15μ pores), but they are not completely filled until 200 psia (0.9μ pores) is reached. These data were used as a zero-pore base line in determining the true pore volume of the 170x200-mesh samples tested. A typical penetration-volume curve for 170x200-mesh particles of marl is shown in figure 1c. The large first step represents the filling of voids, and the second step represents the filling of pores within the particles. Hence, pores much larger than 10μ in 100μ particles cannot be distinguished from voids. In practice, voids larger than 15μ (12 psia) were filled with mercury before any data were recorded.

The mean pore size was determined from the pore-volume curve by computing the mean of the pore sizes evaluated at the 16th, 50th, and 84th percentiles of the distribution. The mean calculated by this procedure more adequately characterizes the distribution than does the mean calculated by the 50th percentile alone (Falk, 1958). The standard deviation (S.D.) was computed from the pore sizes (S_i) evaluated at the 5th, 16th, 84th, and 95th percentiles by means of

$$\text{S.D.} = \frac{S_{95} - S_5}{6.6} + \frac{S_{84} - S_{16}}{4} \quad .$$

Apparatus for Calcination and for Surface Area Measurements

A schematic diagram of the apparatus used for calcination of the carbonate rocks tested in the present study and for subsequent measurements of the surface areas of the calcines is shown in figure 2. The U-shaped sample

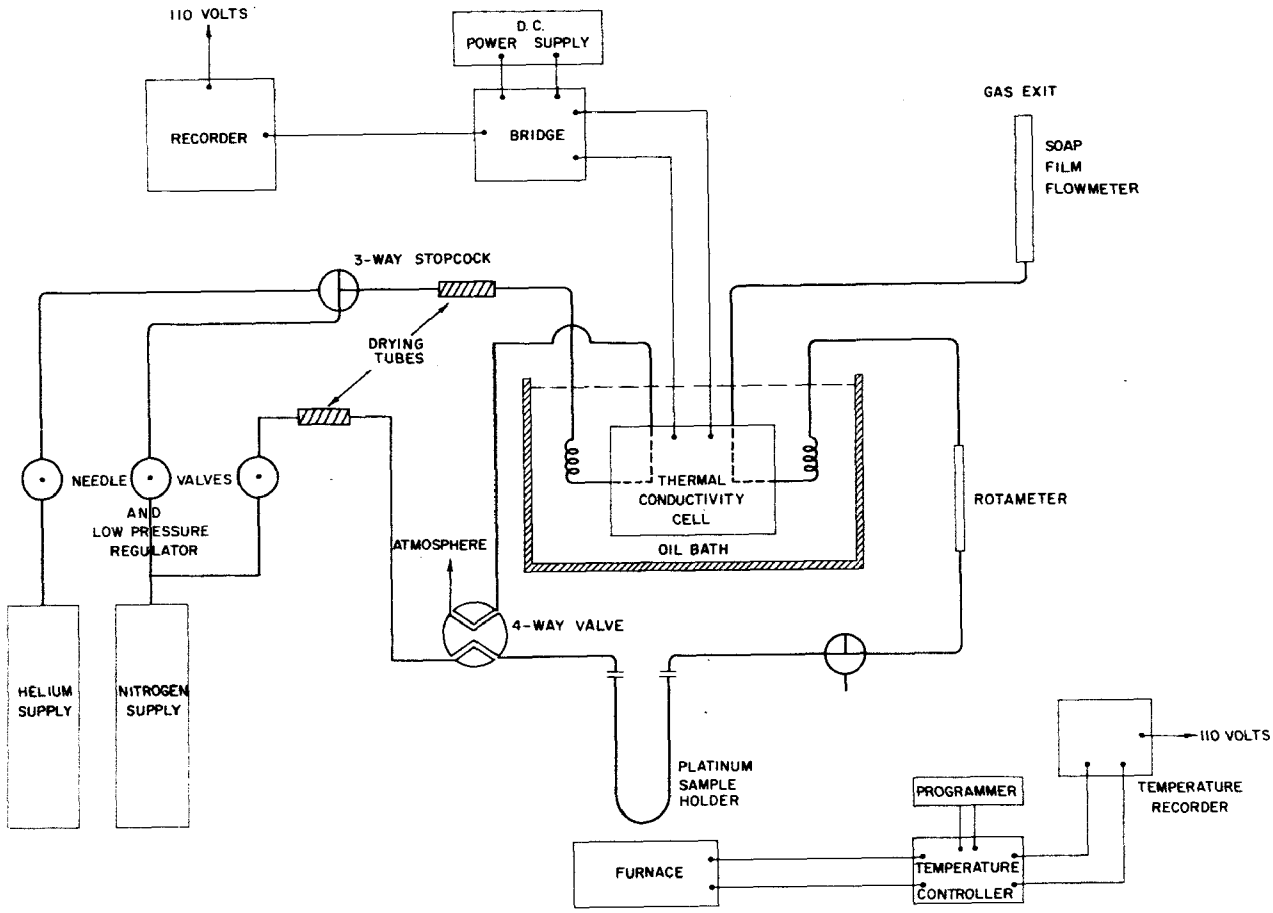

Fig. 2 - Schematic diagram of apparatus used for calcination and for measurement of surface area (after Thomas and Frost, 1972).

holder is made from platinum-5 percent rhodium tubing and is connected to the apparatus with Swagelok "quick connect" fittings, which are cooled by an air stream during calcinations. The furnace, capable of reaching 1000° C, can be quickly raised to, or lowered from, position around the sample holder. Calcination takes place under dynamic gas-flow conditions and the process is monitored by recording the output of the thermal conductivity cell. The recorder is equipped with a Disc integrator for the measurement of the area under recorder traces. The apparatus and procedures are similar to those used by Thomas and Frost (1971).

Surface Area Measurements

The use of a flow system (fig. 2) for surface area measurements was first described by Nelsen and Eggertsen (1958). For these measurements, the 3-way stopcock and the 4-way valve were rotated 90 degrees from the positions shown in figure 2. A known mixture of helium and nitrogen was passed over the

sample. A dewar flask of liquid nitrogen was raised around the sample holder to greatly lower the temperature of the sample, thereby causing nitrogen to be adsorbed from the flowing gas stream. After about 10 minutes, the dewar of liquid nitrogen was removed, the sample was quickly warmed to room temperature, and the adsorbed nitrogen was then desorbed from the sample. The desorbing nitrogen produced a standard gas chromatograph peak on the recorder. The area under the peak was determined by the Disc integrator. From previously prepared calibration curves, the amount of nitrogen adsorbed was determined. The composition of the gas mixture (determined from gas flow rates) defined the nitrogen adsorption pressure. The flow rate of nitrogen was then changed to measure the amount adsorbed at other nitrogen pressures. The classical BET (Brunauer, Emmett, and Teller, 1938) equation was then used to calculate the actual surface area.

In the present study, the surface area of each calcine was calculated from a single adsorption point. The surface areas of rock samples were calculated from multiple adsorption points obtained by using an apparatus similar to the one shown in figure 2. This apparatus is used only for surface area measurements and can handle two samples for consecutive adsorption point measurements.

Calcination Conditions

All samples calcined in the present study were calcined at 850° C under a nitrogen flow rate of 100 cc/min. The calcination time was less than 14 minutes. Calcines of limestones and dolomites (unpublished data of Frost and Thomas) produced under these conditions have large surface areas (20+ m^2/g calcine) and contain fine pores less than 0.2μ in diameter. Similar properties have been reported by Coutant et al. (1971) in dispersed-phase reactor studies with calcination times of 2 seconds or less. According to D. C. Drehmel (personal communication, 1971), calcination of three marls at 980° C, under comparatively less dynamic gas-flow conditions than those used in this study, produced calcines with much lower surface areas (1.6 to 3.9 m^2/g calcine).

Selected marl samples were calcined at 950° C under a nitrogen flow rate of 100 cc/min to study the effect of calcination temperature on calcine pore structure and surface area. Calcination times were less than 6 minutes. Three marls (7133, 7150, and 7162C) were calcined at 950° C under a 10 percent carbon dioxide-90 percent nitrogen (by volume) gas stream at 100 cc/min. A calcination time of 10 minutes was used, but calcination was complete in less than 5 minutes. The three marls were also calcined at 950° C for 60 minutes under both the pure nitrogen and the 10 percent carbon dioxide-90 percent nitrogen gas streams.

Experimental Procedure

A 0.2 to 0.3 g carbonate sample was weighed and placed in the sample holder, which was then connected to the apparatus. When a stable output signal from the thermal conductivity cell was observed on the recorder, the furnace (preheated to 850° C or 950° C) was raised over the sample holder. The calcination

process was completed in 4 to 12 minutes and was monitored on the recorder. About 2 minutes after the apparent completion of calcination, the furnace was removed. The sample holder cooled rapidly to room temperature. The calcine surface area was then measured. The calcined sample was removed from the sample holder, weighed, and transferred to a mercury-penetration cell for the pore-structure measurements.

Observations on Calcination of Samples

Three typical calcination recorder traces are shown in figure 3. The trace shown in figure 3a is representative of chalks, chalky limestones, and shells calcined at 850° C. The height of the trace above the base line is proportional to the CO_2 concentration in the gas stream. Hence, the area under the trace is proportional to the CO_2 content of the carbonate sample. There is no readily available explanation for the small dip at the front of the trace. The general shape of the trace suggests a receding shell calcination model.

Traces typical of lake marls and bog marls calcined at 850° C (fig. 3b) have three distinct regions. The large initial negative dip (cut off by a recorder stop) resulted from the decomposition of the relatively large quantities of organic matter present in the sample. An appreciable quantity of CO_2 from carbonate decomposition was included in the negative peak, as evidenced by observed flow rates and time of appearance of the CO_2 peak, and by the considerably less area than expected under the positive portion of the calcination trace. A possible explanation for the two distinct positive regions on the observed trace is that they represent decomposition of carbonate grains widely differing in size. Since carbonates will not calcine in high concentrations of CO_2, the calcination of the largest grains may be suppressed by the rapid calcination of the very fine grains. It is also possible, because of the charring of the organic carbon, that the suggested grain-size groups are actually one group and that traces like figure 3a, which has a small secondary hump, would be observed if the organic carbon were absent.

The trace shown in figure 3c is typical of the traces of marls calcined at 950° C under both the pure nitrogen and the 10 percent carbon dioxide-90 percent nitrogen gas streams. The effect of the increased temperature on the actual time for complete calcination is readily seen by comparing figures 3b and 3c. The calcination trace at 950° C is characterized by two regions instead of the three observed for calcinations at 850° C. The absence of the third region in the calcination trace (950° C) must be directly related to the increase in calcination temperature. At 950° C, calcium carbonate will calcine under considerably higher carbon dioxide concentrations than at 850° C. Therefore, at 950° C, the rate of calcination for all carbonate grains present in a marl sample is so rapid that all grains calcine more or less at the same time.

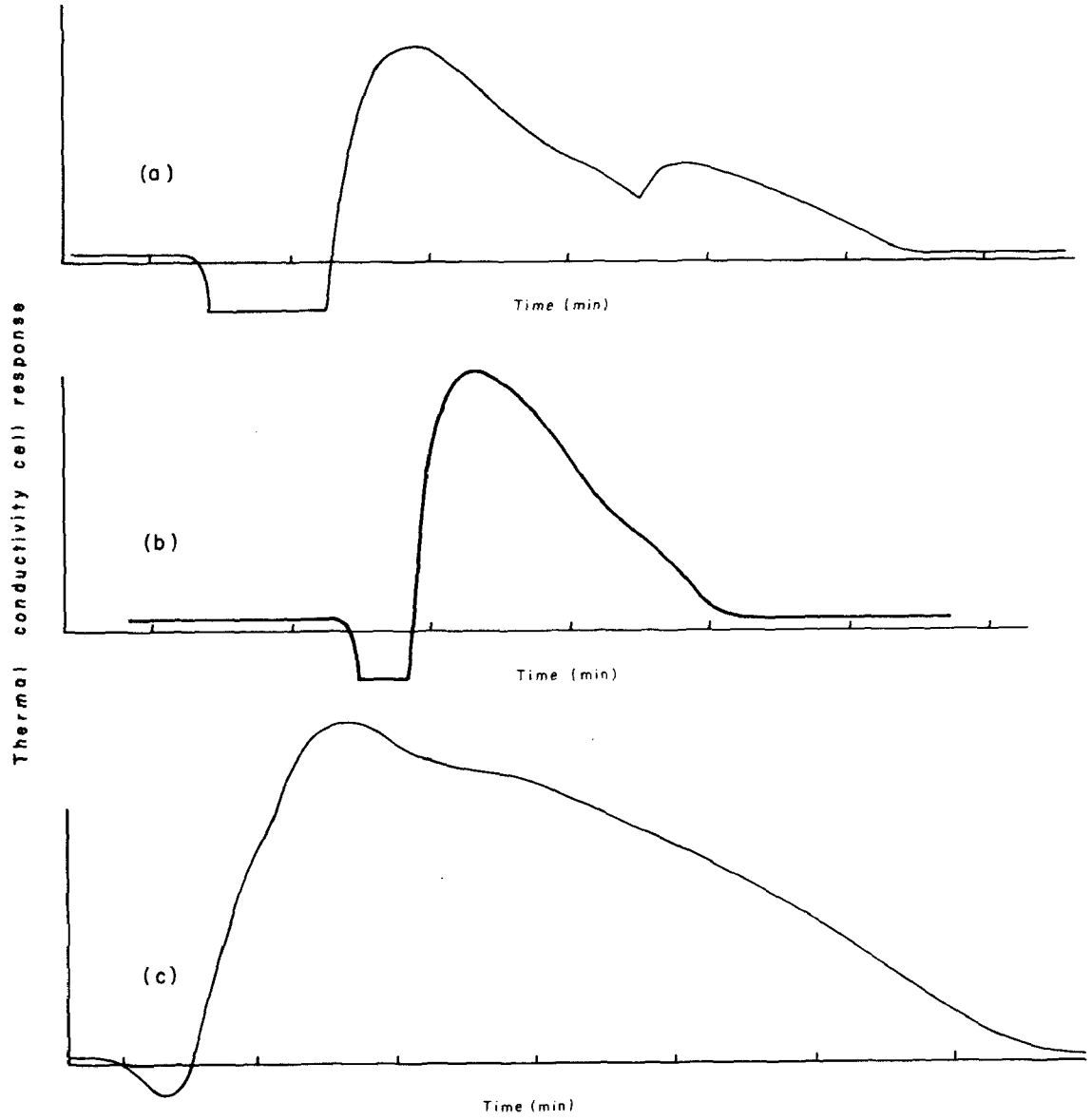

Fig. 3 - Typical calcination recorder traces for (a) marls calcined at 850° C, (b) marls calcined at 950° C, and (c) chalks, limestones, and shells calcined at 850° C.

MARL INVESTIGATIONS

Uses and Production of Marl

During the early 1900's, considerable use was made of marl as a source of CaO for the manufacture of natural and portland cement. Processing plants were located principally in New York, Pennsylvania, Ohio, and Indiana. Production for use in cement decreased in the 1930's, and by 1940 little or no marl was used for this purpose.* However, marl has long been used as a source of agricultural limestone, and marl, as defined here, continues to be produced almost entirely for this purpose. In 1968, 1,211,015 tons of calcareous marl* was produced in the United States (U.S. Bureau of Mines, 1969). In 1969, production increased to 2,490,000 tons (U.S. Bureau of Mines, 1971). Indiana and Michigan are the major marl-producing states. In 1971, there were 22 producers of marl at 24 pits in Michigan (Segall, 1972), and 29 pits were active in Indiana (Purdue University Cooperative Extension Service, 1971). During the summer of 1971, there were two active marl pits in Minnesota and one active pit in each of the states of Virginia, New York, and Wisconsin.

Marl occurs in basins occupied by lakes and bogs. The basins may be small, occupying a few acres, or as large as several hundred acres. Most deposits are of the order of 50 to 100 acres and 10 to 30 feet thick. Production from most marl pits is small compared to that from most limestone quarries. However, operators of marl pits report that if a new market or a new use for marl were developed, production could be increased.

With few exceptions, marl is mined by dredging a channel through the deposit and stockpiling marl along the bank, allowing the water to drain (fig. 4). The stockpiled marl is turned over occasionally to promote drying. However, the marl produced from one pit examined was dry enough to be disked and then later loaded into trucks for delivery; another pit was pumped sufficiently dry that the marl was loaded directly into trucks.

Sources and Samples of Marl

Geologic literature was surveyed to find localities of marls in the contiguous states of the United States. With rare exception, all known lake marls occur in the northeastern part of the country (fig. 5). These marls are associated with the fresh-water glacial lakes and bogs. An annotated bibliography of the occurrences and geology of marls in the northeastern part of the country is given in appendix 1.

Lake marls consist of very fine grained gray to near white, soft and incoherent mud-like material, mainly calcite ($CaCO_3$). Marl frequently contains

---

* Coquina continues to be used in the manufacture of portland cement in Virginia and elsewhere and is included in U. S. Bureau of Mines production tables under the heading "calcareous marl."

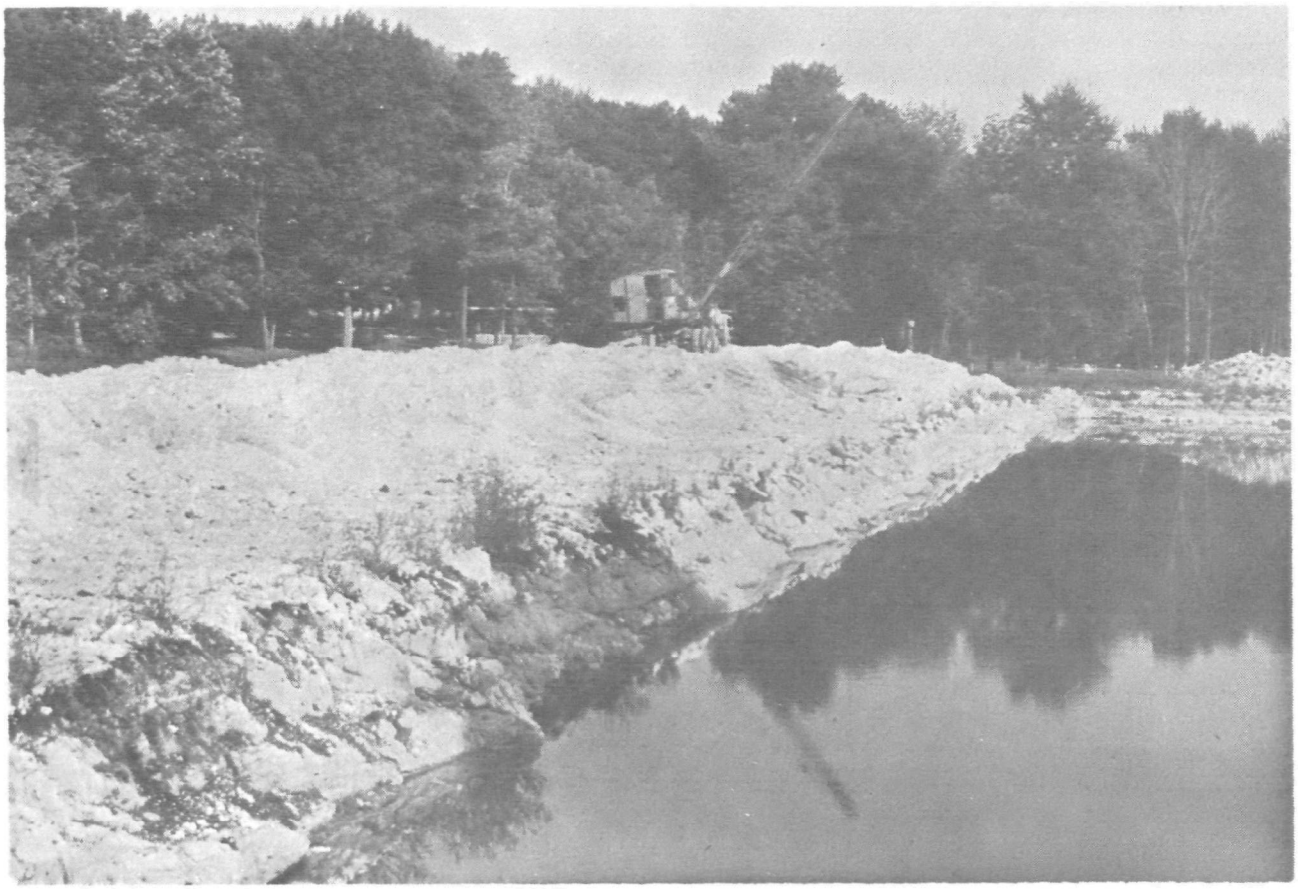

Fig. 4 - Marl production pit.

organic remains of plants, the source of the gray color, and also scattered mollusk shells. In most deposits, some degree of stratification of marl occurs. Snail shells are concentrated into a few lenticular beds 1 to 3 inches thick and 4 to 10 feet in length, and other stratification is evidenced by thin interlaminations of dark and light colored marl.

Lake marls in the areas around the Great Lakes are all geologically very young, Pleistocene in age,* and $CaCO_3$ in the form of marl is being deposited during spring months in at least one fresh-water lake in New York (Terlecky, in press). Many of the marl localities identified in the literature were examined and sampled for this study (fig. 5), and the locations and specific remarks on the samples and deposits are given in appendix 2. In August 1971, samples were obtained from all known marl deposits in commercial production in Virginia, New York, and Minnesota and from most of the commercial deposits in Indiana and Michigan.

---

* The Pleistocene Epoch covers the time interval popularly known as the "Ice Age," which began approximately 2 million years ago and includes the Holocene (Recent) Stage. Marl appears to be forming in some lakes today.

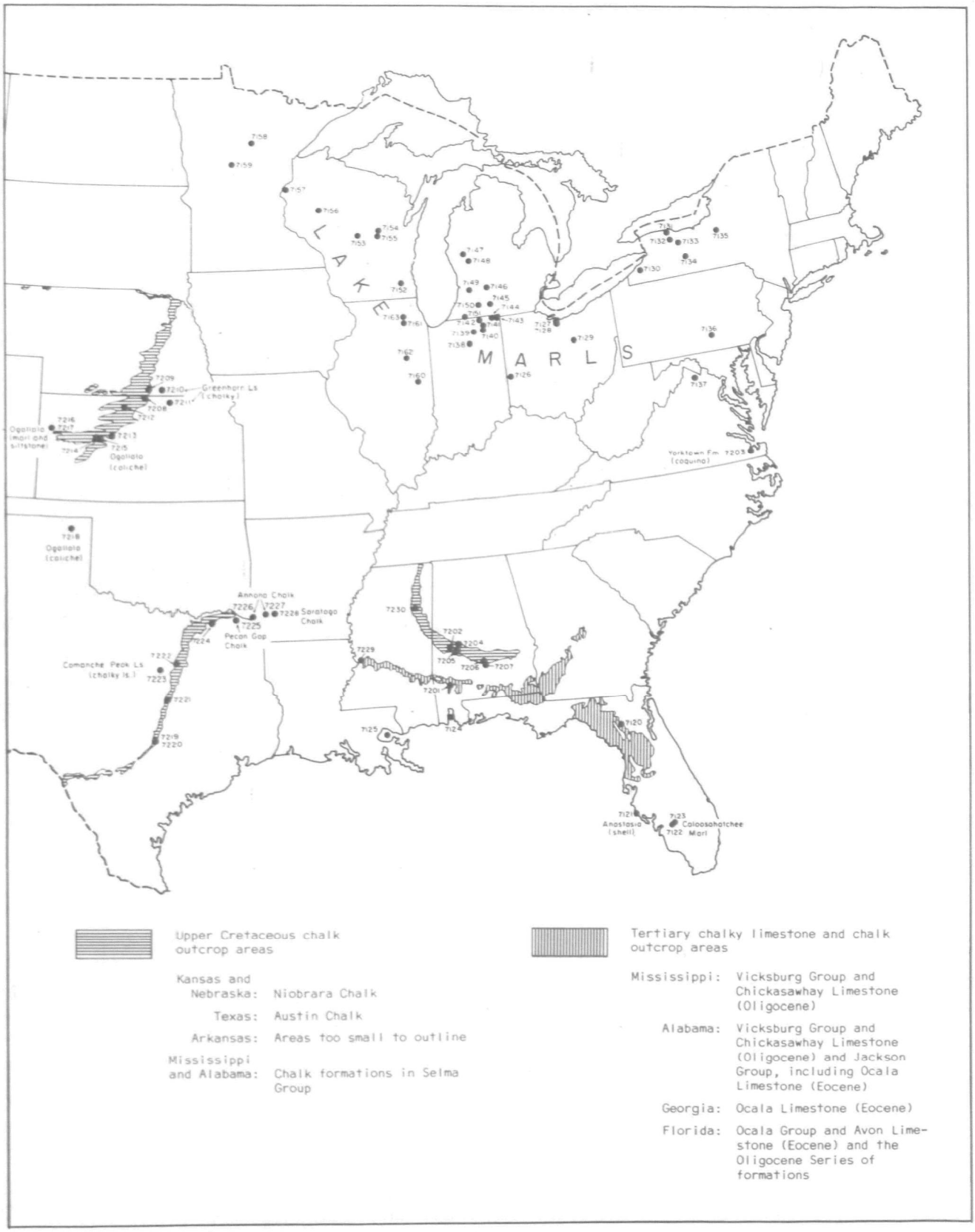

Fig. 5 - Localities of marls and other rocks sampled and the outcrop areas of principal chalk and chalky limestone strata. Sources: Alabama - Copeland (1968); Florida - Vernon and Puri (1965); Georgia - Georgia Division of Mines, Mining and Geology (1939); Kansas - Kansas Geological Survey (1964); Mississippi - Bicker (1969); Nebraska - Burchett (1969); Texas - Oetking (1959).

Marl resources in Indiana are described and chemical analyses of core samples of five deposits are given by Wayne (1971).

The Ogallala Formation (Pliocene in age) of western Kansas contains deposits of lake marl (Frye and Leonard, 1959). Samples for study were obtained from two localities. One was collected from an operating quarry in Ogallala marl where the deposit (7217) was mined for its diatomaceous content by the NL Industries of St. Louis, Missouri. The other was collected from a nearby deposit (7216); however, this sample was later proved in laboratory studies to be a calcareous siltstone with a smaller calcite content than anticipated.

Several deposits of marl and related soft and porous carbonates are known to occur in widely scattered localities in the western states but were not sampled for the present study. The following remarks will serve as a guide for further investigation in these areas. In south-central Oklahoma, in the vicinity of Ravia, marly and chalky limestones of the Baum Limestone (Lower Cretaceous) occur in considerable quantities, and samples contain 93.1 to 99.5 percent $CaCO_3$ (Wayland and Ham, 1955).

In western Utah, according to William P. Hewitt of the Utah Geological Survey, Salt Lake City (personal communication, May 28, 1971), impure marls occur in sediments left by the former Lake Bonneville, north of Ogden. Also in Utah, a pisolitic and chalky limestone of high purity occurs in Tertiary-Pleistocene sediments on the eastern slopes of the Confusion Range, west of Delta (W. Walker, Marblehead Lime Co., Thornton, Illinois, personal communication, May 17, 1973).

Lake marls occur in north-central and northeastern Washington. These are described in some detail by Valentine (1960, p. 58 and 59).

In Nevada, according to Keith G. Papke of the Mackay School of Mines, Reno, Nevada (personal communication, June 3, 1971), extensive deposits of relatively pure unconsolidated calcium carbonate occur in two areas. One is in the vicinity of Pyramid Lake, and the other is in southern Nye County, north of Ash Meadows. The latter deposits were previously mined for whiting.

Many rock types described in geologic literature as marls are sands, calcareous siltstones, and calcareous claystone, all deposited in marine waters. Many of these rocks are associated with chalks in the Upper Cretaceous rocks from Texas to Alabama; examination showed they are too low in $CaCO_3$ content for inclusion in this study. Thus, the Corsicana Marl, Arkadelphia Marl, Marlbrook Marl, and Brownstown Marl Formations were excluded.

Illinois Marl Deposits and Samples

Two deposits of marl in Illinois are of special interest. Marl was produced from a bog deposit near Chatsworth, Illinois (locality 7162), during the late 1930's. Samples from this site were obtained from stockpiles that remain from past workings (7162 A-D). Exact marl reserves in this locality

are not known, but it is thought that only a relatively small portion of the marl was removed during past operations. The bog is about 60 acres in area and was reported at the time of production to be 24 feet thick in the central part. A small lake now stands where the marl was previously produced.

The other known sizable deposit of marl in Illinois occurs beneath a peat (Grayslake Peat) deposit near Batavia, Illinois, about 30 miles west of Chicago (locality 7163). The peat is currently being produced from the surface and processed by the Batavia Soil Builders Company. Samples 7163A-C were obtained from a boring near the northwest edge of the bog. Marl was observed to occur from 3 to more than 13.2 feet (the maximum extension of our auger). Sample 7163D was taken from a pile of marl dug previously near the center of the north end of the bog. The bog occupies an area of about 230 acres and if the marl averages 10 feet in thickness, about 10 million cubic yards of marl are present in this deposit. As a cubic yard of marl weighs close to one ton, this deposit is estimated to contain about 10 million tons of marl. The topographic quadrangle map of the area (Geneva, Illinois) shows the presence of other bog areas in the vicinity of 7163 that which may contain marl.

Characterization of Marl Samples

The distinction between lake marls and bog marls is based on the presence or absence of a natural lake immediately above the collection site. The samples designated as lake marls (app. 2) do not differ greatly from bog marls. Both types consist overwhelmingly of very fine grained gray to light buff calcite. They are very soft and incoherent mud-like materials and frequently contain organic remains of plants. Conspicuously scattered throughout marls are mollusk shells (pl. 1), with specimens and varieties of gastropods being more abundant than those of bivalves. Both pulmonate (with lungs) and branchiate (with gills) gastropods occur. The mollusk shells are very easily broken, and in all specimens examined they consist of the aragonite form of $CaCO_3$. Gastropod specimens are frequently 1/2 to 1 cm across, whereas the other types of shells present are usually 1 to 2 mm or less across. The larger shells are conspicuous in the marl because their color is milky white whereas the surrounding fine-grained calcite is light to dark gray. Marls containing little or no organic matter are nearly white when dry. The darker color is due principally to the occurrence of organic matter and moisture.

The major inorganic impurities in marls are quartz, as partly rounded grains 4μ to 30μ in diameter, and a few similarly sized and shaped grains of feldspar. These impurities are present in nearly every sample of marl and are scattered throughout the marl material rather than concentrated in certain layers. The abundance of these grains is proportional to the amount of SiO_2 and Al_2O_3 observed in the samples, as will be discussed later.

Study of lake marls by electron microscopy (pl. 2, A-F) shows the character of the grains and the high porosity of the samples. The micrographs shown illustrate characteristic textural features of the lake marls studied. Crystallite grain size, measured from more than five micrographs of each sample

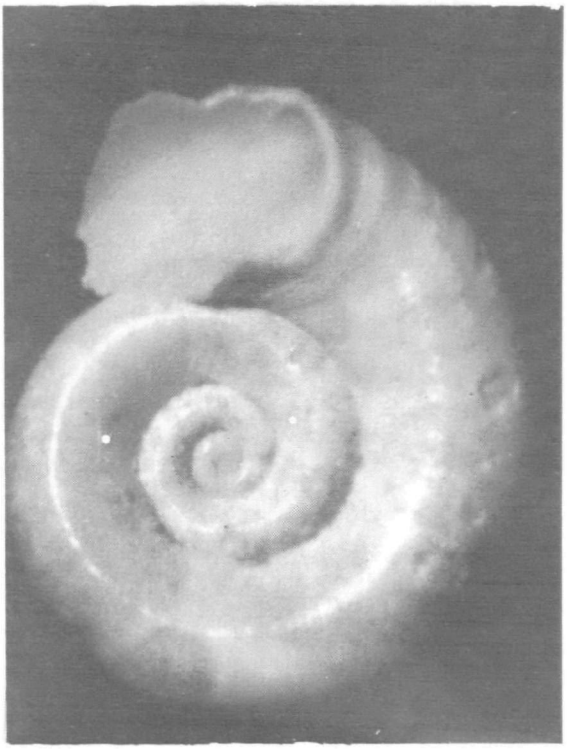

A. Pulmonate gastropod, Gyraulus altissimus (Baker)

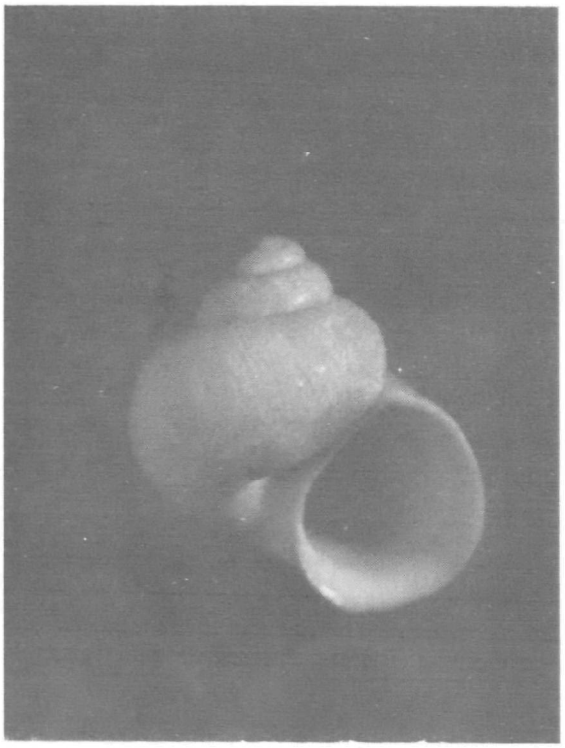

B. Branchiate gastropod, Amnicola leightoni (Baker)

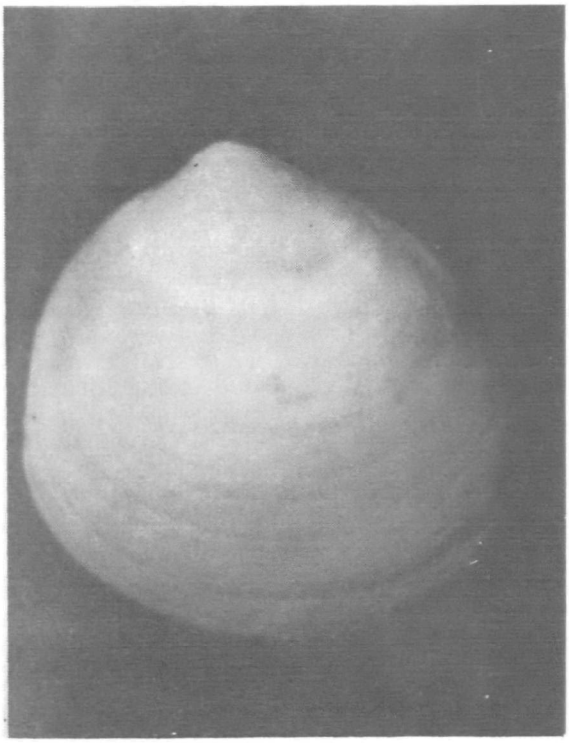

C. Bivalve, Pisidium sp.

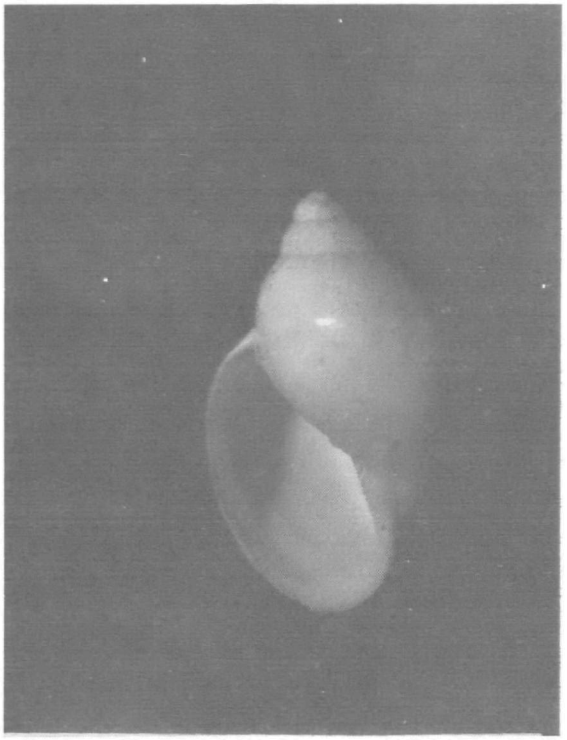

D. Pulmonate gastropod, Physa sp.

Plate 1 - Common mollusks from Pleistocene marls (x 10).

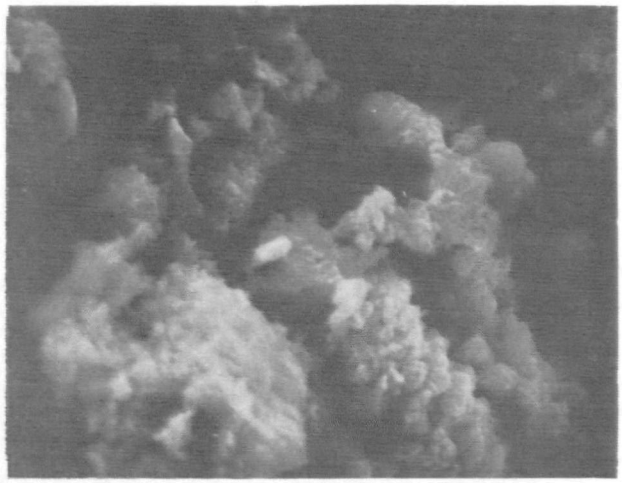

A. Sample 7138 5μ (x 2540)

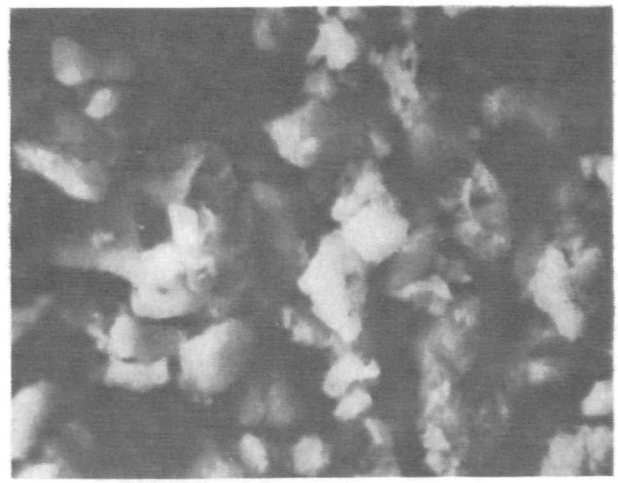

B. Sample 7142 5μ (x 2510)

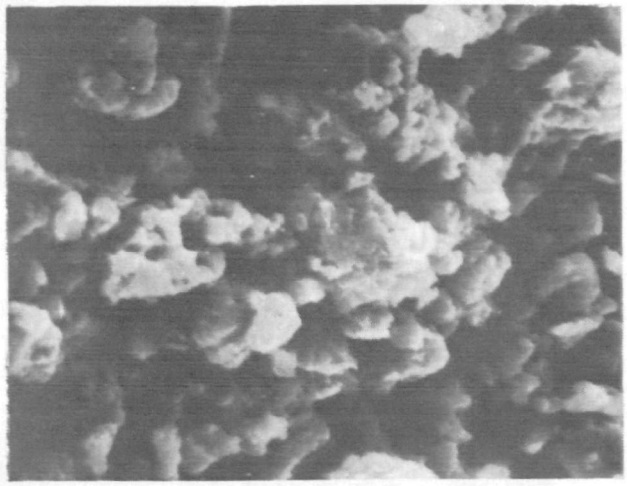

C. Sample 7142 5μ (x 2240)

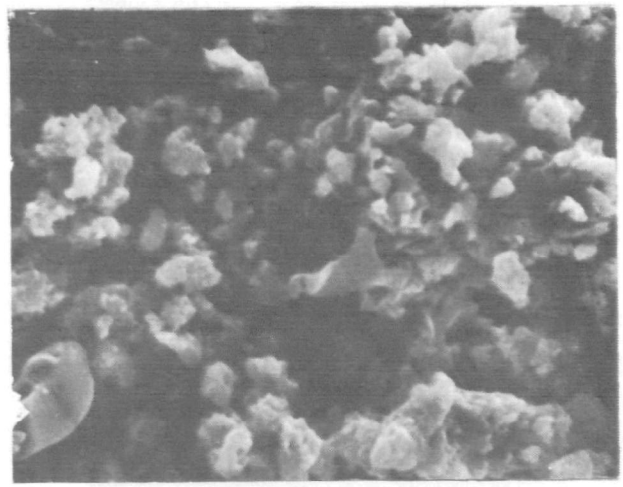

D. Sample 7134A 5μ (x 1970)

E. Sample 7158 5μ (x 2670)

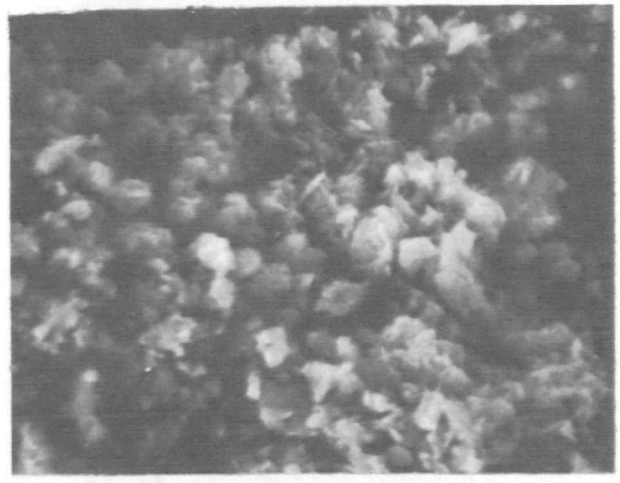

F. Sample 7157C 5μ (x 2210)

Plate 2 - Characteristic textural features of lake marls.

of the 14 lake marls, ranges from 0.1μ to more than 16μ; most grains have a diameter between 0.5μ and 2μ. In large part, these marls consist of agglomerate particles composed of several grains or crystallites weakly held together to form porous particles (especially noted in pl. 2F). In some areas, grains and particles are not clearly distinguished, such as in the right hand part of the large particle in the lower left of plate 2A. It is interpreted that the nodes present there are grains. Similarly, the nodes on the particle in the center of plate 2C are interpreted to be grains.

Marl in bogs consists mainly of very fine grained calcite (pl. 3, D, E, and F) and resembles lake marl in all important respects. Bog marl tends to be somewhat coarser grained than lake marl.

Tubular particles are found in 75 percent of the marls and are usually most abundant in bog marls. These particles are about 1/4 to 1 mm in diameter and 1 to 10 mm long (pl. 4C). The interior of these particles contains several open channels that run parallel to the long axis. Inspection of the outer surface of the tubules (pl. 3, A, B, and C) shows randomly oriented, interlocking grains of calcite that are larger than most of the other calcite grains in the marl. These tubules are the most coherent particles in marls, although they readily break apart when a few are rolled together between one's fingers. When these tubules are very abundant, the marl is designated as tufaceous (app. 2).*

Unusual and rare particles, found in a few samples of marls, are spores (pl. 4A); framboidal pyrite (pl. 4B)—spheroids 10μ to 30μ in diameter that consist of crystals (mainly 1μ octahedrons in this case) of pyrite (FeS_2); diatoms (pl. 4D)—delicate, siliceous skeletons of aquatic algae, especially abundant in 7162A; and ostracod carapaces (pl. 4E)—shells of minute bivalve crustacean fossils.

Grain Size and Particle Size

Averages of the 50 or more values of $\bar{C}$ (mean grain chord length) and of B (grain boundary length) determined from petrographic thin sections by Quantimet procedures for each marl were computed and considered to be characteristic of the sample (table 1). In addition, many of the scanning electron micrographs of specimens taken at extra high magnification were of sufficient quality for Quantimet analyses (table 1).

The Quantimet analyses show the mean chord length of the bog marls to range from 1.8μ to 5.7μ. The average is 3.4μ. The range of $\bar{C}$ for lake marls is 2.1μ to 4.4μ, with an average (2.8μ) slightly smaller than the average for bog marls. In many samples, though not all, the mean chord length measured on

---

* Davis (1901), Thiel (1930), and others have made detailed studies of such tubular structures and concluded that they were formed by the precipitation of $CaCO_3$ on the stems of Chara plants and, in places, several crystallites were sufficiently interlocked to form a coherent sediment particle, which was deposited on the bottom of the bog after the death of the plant.

A. Sample 7128A 5μ (x 3020)

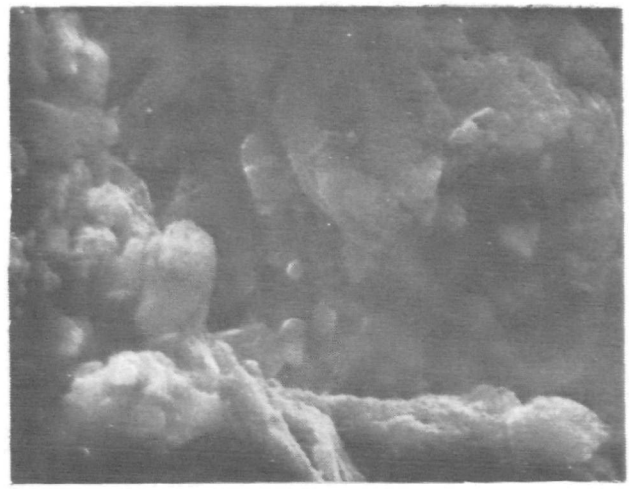

B. Sample 7133 5μ (x 2580)

C. Sample 7133 5μ (x 2150)

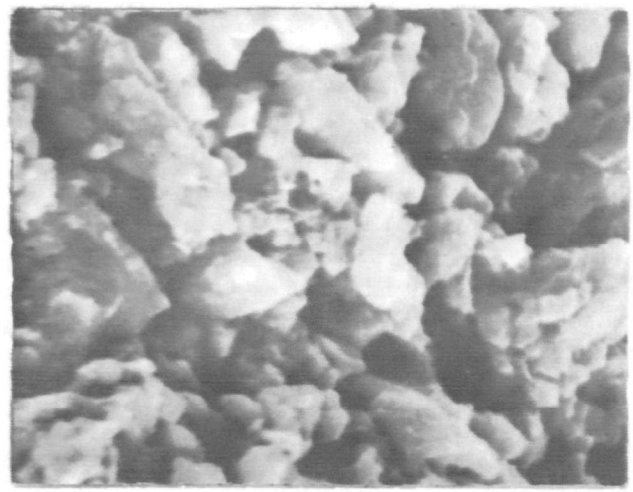

D. Sample 7151B 5μ (x 3250)

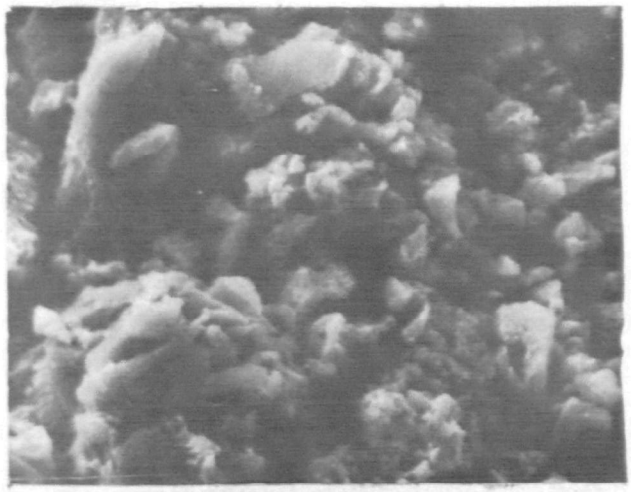

E. Sample 7162B 5μ (x 1890)

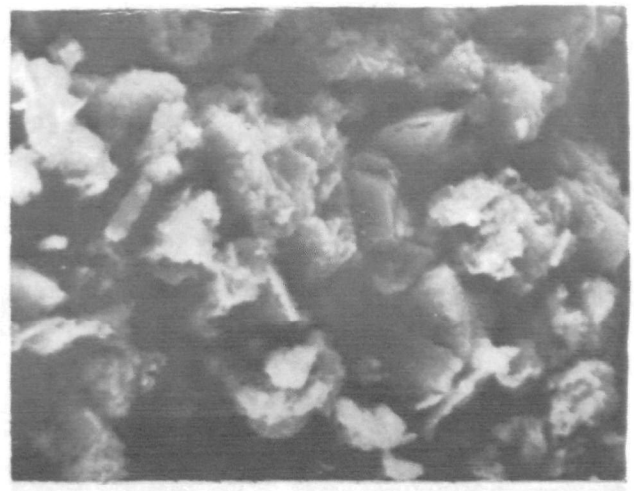

F. Sample 7163B 5μ (x 2350)

Plate 3 - Characteristic textural features of bog marls.

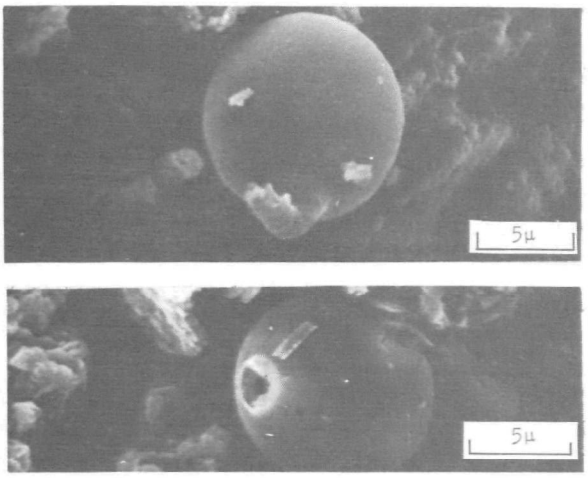

A. Spores in 7162C (x2500)

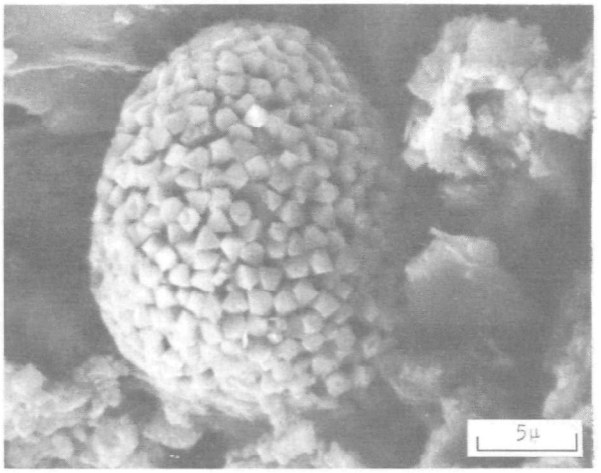

B. Framboidal pyrite (x2430)

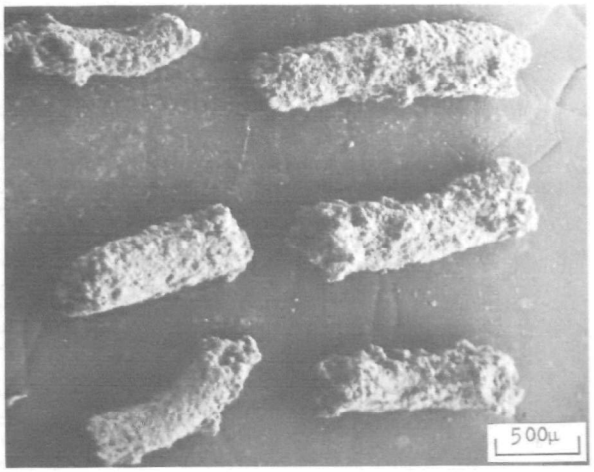

C. Tubules in tufaceous marls (x20)

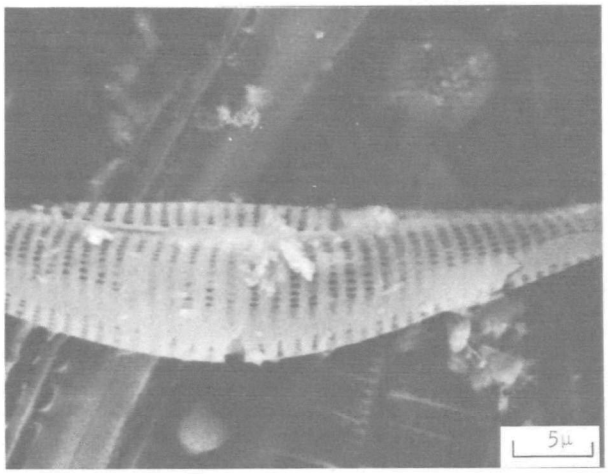

D. Diatom Cymbella sp. (x1990)

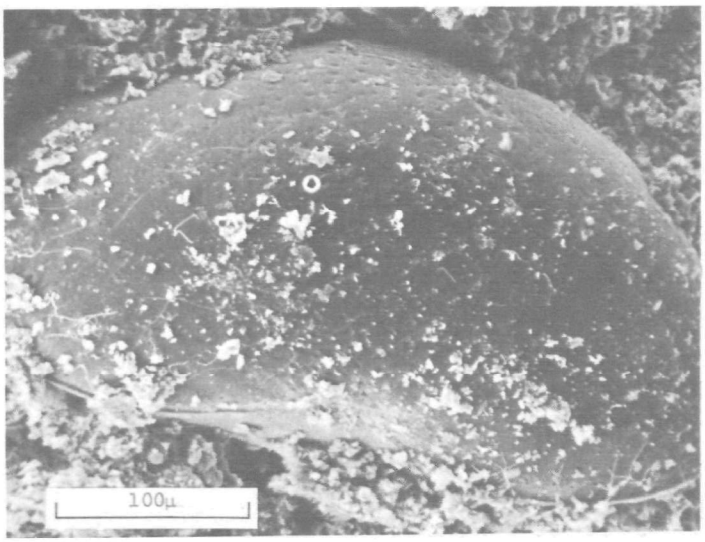

E. Ostracod valve (x244)

Plate 4 - Selected types of particles that occur in marls.

TABLE 1 — TEXTURAL ANALYSES OF MARLS

Sample number	Quantimet results				Median particle size† (μ)
	Mean grain chord length, $\bar{C}$ (μ)		Total grain boundary length, B (mm/mm^2)		
	Thin sections*	Electron micrographs	Thin sections	Electron micrographs	
7126A	3.8	—	2945	—	40.0
7127A	6.6	—	2964	—	—
7127D	2.6	—	2185	—	—
7128A	4.2	—	2622	—	—
7128B	5.7	1.54	2394	680	42.0
7129	3.5	—	2698	—	—
7130	3.3	—	2926	—	—
7131A	3.2	—	3059	—	—
7131B	2.7	—	2090	—	—
7131C	4.0	—	3002	—	—
7132A	3.8	—	4180	—	—
7132B	4.3	2.05	1881	611	—
7132C	2.7	2.22	2964	1264	—
7132D	3.1	1.84	2964	950	8.2
7133	4.1	4.24	2375	482	22.0
7134A	2.2	1.71	2983	876	—
7136	3.0	—	2052	—	—
7137	3.0	—	3610	1083	6.7
7138	2.4	3.74	3211	447	35.4
7139	2.7	3.11	2185	667	—
7140	3.2	—	2679	—	30.0
7141	2.7	2.85	2489	755	10.5
7142	2.1	1.81	2888	965	24.2
7143A	2.6	1.41	2812	1300	22.3
7144A	2.6	—	2527	918	—
7145A	2.1	1.53	2755	966	—
7146A	3.0	—	3192	—	—
7147A	2.8	2.17	2926	740	—
7148	3.4	1.62	3078	1103	—
7149A	2.8	2.21	2432	842	39.0
7149B	—	2.37	—	849	22.1
7150	4.4	0.41	2869	1161	7.6
7151A	3.3	4.05	1254	389	—
7151B	2.9	1.48	2774	1008	—
7151C	2.7	2.00	4237	848	—
7152	1.8	—	4294	—	29.5
7154	3.9	—	2546	—	—
7155	3.0	—	2831	—	—
7157A	3.2	2.85	3686	794	9.9
7157B	3.1	—	1900	—	—
7157D	2.5	—	1672	—	—
7158	2.4	1.30	1824	1308	—
7159	2.5	2.66	1938	742	—
7160	3.4	—	2546	—	—
7161	3.5	—	—	—	—
7162A	4.7	3.90	1634	497	—
7162B	4.0	2.01	1463	453	—
7162C	4.0	1.54	2831	783	—
7162D	3.9	1.72	1330	617	—
7163A	—	1.72	—	702	—
7163C	4.0	—	1976	—	8.6

*Excludes grains less than 1μ in diameter, the limit of optical resolution of the microscope.

†The size corresponding to the 50% point on the cumulative curves (figs. 6-9); determined by sedimentation methods on samples dispersed and vigorously stirred in water for 15 minutes.

the electron micrographs is smaller than that from the thin sections of the same samples. Two disadvantages are inherent in an analysis by electron microscopy: (1) to obtain a representative sample of grains, one must take a very large number of micrographs, and (2) the contrast of the grains is not sufficient in many micrographs to obtain accurate results with the Quantimet.

The results of particle-size analyses are shown graphically in figures 6 to 9. Interpolation of the curves at the 50 percent point gives the median particle size listed in table 1. Some marls, especially the tufaceous marls 7128B (fig. 7) and 7149A (fig. 8) have particle-size distributions with median values up to 40μ. Clearly the vigorous stirring in water did not disperse a sizable fraction of the particles in these samples. For comparison, the particle-size distributions of three limestones (Types 2, 3, and 4 in Harvey and Steinmetz, 1971) crushed and pulverized for 2.5 hours in a ball mill are shown in figure 6. It is clear that the ball milling of dense limestones does not yield a size distribution as fine as that observed for marls.

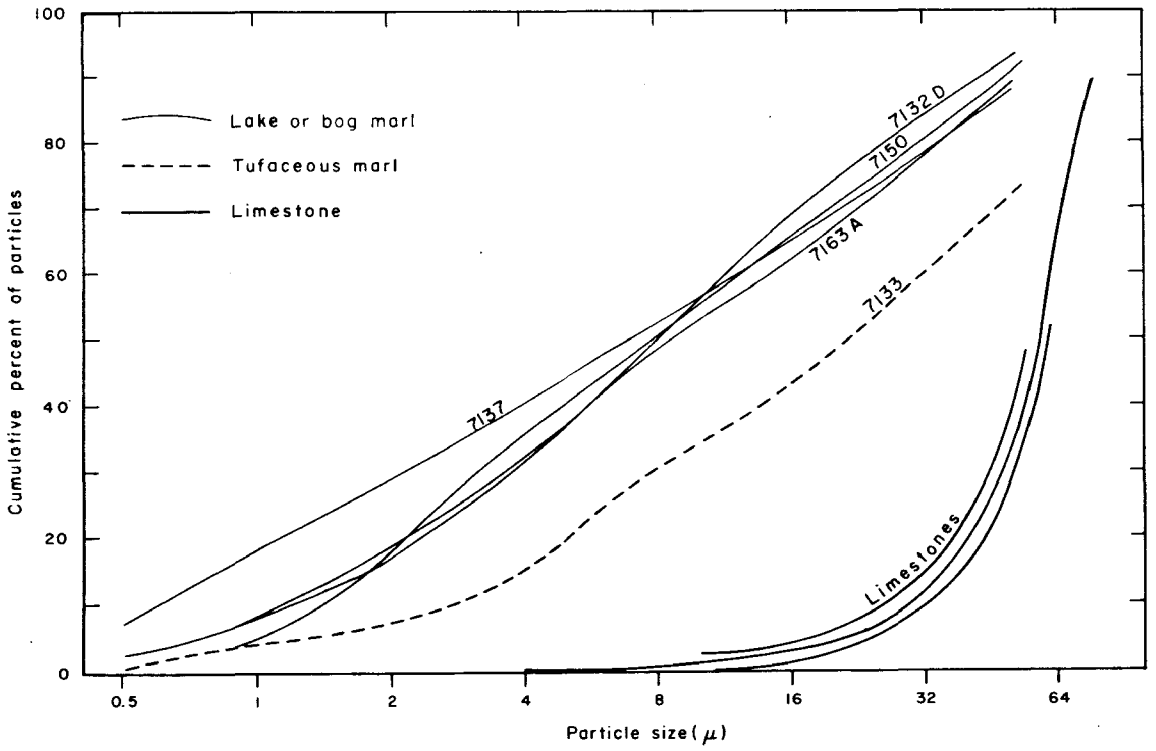

Fig. 6 - Particle-size distribution of selected marls. For comparison, results are also shown for three coherent and hard limestones (Types 2, 3, and 4, Harvey and Steinmetz, 1971) that were crushed and pulverized for 2.5 hours in a laboratory ball mill.

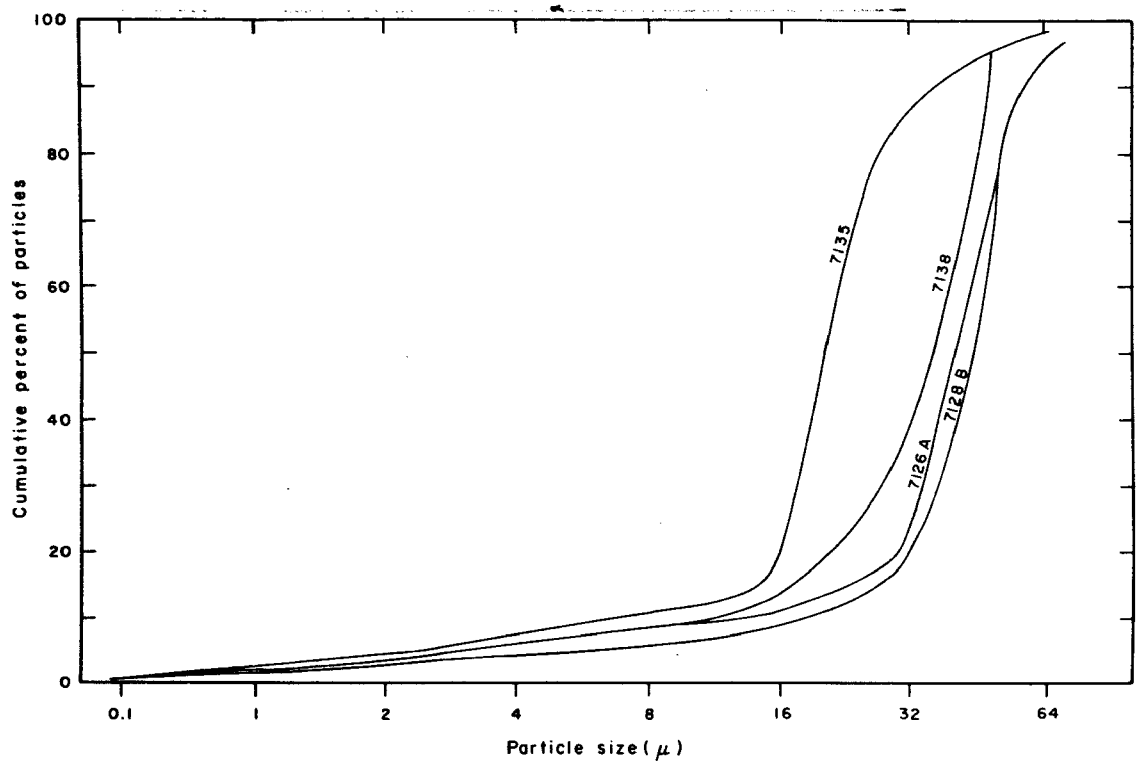

Fig. 7 - Particle-size distribution of marl samples.

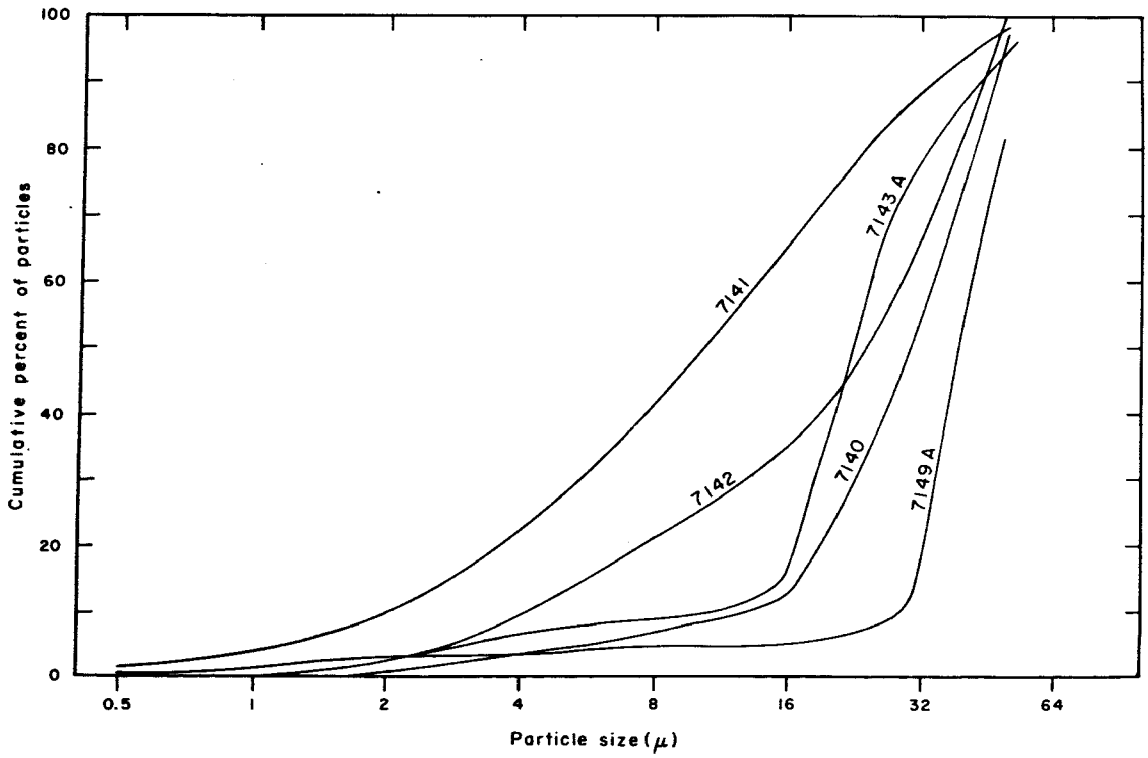

Fig. 8 - Particle-size distribution of marl samples.

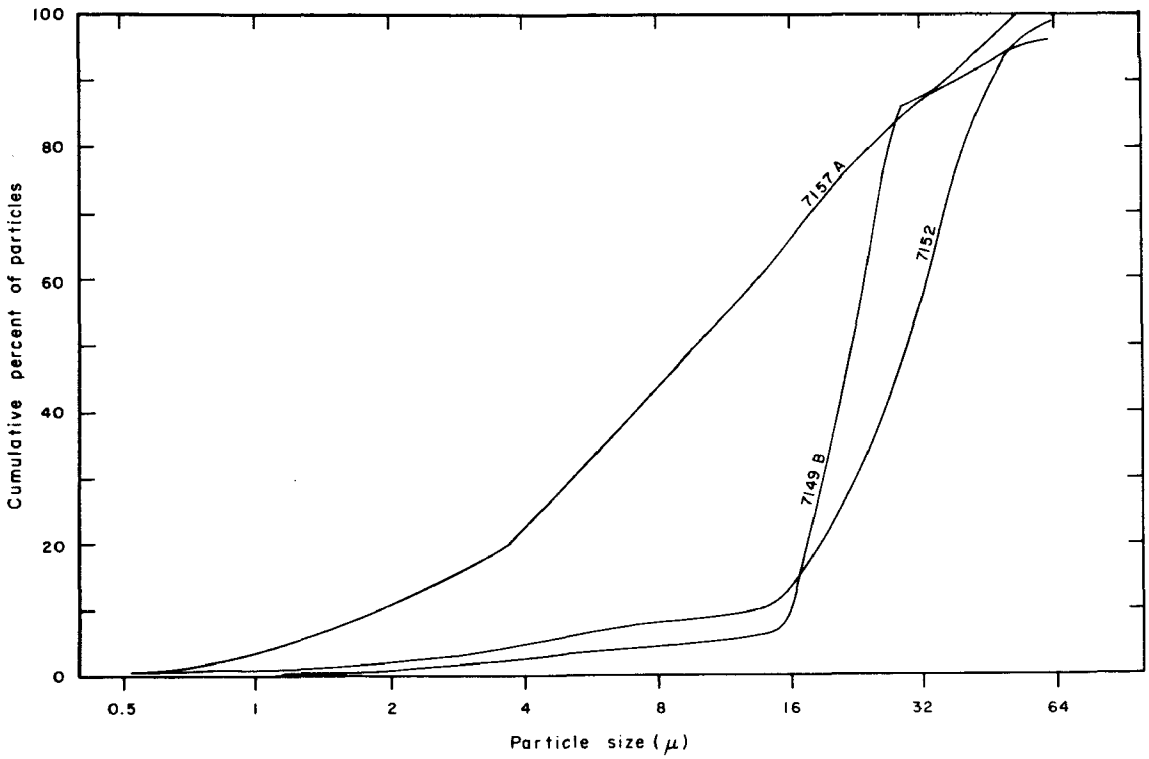

Fig. 9 - Particle-size distribution of marl samples.

Mineral and Chemical Analyses

The results of mineralogical analyses of marl samples are shown in table 2. The major mineral component in the samples is calcite, the rhombohedral form of $CaCO_3$. Trace and minor minerals in marls (table 2) are quartz (in the form of silt grains 4μ to 30μ across); feldspar (silt); aragonite, which occurs in the fossil shells common in marls; dolomite; pyrite; and clay minerals.

Results of chemical analyses of all but the most impure samples are shown in table 3. In addition to those oxides shown (table 3), trace amounts of TiO_2 and MnO were detected in several of the samples. The higher TiO_2 values (between 0.11 and 0.43 percent) were observed in the most silty (quartz) samples. All samples containing less than 20 percent SiO_2 have less than 0.10 percent TiO_2. MnO content was determined on all samples. Sample 7129 contained 0.22 percent. Three samples contained 0.05 to 0.06 percent MnO (7130, 7133, and 7138). All other samples contained less than 0.04 percent MnO.

The two columns on the far right in table 3 are values calculated from loss-on-ignition data and the CaO values. The "CaO in calcine" represents the weight percentage of the CaO in the sample after being heated to 1000° C. The $CaCO_3$ values refer to the oven-dried sample.

For the marls, the silica (SiO_2) content ranges from nil to 55.6 percent. Approximately half the samples of marls have less than 8 percent silica. Alumina values in the marls range from 0.03 to 6.79 percent. Of 38

TABLE 2 — MINERALOGY OF MARLS

Sample number	Major	Minor*	Trace*
7126A	calcite	aragonite & quartz	—
7126F	calcite	—	aragonite
7127A	quartz	calcite & clay	feldspar
7127B	quartz	clay	feldspar
7127C	quartz	clay & dolomite	calcite
7127D	calcite	—	—
7128A	calcite	quartz	—
7128B	calcite	—	—
7129	calcite	quartz	—
7130	calcite & quartz	—	dolomite
7131A	calcite	quartz	aragonite & feldspar
7131B	calcite	quartz	feldspar
7131C	quartz & calcite	dolomite & feldspar	clay
7132A	calcite	—	feldspar (?)
7132B	calcite	—	—
7132C	calcite	—	—
7132D	calcite	—	—
7133	calcite	—	—
7134A	calcite	quartz	pyrite
7135	calcite	—	—
7136	calcite & quartz	dolomite	feldspar (?)
7137	calcite	quartz	—
7138	calcite	—	quartz & aragonite
7139	calcite	quartz	—
7140	calcite	—	quartz
7141	calcite	—	quartz, dolomite, & aragonite
7142	calcite	—	quartz & dolomite
7143	calcite	—	aragonite, quartz, & dolomite
7144A	calcite	quartz	dolomite
7145A	calcite	—	quartz
7146A	calcite	quartz	feldspar
7147A	calcite	quartz	—
7148	calcite	gypsum	—
7149A	calcite	—	quartz
7149B	calcite	—	aragonite
7150	calcite	quartz	dolomite & feldspar
7151A	calcite	—	—
7151B	calcite	quartz	dolomite & pyrite
7151C	calcite	—	quartz
7152	calcite	quartz	aragonite
7154	calcite	quartz	aragonite
7155	calcite	quartz	aragonite
7156	calcite & quartz	—	aragonite & feldspar
7157A	calcite	quartz	aragonite
7157B	calcite	—	quartz, aragonite, & dolomite
7157C	calcite	—	quartz
7157D	calcite	quartz	dolomite
7158	calcite	—	quartz & aragonite
7159	calcite	—	—
7160	calcite & quartz	dolomite	aragonite
7161	quartz	calcite, dolomite, & feldspar	aragonite & clay
7162A	calcite	quartz	aragonite
7162B	calcite	—	quartz, argonite, & feldspar
7162C	calcite	—	dolomite (?)
7162D	calcite	quartz & aragonite	feldspar (?)
7163A	calcite	aragonite & quartz	dolomite & pyrite
7163B	calcite	aragonite	quartz
7163C	calcite	aragonite & quartz	dolomite
7163D	calcite	quartz & aragonite	dolomite
7217	calcite	quartz	limonite & magnetite

*Dash indicates that no minor and/or trace minerals were observed.

TABLE 3 — CHEMICAL ANALYSES OF MARLS
(Analyses by Analytical Chemistry Section, Illinois State Geological Survey)

Sample number	SiO_2	Al_2O_3	Fe_2O_3	MgO	CaO	Na_2O	K_2O	H_2O+	CO_2	SO_3	Organic carbon	CaO in calcine	$CaCO_3$
7126A	2.46	1.09	0.77	1.36	49.4	0.051	0.46	2.03	40.97	0.06	0.96	88.2	88.2
7128B	2.34	1.13	0.27	nil	50.5	0.047	0.12	2.56	39.08	1.74	1.90	89.4	90.1
7129	26.9	5.91	1.57	1.62	38.1	0.147	0.40	2.59	18.24	0.18	2.83	49.9	68.0
7130	40.5	5.79	3.15	2.26	23.3	0.546	1.20	0.03	19.84	0.36	2.53	30.0	41.6
7131B	13.5	2.13	0.89	1.33	40.2	0.331	0.49	2.79	33.15	0.28	3.72	66.6	71.7
7132D	1.21	0.28	0.13	0.03	51.7	0.027	0.05	1.71	40.89	1.20	1.56	92.7	92.3
7133	1.59	0.51	0.16	0.53	51.5	0.041	0.10	1.39	40.17	1.70	1.24	90.0	91.9
7134A	4.33	1.08	0.47	0.64	49.01	0.091	0.15	4.22	36.94	0.15	1.65	85.5	87.5
7135	0.28	0.15	0.12	0.38	47.98	0.030	0.04	5.19	36.50	1.48	6.29	92.4	85.7
7137	1.38	0.47	0.40	0.19	52.7	0.019	0.24	1.61	41.09	0.30	0.40	92.6	94.1
7138	0.43	0.23	0.36	1.18	51.3	0.023	0.03	1.88	41.61	0.12	1.74	93.7	91.6
7139	10.6	2.16	1.05	1.16	42.76	0.186	0.34	1.64	34.50	1.97	2.50	69.7	76.4
7140	0.85	0.08	0.25	1.36	50.9	0.025	0.01	1.88	41.78	0.06	1.65	93.1	90.8
7141	1.70	0.89	0.58	1.75	46.2	0.065	0.06	4.14	37.30	0.13	6.82	87.6	82.5
7142	1.40	0.22	0.66	1.27	49.2	0.037	nil	2.93	39.78	0.23	2.99	90.6	87.8
7143A	0.32	0.12	0.49	1.18	51.1	0.025	0.02	2.91	40.40	0.15	2.99	95.2	91.2
7144A	4.85	0.73	0.54	0.99	47.5	0.103	0.06	2.40	37.98	0.13	3.49	84.6	84.8
7145A	1.53	0.44	0.77	1.46	48.03	0.055	0.02	4.17	37.99	0.12	4.30	89.7	85.7
7146A	9.95	1.38	0.95	1.25	41.02	0.166	0.17	5.33	32.45	0.57	5.91	72.8	73.2
7149A	0.41	0.17	0.13	1.69	52.2	0.030	nil	1.25	42.55	0.07	0.64	94.0	93.2
7149B	0.83	0.12	0.17	1.58	50.59	0.030	nil	2.21	41.69	0.18	1.57	92.8	90.3
7150	7.99	0.83	0.47	1.16	46.6	0.054	0.06	1.82	38.24	0.06	1.48	79.7	83.2
7151A	0.55	0.24	0.99	1.01	41.7	0.044	0.02	9.32	31.56	0.55	13.24	90.9	74.4
7151B	2.83	0.19	1.23	1.33	47.69	0.034	nil	3.10	37.56	0.39	4.86	87.5	85.1
7151C	1.80	0.03	0.42	1.38	49.7	0.036	0.01	2.14	40.99	0.19	2.07	90.7	88.7
7152	1.17	0.34	0.20	1.80	50.3	0.036	nil	1.68	41.77	0.08	1.45	91.3	89.8
7155	7.82	0.15	0.10	1.33	46.24	0.108	0.10	2.40	37.89	0.05	2.65	81.0	82.5
7156	35.4	4.19	1.09	1.65	26.16	0.048	0.65	3.84	20.99	0.06	4.77	37.2	46.8
7157A	12.9	2.27	0.85	1.08	42.26	0.196	0.27	2.20	34.32	0.03	2.24	69.0	75.5
7158	6.42	0.66	0.65	3.05	44.86	0.164	0.07	3.01	36.95	0.27	2.94	78.6	80.1
7159	8.88	0.77	0.66	2.26	41.0	0.140	0.01	4.03	34.00	0.20	7.89	75.8	73.2
7160	48.7	6.79	2.46	3.69	17.08	0.701	0.99	1.88	16.43	0.12	0.85	21.1	30.5
7161	55.54	6.52	2.83	1.62	12.55	0.890	1.14	4.27	10.67	nil	3.20	15.3	22.4
7162A	17.6	4.54	1.43	1.52	35.8	0.227	0.39	4.17	29.06	0.62	4.45	57.4	63.9
7162B	8.45	1.41	1.48	1.55	40.7	0.129	0.26	5.88	31.88	0.24	6.64	73.2	72.6
7162C	3.43	0.43	0.86	1.07	48.13	0.046	0.07	2.87	39.24	0.16	2.57	87.0	85.8
7162D	22.0	3.72	2.02	1.47	29.98	0.238	0.48	7.75	23.14	0.61	8.50	49.5	53.5
7163A	14.4	1.55	1.13	0.9	40.6	0.25	0.28	3.27	32.84	0.09	3.89	67.7	72.5
7163B	6.74	0.98	1.11	1.07	44.7	0.13	0.21	3.10	36.32	0.35	4.44	79.6	79.8
7163C	10.88	1.87	2.11	2.99	38.8	0.10	0.57	4.07	33.65	0.27	4.00	66.6	69.3
7163D	12.39	1.86	1.29	1.81	40.3	0.11	0.53	2.78	33.10	1.07	4.34	67.3	71.9
7217	19.6	1.38	0.20	nil	42.34	0.12	0.27	1.82	32.97	nil	0.05	63.8	75.6

samples of marl analyzed, 23 contain less than 0.89 percent Al_2O_3. It is estimated that one-fourth to three-fourths of the alumina occurs in silt-size feldspar grains and that the remaining trace amounts are in clay minerals. Few marls contain more than 0.15 percent Na_2O, probably present in clays. The MgO occurs mainly in dolomite grains detected in many marls. Most marls contained from 1 to 6 percent organic carbon, but one sample (7151A) had more than 13 percent.

Moisture-Density Relations of Marls

To evaluate the possibility of successfully predicting the pore structure and surface area of marls and/or other important properties related to the reactivity of marls and their calcines with SO_2, a density measurement was deemed important. Because marls are fine grained and have soil-like properties and most marl deposits under exploitation contain about 50 percent water before being excavated, a moisture-density relations test (commonly called the "Standard Proctor Test") was thought to be useful. Because of the small quantity of sample available, the miniaturized Proctor test—the Harvard compaction test (Wilson, 1970)—was selected and was run on most of the marls. The results are listed in table 4. The optimum dry density and corresponding moisture content were taken from the maximum point of a density versus moisture curve determined for each sample. Preliminary evaluation of these results indicates that samples with low density have high pore volumes and high organic carbon and H_2O contents.

TABLE 4 — HARVARD MINIATURE COMPACTION TEST RESULTS OF MARLS

Sample	Optimum density (g/cm^3)	Moisture content (%)
7132D	1.20	38
7133	1.17	36
7134A	1.17	44
7137	1.57	24
7140	1.17	41
7141	0.99	53
7142	1.03	53
7144A	1.04	51
7145A	0.91	60
7146A	0.91	58
7149B	1.07	48
7150	1.25	38
7153	1.23	38
7157A	1.23	38
7158	0.99	57
7159	0.96	54
7163C	0.96	56

Results and Discussion of Pore Structures and Surface Areas of Marls and Their Calcines

Pore Structures and Surface Areas of Marls

For a majority of the samples, only the 16x18-mesh size fraction of particles was tested. However, for selected samples, other size fractions were also tested. The pore-structure data are summarized in table 5.

The pore volumes of the lake and bog marls range from 0.21 to 1.08 cc/g, with a majority of the values in the 0.3 to 0.6 cc/g range. The pore volumes of the tufaceous marls are on the low end of the pore-volume range for marls. Variation in pore volume exists between samples of marls taken from the same deposit, especially 7126, 7131, 7151, 7157, and 7162. These differences are probably due to the variations in contents of quartz and organic matter.

The mean pore-size values (0.47μ to 5.80μ) vary significantly between the samples tested—in some cases, even between samples from the same deposit. The size of the pores in the marls is rather evenly distributed from 0.1μ to larger than 10μ in diameter. The average of the mean pore sizes of the lake and bog marls is 1.7μ.

With the exception of marls 7129 and 7132D, the pore volume of the 170x200-mesh particles is less than that of the 16x18-mesh particles, as expected. It is possible that the pore volumes listed for 170x200-mesh particles of 7129 and 7132D still contain appreciable void space volume and/or that the pore volumes of the 16x18-mesh particles are low.

The estimated average pore size for the 170x200-mesh particles is less than the mean pore size calculated for the 16x18-mesh particles of the same sample except in sample 7132D. The larger pores (>15μ) present in the 16x18-mesh particles shift the mean pore size to a higher value, but these large pores are not detected in measurements of the smaller particles.

The surface area values for the marl samples are given in table 6.

Pore Structure and Surface Area of Calcined Marl

A few of the samples, the pore structures of which were determined, were not calcined as part of the calcination tests. The samples eliminated from the calcination test program are of low purity (<70 percent $CaCO_3$ content), and all contain in excess of 20 percent quartz.

16x18-Mesh Particles

Pore-volume and surface-area data for the 16x18-mesh fraction of marls and their calcines (850° C) are given in table 6. The calcine pore-volume and surface-area data were determined on calcined marl samples, but the values in table 6 are reported in terms of "per g (gram) marl" used to prepare

TABLE 5 — PORE VOLUMES AND MEAN PORE SIZES OF MARLS

Sample number	Mesh size (U.S.)	Pore volume (cc/g)	Mean pore size (μ)	Standard deviation (μ)
7126A	16x18	0.2325	1.65	0.09
7126A	170x200	0.1500	0.60*	—
7126B	16x18	0.3720	5.80	0.13
7127A	16x18	0.1740	0.43	0.16
7127B	16x18	0.1235	0.16	0.16
7127C	16x18	0.1375	0.16	0.16
7127D	3 pieces	0.2880	4.21	0.12
7127D	16x18	0.2505	1.43	0.19
7128A	16x18	0.1990	1.51	0.15
7128B	16x18	0.2080	1.43	0.20
7128B	170x200	0.2000	1.00*	—
7129	16x18	0.1385	1.38	0.17
7129	170x200	0.2100	0.60*	—
7130	16x18	0.2735	0.81	0.37
7131A	16x18	0.5745	0.50	0.45
7131B	16x18	0.5700	0.57	0.33
7131C	16x18	0.2335	0.35	0.28
7132A	40x50	0.4535	0.84	0.38
7132B	40x50	0.3995	3.45	0.22
7132C	16x18	0.4865	0.87	0.26
7132D	1 piece	0.4667	0.58	0.28
7132D	16x18	0.3805	0.86	0.24
7132D	170x200	0.5680	2.00*	—
7133	1 piece	0.3904	3.13	0.23
7133	16x18	0.3150	4.44	0.15
7133	170x200	0.0700	1.00*	—
7134A	16x18	0.4905	1.21	0.42
7135	16x18	0.5740	1.63	0.18
7137	16x18	0.2770	0.47	0.23
7138	16x18	0.5440	1.28	0.27
7139	16x18	0.5225	1.31	0.37
7140	16x18	0.4840	1.34	0.34
7141	16x18	0.6725	1.72	0.22
7142	16x18	0.5505	1.22	0.38
7143A	16x18	0.5750	1.68	0.18
7144A	16x18	0.5545	1.27	0.36
7145A	16x18	0.6250	1.07	0.27
7146A	16x18	0.5435	0.69	0.26
7147A	16x18	0.6189	1.12	0.31
7148	16x18	0.1260	4.26	0.11
7149A	16x18	0.4099	4.85	0.14
7149B	16x18	0.5808	2.14	0.21
7150	1 piece	0.4658	1.25	0.45
7150	16x18	0.4724	1.30	0.24
7150	170x200	0.2500	0.80*	—
7151A	16x18	0.5997	2.58	0.23
7151B	16x18	0.5732	1.15	0.33
7151C	16x18	0.4460	0.78	0.51
7152	16x18	0.3995	1.07	0.32
7154	16x18	0.6390	3.22	0.17
7155	16x18	0.4205	2.25	0.15
7156	16x18	0.4580	1.93	0.24
7157A	16x18	0.3670	1.38	0.29
7157B	16x18	0.3580	0.60	0.42
7157C	16x18	0.5000	0.90	0.38
7157D	16x18	0.4005	0.70	0.29
7158	16x18	0.5045	1.02	0.26
7159	16x18	0.6220	1.28	0.33
7160	16x18	0.2190	2.06	0.16
7161	16x18	0.2135	0.83	0.26
7162A	1 piece	0.7942	5.65	0.22
7162A	16x18	0.5125	2.98	0.15
7162A	170x200	0.3200	1.50*	—
7162B	16x18	1.0780	3.98	0.19
7162C	16x18	0.9340	3.10	0.24
7162C	40x50	0.7825	2.66	0.17
7162C	170x200	0.3200	1.50*	—
7162D	16x18	0.7450	3.38	0.16
7163A	16x18	0.7750	1.70	0.17
7163C	16x18	0.5910	2.64	0.19
7163C	170x200	0.3400	0.80*	—
7163D	3 pieces	0.8311	2.72	0.16
7163D	16x18	0.7190	2.44	0.15

*An estimated mean pore size.

TABLE 6 — PORE STRUCTURES AND SURFACE AREAS OF MARLS AND THEIR CALCINES (16x18 MESH PARTICLES)

Sample number	Marl					Calcined marl				
	Type	Pore volume (cc/g)	Mean pore size (μ)	Standard deviation (μ)	Surface area (m^2/g)	Observed pore-volume increase* (cc/g marl)	Theoretical pore-volume increase** (cc/g marl)	Pores <0.1μ diameter†		Surface area (m^2/g marl)
								Pore volume (cc/g marl)	Average pore diameter (μ)	
7128B	Tufaceous bog marl	0.208	1.43	0.20	—	0.202	0.180	?	0.06	5.2
7131B	Bog marl	0.570	0.57	0.33	—	0.194	0.143	0.150	0.045	11.1
7132D	Bog marl	0.380	0.86	0.24	3.8	0.258	0.184	0.155	0.05	11.0
7133	Tufaceous bog marl	0.315	4.44	0.15	0.8	0.245	0.184	0.180	0.07	8.5
7134A	Lake marl	0.490	1.21	0.42	—	0.169	0.175	0.150	0.043	12.7
7135	Bog marl	0.574	1.63	0.18	—	0.196	0.171	0.145	0.05	13.7
7137	Bog marl	0.277	0.47	0.23	—	0.207	0.188	?	0.10	5.3
7138	Lake marl	0.544	1.28	0.27	4.4	0.244	0.183	0.150	0.05	10.3
7139	Bog marl	0.522	1.31	0.37	—	0.146	0.153	0.120	0.035	13.2
7140	Lake marl	0.484	1.34	0.34	2.7	0.232	0.182	0.165	0.04	14.3
7141	Bog marl	0.672	1.72	0.22	—	0.172	0.165	0.135	0.044	13.7
7142	Lake marl	0.550	1.22	0.38	—	0.189	0.176	0.150	0.044	12.1
7143A	Bog marl	0.575	1.68	0.18	—	0.185	0.182	0.150	0.044	14.3
7144A	Lake marl	0.554	1.27	0.36	—	0.188	0.170	0.145	0.04	13.8
7145A	Lake marl	0.625	1.07	0.27	—	0.261	0.172	0.110	0.044	12.3
7146A	Lake marl	0.543	0.69	0.26	—	0.145	0.146	0.090	0.035	16.2
7149A	Bog marl	0.410	4.85	0.14	2.1	0.168	0.187	0.160	0.04	15.7
7149B		0.581	2.14	0.21	—	0.135	0.182	0.145	0.037	14.6
7150	Lake marl	0.472	1.30	0.24	3.9	0.088	0.167	0.140	0.04	13.4
7151A		0.600	2.58	0.23	—	0.160	0.149	0.120	0.03	31.0
7151B	Bog marl	0.573	1.51	0.33	—	0.193	0.170	0.155	0.04	14.2
7151C		0.446	0.78	0.51	—	0.173	0.178	0.170	0.044	12.2
7152	Bog marl	0.400	1.07	0.32	—	0.210	0.179	0.160	0.037	15.8
7155	Lake marl	0.420	2.25	0.15	—	0.258	0.165	0.130	0.037	13.0
7157A	Lake marl	0.367	1.38	0.29	—	0.163	0.155	0.125	0.035	12.5
7158	Lake marl	0.504	1.02	0.26	5.2	0.194	0.161	0.120	0.037	14.2
7159	Bog marl	0.622	1.28	0.33	—	0.212	0.147	0.140	0.045	14.9
7162C	Bog marl	0.934	3.1	0.24	6.8	0.094	0.172	0.100	0.04	13.6
7163A		0.775	1.7	0.17	—	0.119	0.146	0.110	0.032	15.3
7163C	Bog marl	0.591	2.64	0.19	5.2	0.201	0.139	0.105	0.035	14.1
7163D		0.719	2.44	0.15	—	0.140	0.144	0.110	0.035	14.0

*Column 4 minus column 1. **Based on $CaCO_3$ content of rock sample, assuming no shrinkage of $CaCO_3$ grains on calcination. †Calculated from the less than 0.1μ portion of the pore volume versus pore size graph.

the calcines in order that direct comparisons between the calcine data and the marl data could be made. It would not be correct to compare the calcine data on a "per g calcine" basis with the marl data on a "per g marl" basis since, of course, 1 g of marl produces less than 1 g of calcine, depending in part on the $CaCO_3$ content of the marl. The calcine pore-volume and surface-area data in table 6 can easily be converted from "per g marl" to "per g calcine" by multiplying the values given by $100/[100 - (\%H_2O + \%CO_2 + \%SO_3 + \%\text{Org. C})]$. These percentages can be found in table 3.

Pore-volume curves for marls 7132D, 7149A, 7137, and their calcines are shown in figures 10, 11, and 12. The pore-volume curves for marl 7132D and its calcine (fig. 10) are typical of those obtained for most of the marl samples. The second step on the calcine pore-volume curves (figs. 10 and 11) is interpreted as resulting from creation of new pores by calcination of the $CaCO_3$ in the marls. The vertical displacement of the calcine pore-volume curve for marl 7132D (fig. 10) from the marl pore-volume curve cannot be attributed to any one factor but is probably due to loss of volatile impurities on calcination, opening of any closed pores, and other unknown factors. The lack of vertical displacement of the calcine pore-volume curve for marl 7149A (fig. 11) from the marl pore-volume curve can be attributed, in part, to a lower content of volatile impurities in the marl. Marl 7137 is a unique sample in that no fine pores less than 0.1μ in diameter are seen in the calcine pore-volume curve (fig. 12). On the basis of chalk calcination test results to be discussed later, it appears that in marl 7137, which contains very fine pores, calcination results in the enlargement of those pores as opposed to the creation of new pores.

The theoretical pore-volume increase on calcination of pure nonporous $CaCO_3$ (Iceland spar) is simply the result of CO_2 loss; however, some particle shrinkage usually occurs on calcination and hence, the actual increase in pore volume on calcination of $CaCO_3$ is usually less than the theoretical increase. The amount of particle shrinkage will depend upon the harshness of calcination conditions, with the limit being a dead-burned nonporous calcine. The calcination conditions used in the present study are fairly mild and produce a porous calcine. For typical samples, which are porous and somewhat impure, the pore-volume increase on calcination and calcine pore structure will depend upon loss of any volatile impurities present (such as moisture) and CO_2, opening of any closed pores, and particle shrinkage. Pore-volume increase can be larger or smaller than the theoretical increase based on $CaCO_3$ content only. The theoretical pore-volume increase due to calcination, assuming no particle shrinkage and based on the $CaCO_3$ analyses (table 3), was calculated* and is included in table 6. The increase in pore volume on calcination of the marls was computed from measured data by two methods. In the first method, it was assumed that the increase in pore volume was simply the difference between the total pore volumes of the calcined and uncalcined marl. In the second method, the increase in pore volume was computed from the second step of the calcine pore-volume curve.

* 1 g pure $CaCO_3 \rightarrow 0.56$ g CaO. On the basis of densities of 2.71 g/cc for $CaCO_3$ and 3.32 g/cc for CaO, one obtains the theoretical volumes of 0.369 cc/(g of $CaCO_3$) and 0.169 cc/(0.56 g of CaO) and hence, 0.200 cc increase in pore volume when 1 g of pure $CaCO_3$ is calcined. For impure samples, the theoretical pore volume increase per g rock is $0.200 \times \%CaCO_3/100$.

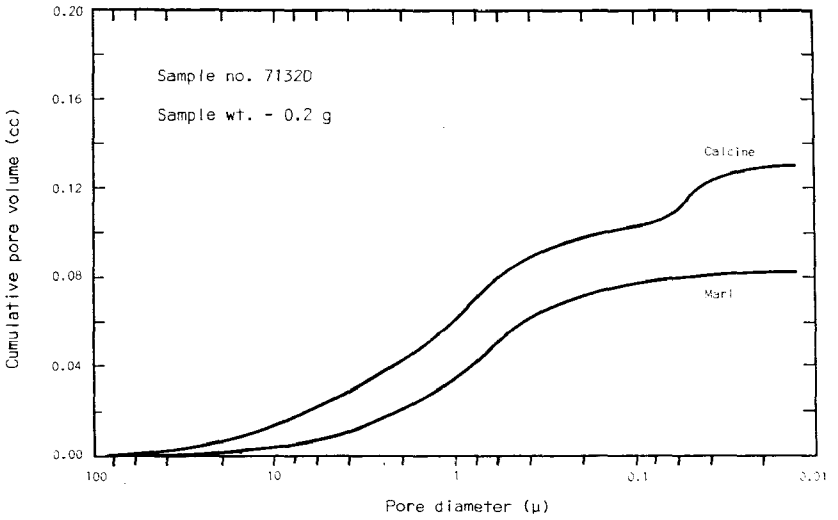

Fig. 10 - Pore-volume curves for 16x18 mesh particles of bog marl 7132D and its calcine.

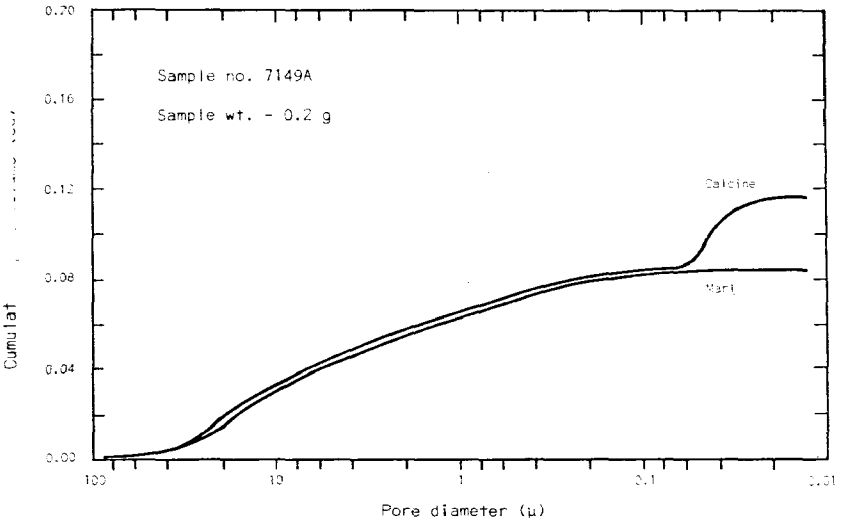

Fig. 11 - Pore-volume curves for 16x18 mesh particles of bog marl 7149A and its calcine.

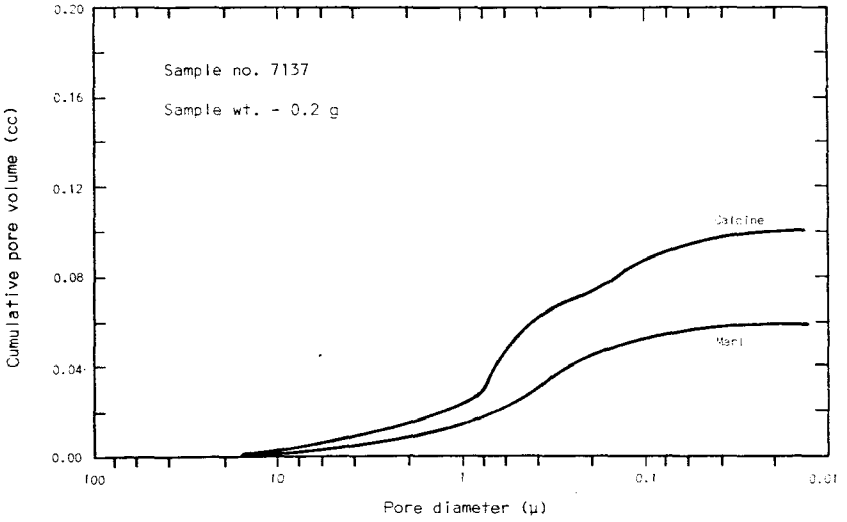

Fig. 12 - Pore-volume curves for 16x18 mesh particles of bog marl 7137 and its calcine.

The pore-volume increase of the marls (16x18-mesh) on calcination (at 850° C), computed from total pore volumes, ranges from 0.094 to 0.261 cc/g marl; in the majority of the samples, the increase is between 0.18 and 0.22 cc/g marl. The pore-volume increase computed from the second step of the calcine pore-volume curve ranges from 0.09 to 0.180 cc/g marl. The theoretical pore-volume increase ranges from 0.143 to 0.188 cc/g marl. A sample-by-sample comparison of the data in table 6 shows that the pore-volume increase determined from total pore volumes is usually higher than the theoretical increase, while all values calculated from the second step of the calcine pore-volume curves are slightly lower than the theoretical values. Thus, the interpretation that the second step of the calcine pore-volume curves is due to calcination of $CaCO_3$ is correct. However, it is impossible to say specifically why considerable variations in the actual pore-volume increase on calcination are obtained.

Electron micrographs of marls 7151A and 7150 calcined at 850° C are shown in plate 5A and 5B. The CaO grains, about 0.2μ to 7μ in diameter, are aggregated into particles about 2μ to 7μ across. These particles likely were derived from individual calcite grains (up to 7μ) in the original marls. The largest pores observed are those existing in the uncalcined marls. The very fine pores (<0.1μ in diameter) are within the particles composed of the very fine CaO grains.

The surface areas of the marls are indicative of the fine grains present in the marls and show that very fine pores do not exist to any appreciable extent in the marls. The surface areas of the marl calcines are greater than those of the marls as a result of the creation of fine pores within the $CaCO_3$ grains by calcination. Also, surface area and pore volume are created by removal of the volatile impurities by calcination. Presumably some of the carbon in the organic matter remains in the calcines and adds surface area to the calcines. The surface area, 31.0 m^2/g marl, for sample 7151A can be attributed only to the sample's high (13.4 percent) organic carbon content.

Data in table 7 illustrate the effect of different calcination conditions on pore structures of calcined 16x18-mesh marl particles. With the exception of marl 7162C, only small changes in the total calcine pore volume are observed here. An appreciable fraction of the 16x18-mesh particles of marl 7162C disintegrated when calcined at 950° C, thereby decreasing the total pore volume in the calcine. The pore-volume curves for five different calcination conditions are given for marls 7133, 7150, and 7162C in figures 13, 14, and 15. Simply increasing the calcination temperature from 850° C to 950° C has only a small effect, if any, on the pore-size distribution. The addition of 10 percent carbon dioxide to the nitrogen gas stream promotes growth of the CaO grains and a corresponding widening of the fine pores created during the calcination process. Longer calcination times of 60 minutes under both the pure nitrogen and the 10 percent carbon dioxide-90 percent nitrogen gas streams usually resulted in further widening of the fine pores. The large pores existing in the marl were usually not affected either by raising the calcination temperature to 950° C or by increasing the total calcination time to 60 minutes.

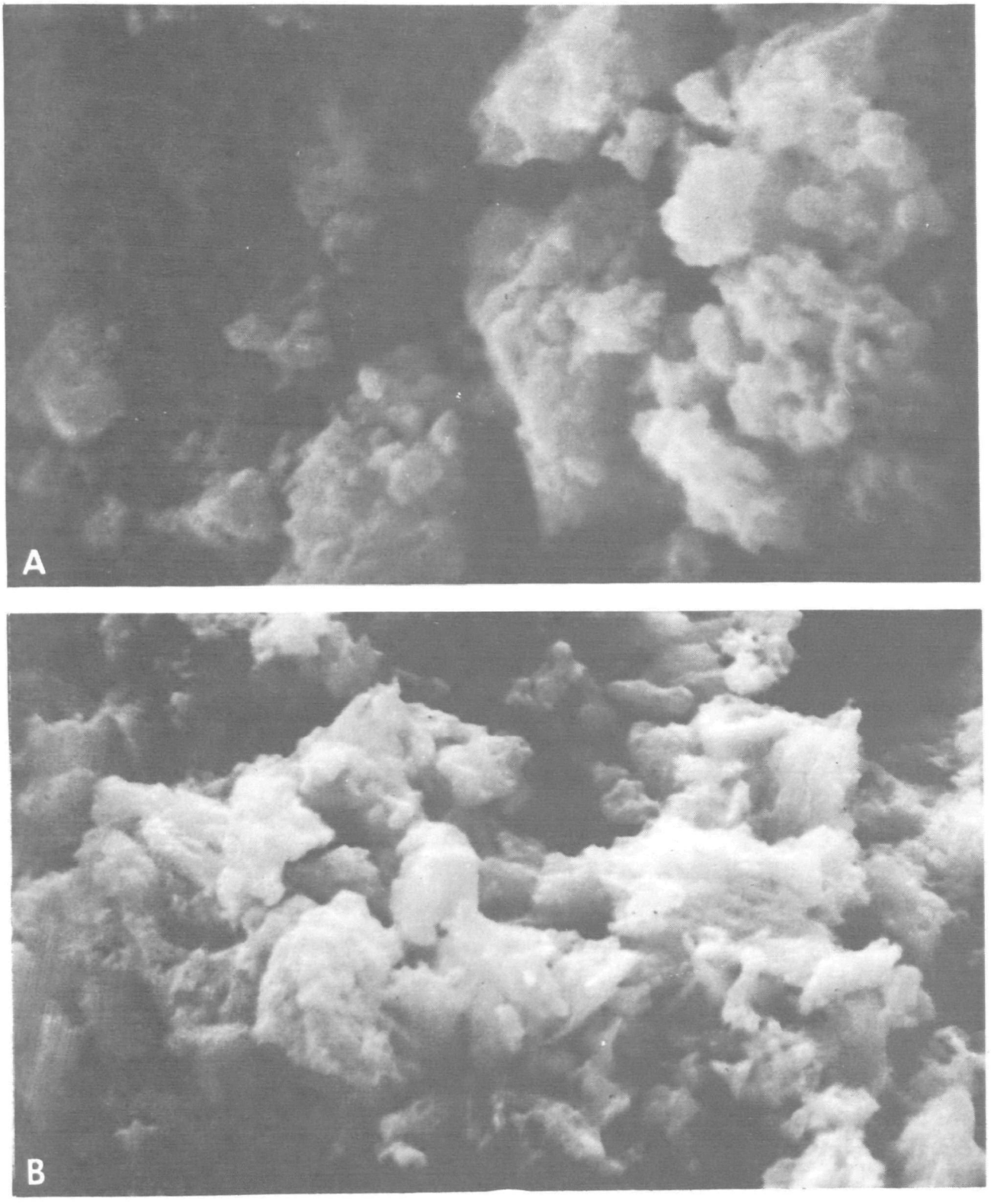

Plate 5 - Typical textural features of lime in calcined marl; A. marl sample 7150 (x 10,100), B. marl sample 7151A (x 4400).

TABLE 7 — EFFECT OF CALCINATION CONDITIONS ON CALCINE PORE STRUCTURE AND SURFACE AREA OF 16x18 MESH PARTICLES OF MARL

Sample number	Calcination conditions*	Calcine pore volume (cc/g marl)	Pore-volume change on calcination** (cc/g marl)	Average diameter of pores created by calcination (μ)	Surface area (m^2 g marl)
7132D	(a)	0.638	0.258	0.05	11.0
	(b)	0.646	0.266	0.06	7.1
7144A	(a)	0.742	0.188	0.04	13.8
	(b)	0.723	0.169	0.04	11.4
7145A	(a)	0.886	0.261	0.044	12.3
	(b)	0.755	0.135	0.05	8.7
7149A	(a)	0.578	0.168	0.04	15.7
	(b)	0.588	0.178	0.04	12.1
7133	(a)	0.560	0.245	0.07	8.5
	(b)	0.543	0.228	0.08	5.5
	(c)	0.540	0.225	0.13	3.4
	(d)	0.529	0.214	0.10	4.7
	(e)	0.594	0.279	0.30	1.6
7150	(a)	0.560	0.088	0.04	13.4
	(b)	0.544	0.072	0.04	10.6
	(c)	0.587	0.115	0.08	4.7
	(d)	0.513	0.041	0.08	3.7
	(e)	0.523	0.051	0.20	1.8
7162C	(a)	1.028	0.094	0.04	13.6
	(b)	0.948	0.014	0.05	9.6
	(c)	0.892	-0.042	0.13	3.3
	(d)	0.710	-0.224	?	1.8
	(e)	0.758	-0.176	?	1.3

*Calcination conditions are as follows:
(a) 850°C, about 7 min., 100% N_2 stream
(b) 950°C, about 4 min., 100% N_2 stream
(c) 950°C, 10 min., 10% CO_2-90% N_2 stream
(d) 950°C, 60 min., 100% N_2 stream
(e) 950°C, 60 min., 10% CO_2-90% N_2 stream

**Calculated from calcine pore volume and marl pore volume.

The effect of different calcination conditions on the calcine surface area of 16x18-mesh particles can be seen in table 7. Calcination at 950° C under pure nitrogen lowers the surface areas of the calcines 10 to 40 percent from the values at 850° C. Calcination under a 10 percent carbon dioxide-90 percent nitrogen gas stream reduces the surface areas of the calcines even more. Further reduction in the surface areas of the calcines is observed for calcination times of 60 minutes at 950° C under either the pure nitrogen or the 10 percent carbon dioxide-90 percent nitrogen gas streams. The surface area values obtained at 950° C were generally between 1.7 and 8.5 m^2/g marl and those obtained at 850° C were between 8.5 and 16.0 m^2/g marl. However, inspection of these results in table 7 shows that the addition of 10 percent carbon dioxide to the gas stream has a much greater effect on the surface areas of the calcines than that brought about by simply raising the calcination temperature from 850° C to 950° C.

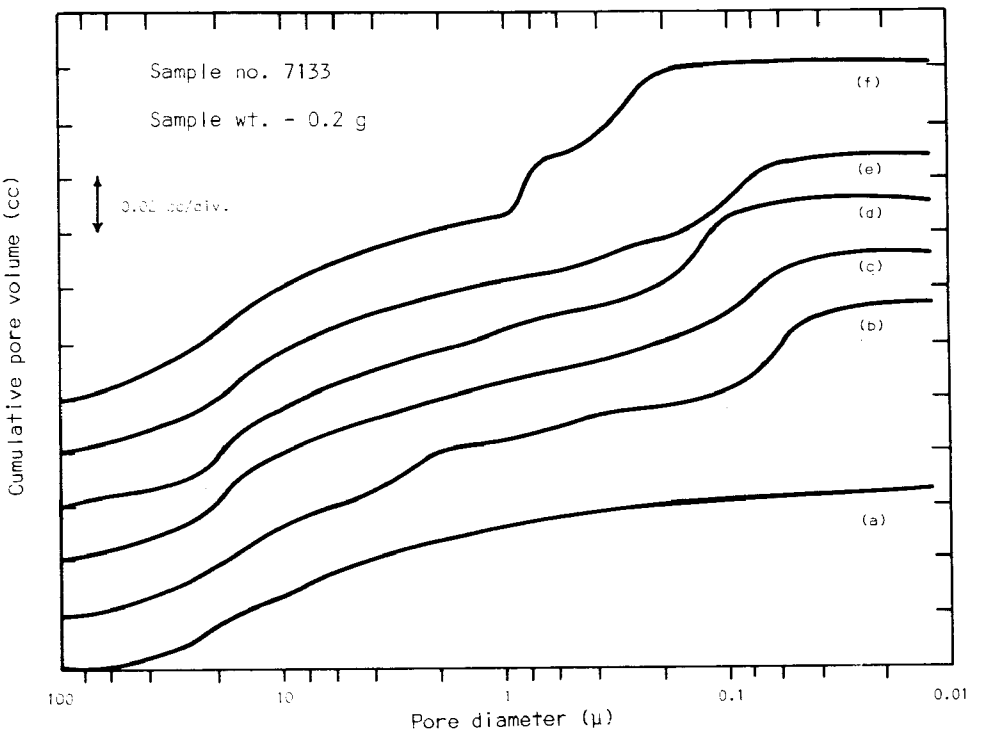

Fig. 13 - Pore-volume curves for 16x18 mesh particles of tufaceous bog marl 7133 (a) and its calcines (b-f). The calcination conditions are: (b) 850° C, about 7 min., 100% N_2 stream; (c) 950° C, about 4 min., 100% N_2 stream, (d) 950° C, 10 min., 10% CO_2-90% N_2 stream; (e) 950° C, 60 min., 100% N_2 stream; (f) 950° C, 60 min., 10% CO_2-90% N_2 stream.

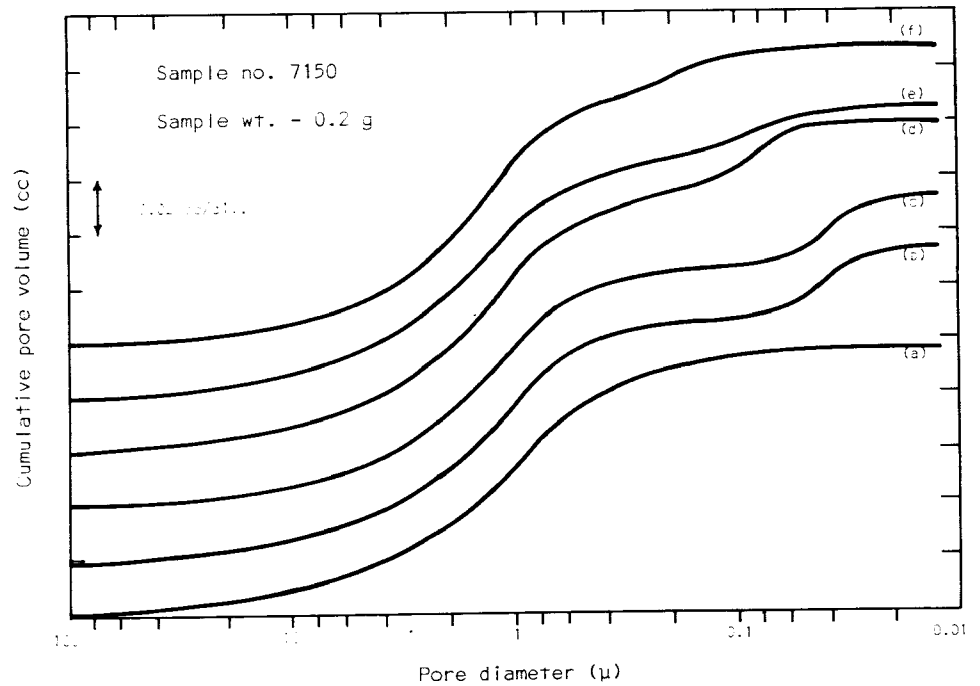

Fig. 14 - Pore-volume curves for 16x18 mesh particles of lake marl 7150 (a) and its calcines (b-f). The calcination conditions are: (b) 850° C, about 7 min., 100% N_2 stream; (c) 950° C, about 4 min., 100% N_2 stream, (d) 950° C, 10 min., 10% CO_2-90% N_2 stream, (e) 950° C, 60 min., 100% N_2 stream, (f) 950° C, 60 min., 10% CO_2-90% N_2 stream.

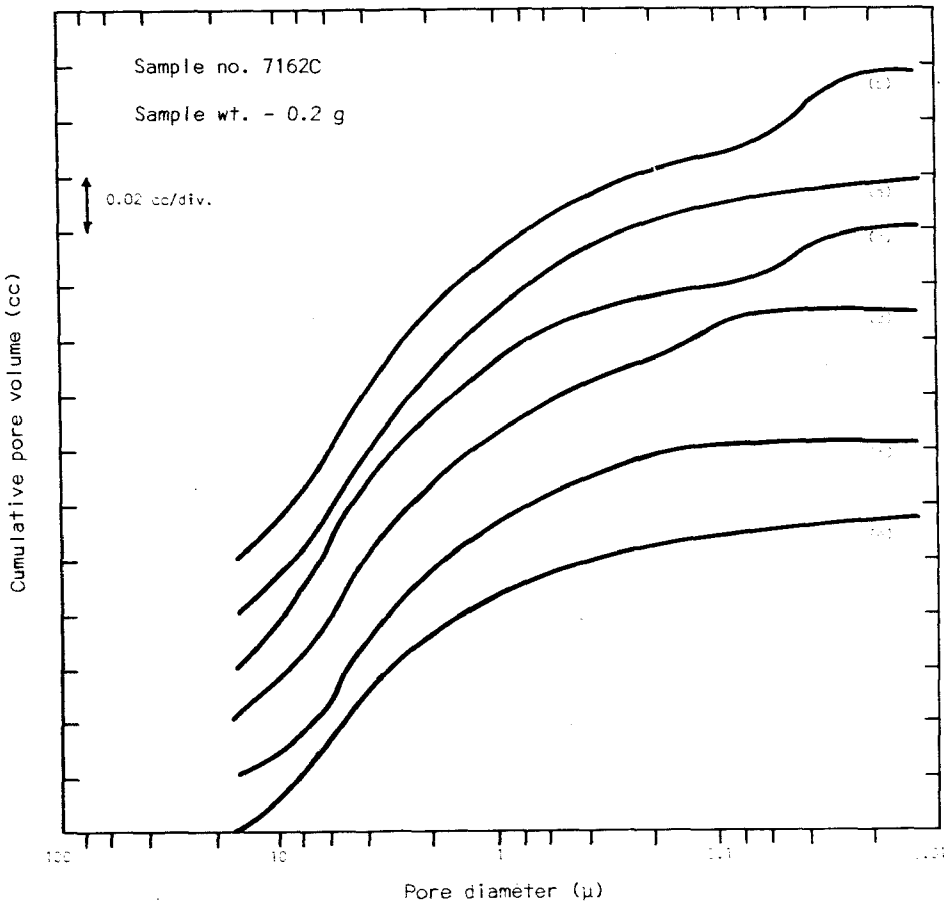

Fig. 15 - Pore-volume curves for 16x18 mesh particles of bog marl 7162C (a) and its calcines (b-f). The calcination conditions are: (b) 850° C, about 7 min., 100% N_2 stream; (c) 950° C, about 4 min., 100% N_2 stream; (d) 950° C, 10 min., 10% CO_2-90% N_2 stream; (e) 950° C, 60 min., 100% N_2 stream; (f) 950° C, 60 min., 10% CO_2-90% N_2 stream.

170x200-Mesh Particles

Table 8 summarizes the data on 170x200-mesh particles of marls calcined at 850° C. Corresponding data for 16x18-mesh particles have been included in table 8. Direct comparison of data for marls 7133, 7150, and 7162C shows that the pore structures (<0.1μ) and surface areas of the calcines are not appreciably dependent upon particle size.

Pore-volume and penetration-volume curves for a tufaceous marl (7133, fig. 16) and a lake marl (7150, fig. 17) show the close similarity in shape in the ≤0.1μ pore range for the 16x18- and 170x200-mesh particles and their calcines. Note that for the 170x200-mesh particle data, both the penetration-volume and void-volume curves are shown in figures 16 and 17 to illustrate the relative importance of the difference between pore volume and penetration volume of these fine-mesh particles. The penetration-volume curve for 170x200-mesh particles of tufaceous bog marl 7133 (fig. 16) is identical with the penetration-volume curve of its calcine in the 2.0μ to 0.1μ range, but the penetration-volume curve for 170x200-mesh particles of the lake marl 7150 (fig. 17) lies below the penetration-volume curve of its calcine. However, the

TABLE 8 — COMPARISON OF TEST RESULTS ON 16x18 AND 170x200 MESH PARTICLES OF MARL

Sample number	Mesh	Marl		Calcine					
		Pore volume (cc/g)	Average pore size (μ)	Pore volume (cc/g marl)	Pore-volume increase* (cc/g marl)	Theoretical pore volume** (cc/g marl)	Pores <0.1μ diameter†		Surface area (m^2/g marl)
							Pore volume (cc/g marl)	Average pore diameter (μ)	
7126A	16x18	0.232	1.65						
7126A	170x200	0.150	0.6	0.320	0.170	0.177	0.180	0.04	13.8
7133	16x18	0.315	4.44	0.560	0.245	0.184	0.180	0.07	8.5
7133	170x200	0.070	1.0	0.230	0.170	0.184	0.170	0.055	10.3
7150	16x18	0.472	1.30	0.560	0.188	0.167	0.140	0.04	13.4
7150	170x200	0.250	0.8	0.425	0.175	0.167	0.155	0.045	15.1
7162C	16x18	0.934	3.1	0.878	0.094	0.172	0.092	0.04	13.6
7162C	170x200	0.320	1.5	0.455	0.135	0.172	0.155	0.045	13.4

*Pore volume of calcine minus that of the marl.
**Based on $CaCO_3$ content of rock sample, assuming no shrinkage of $CaCO_3$ grains on calcination.
†Calculated from the less than 0.1μ portion of the pore volume versus pore-size curve.

pore-volume curve for 16x18-mesh particles of tufaceous bog marl 7133 (fig. 16) lies below the pore-volume curve of its calcine, but the pore-volume curve for 16x18-mesh particles of lake marl 7150 (fig. 17) is identical with the pore-volume curve of its calcine in the 100μ to 0.4μ range. It is not clear at this time why these slight differences between the curves are observed. Both figures were included to show some of the complexities in interpreting pore-volume and penetration-volume data.

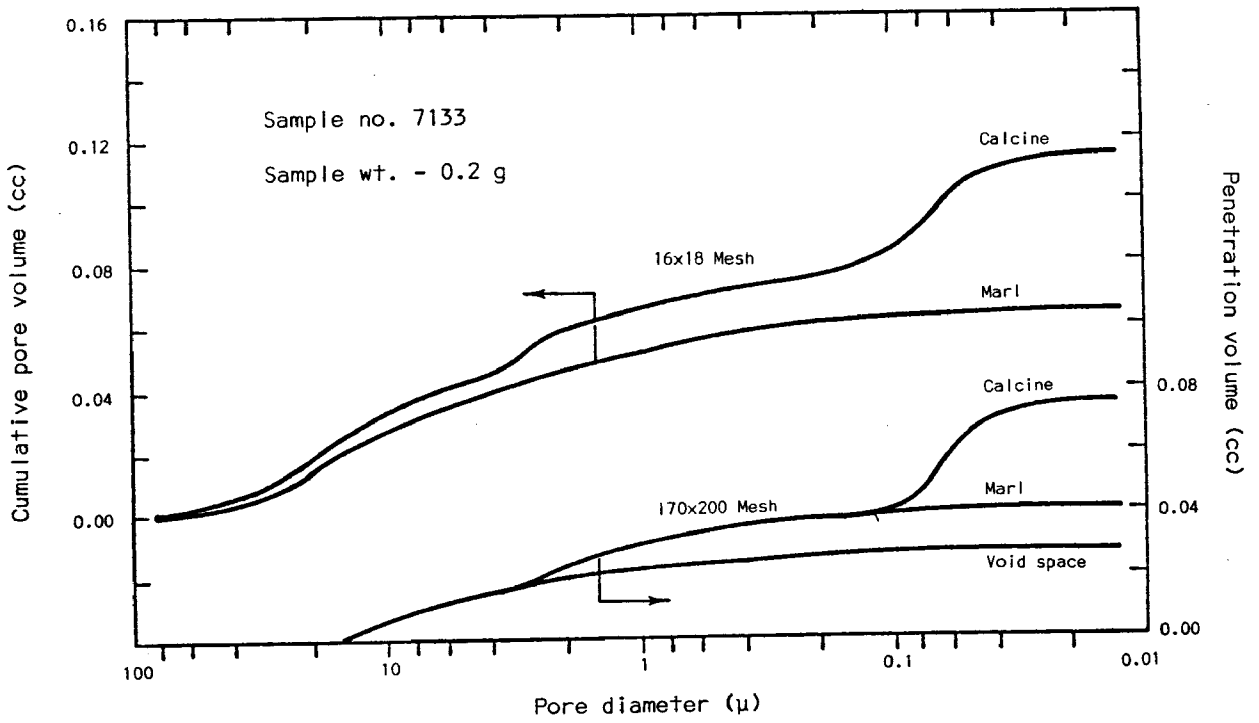

Fig. 16 - Pore-volume curves (left ordinate) for 16x18 mesh particles and penetration-volume curves (right ordinate) for 170x200 mesh particles of tufaceous bog marl 7133 and their calcines.

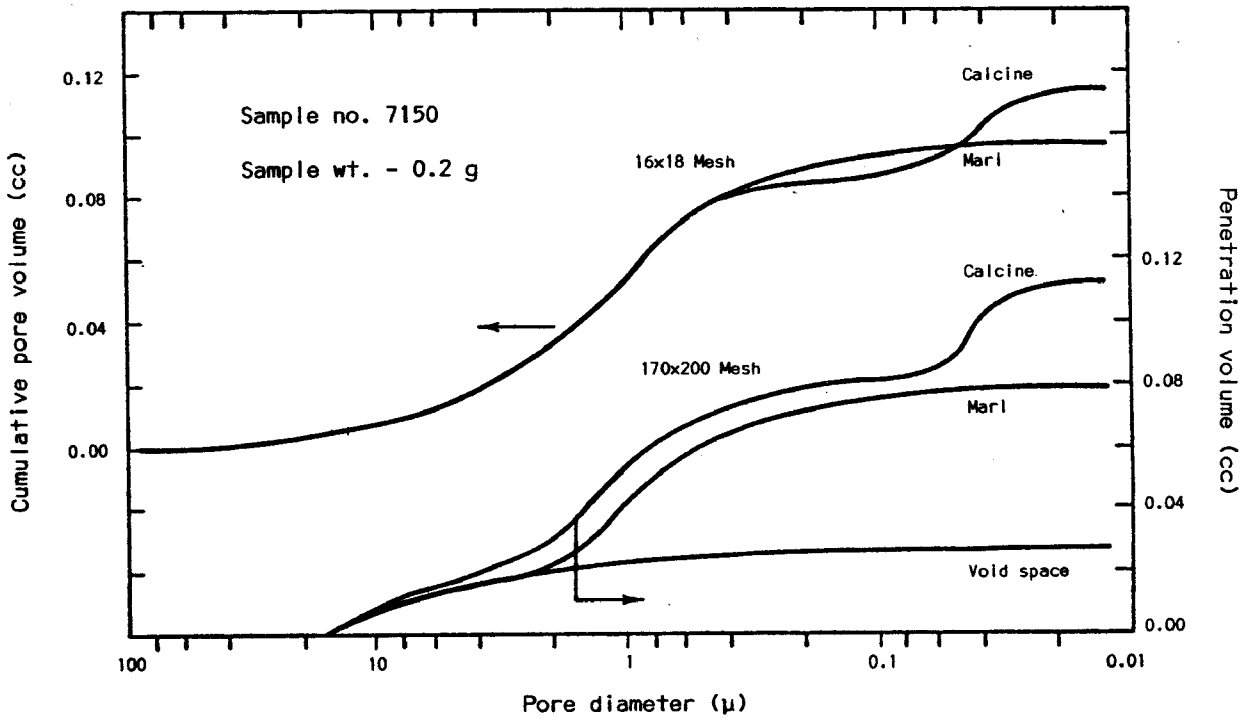

Fig. 17 - Pore-volume curves (left ordinate) for 16x18 mesh particles and penetration-volume curves (right ordinate) for 170x200 mesh particles of lake marl 7150 and their calcines.

CHALK INVESTIGATIONS

General Characteristics and Origin of Chalks

Chalk is a variety of fine-grained limestone that is especially porous, is partly incoherent, and is composed mainly of minute fossil fragments of coccolithophores. These unicellular organisms float in marine waters and secrete $CaCO_3$ platelets, called coccoliths, that cover the outer surface of the organism. The coccoliths are generally disc- or wheel-shaped and consist of 10 or more tabular crystallites of calcite interlocked to form a particle, generally 4μ to 12μ in diameter. Fragments of coccoliths and other very fine grained calcite (probably chemically precipitated in marine sea water) make up the bulk of chalk strata. Also important, however, are other, larger fossils, mainly foraminifera and bivalve shell fragments that are scattered throughout the chalk material. These are composed of coarse-grained calcite.

Other minerals in chalks are quartz, various types of clay (montmorillonite, for the most part, and lesser amounts of illite), mica, iron oxides, and pyrite. Quartz (SiO_2) has the form of discrete grains 4μ to 62μ across; pyrite (FeS_2) and iron oxide (magnetite, hematite, and goethite) occur mainly as 10μ to 20μ opaque grains. Clay occurs in flakes less than 2μ in size scattered throughout the very fine grained calcite, and in some chalks glauconite (green pellets of illite clay) is rather abundant.

Chalks were formed by the settlement of the coccoliths, foraminiferal tests (shells), and probably other crystallites of calcite on the bottom of shallow to moderately deep seas. Tributary rivers and streams carried into the sea quartz silt and clay particles which were deposited simultaneously with the fossil fragments, mainly along the margins of the sea. Periodically, tributary rivers brought extra heavy loads of clay and silt that form thin sheets of shale within otherwise uniform beds of chalk. In cases where the tributary load was especially heavy, the resultant rock is classified as a calcareous siltstone or claystone. It is important to note here that in the geologic literature of the southern states, these impure calcareous rocks are frequently classified as marls but are quite unlike fresh-water lake marls.

Chalks sometimes change laterally and vertically into limestones, with decreasing porosity and increasing hardness of the carbonate rock, and therefore some fairly dense limestone and chalky limestone strata occur interbedded with chalks in some deposits.

Sources and Samples of Chalk and Chalky Limestone

Chalk strata crop out in the United States principally in Kansas, Texas, Arkansas, Mississippi, and Alabama (fig. 5). These strata are geologically related, as shown in figure 18,* by fact of the similarity of fossil content and

---

* References for the correlations of the Upper Cretaceous formations are: Kansas-Texas (Reeside, 1932), Texas-Arkansas (Pessagno, 1969), Arkansas-Mississippi (Boswell and others, 1965), Mississippi-Alabama (Copeland, 1968); for the correlations of the Oligocene formations: Mississippi-Alabama (Deboo, 1965).

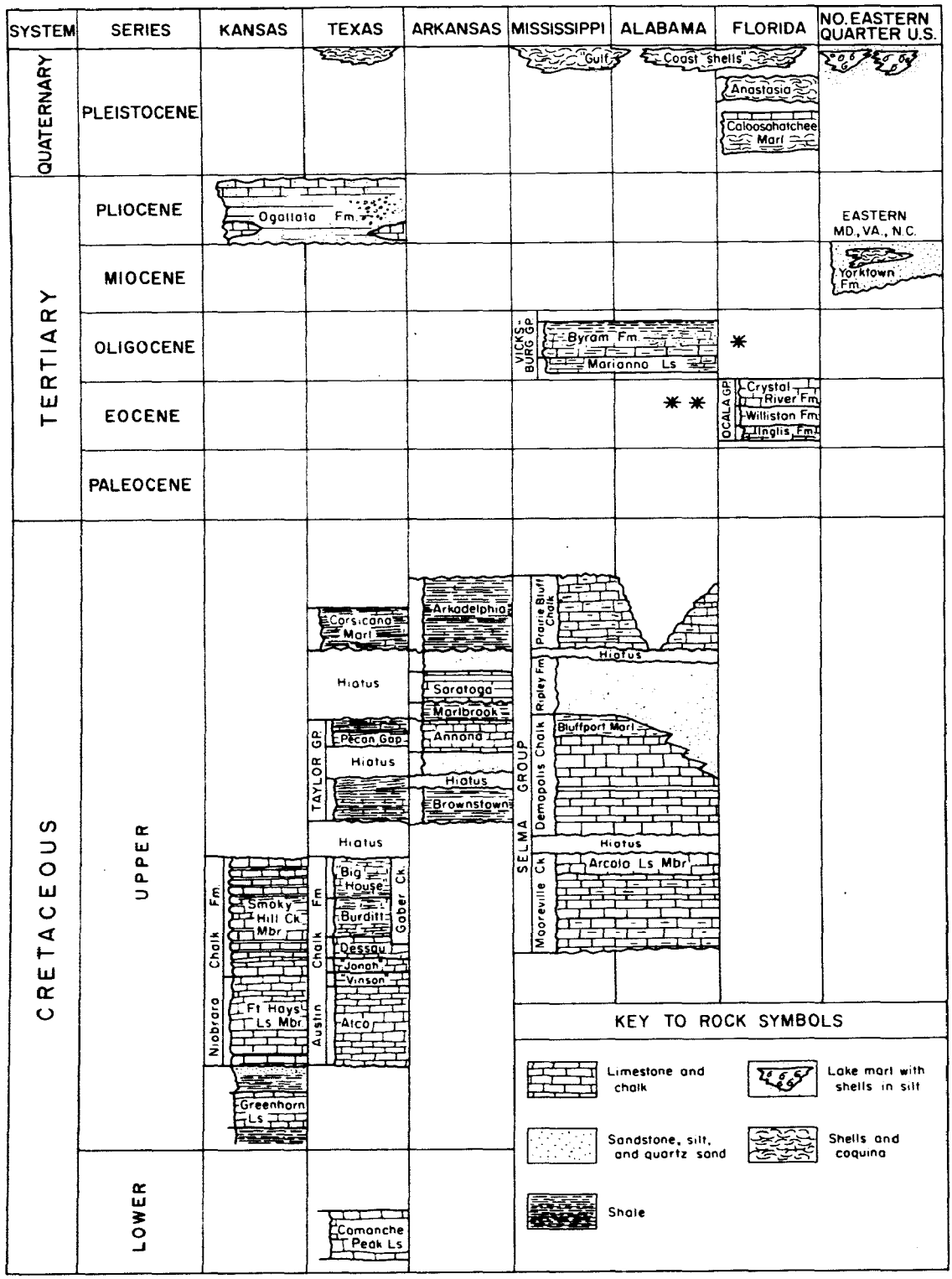

*The Marianna Limestone and the overlying Suwannee Limestone, both Oligocene in age, occur in the Florida panhandle and are in many places high-purity, fine-grained, porous, and chalky limestones (Reves, 1961).

* *The Ocala Limestone of southeastern Alabama (and southwestern Georgia) is composed of chalky and porous limestones very similar in character to the limestones of the Ocala in Florida.

Fig. 18 - Geologic time-rock classification of carbonate rocks studied. The column under each state shows formations that occur in those parts of the state from which samples were collected. In these areas formations of other rock types occur but are not shown here. Vertical scale does not represent true thickness of rock units or duration of time. A hiatus represents a period during which either no sediments were deposited or sediments were eroded prior to deposition of superposed unit.

age relations of the strata that overlie and underlie the chalks. The principal chalk strata are geologically classified as the Niobrara Chalk in Kansas and adjacent states, the Austin Chalk in central and northeastern Texas, the Annona Chalk in Arkansas, and the Selma Group in the Alabama-Mississippi area. Each of these units is recognized as part of the rock strata of the Upper Cretaceous Series. The Cretaceous Period, approximately 70 million to 135 million years ago, is the geologic time during which rocks of the Cretaceous System were deposited. Some chalks and chalky limestones occur in rocks deposited during the Tertiary Period (2 million to 70 million years ago).

Niobrara Chalk

According to Runnels and Dubins (1949), the purer chalk strata of the Niobrara Chalk occur in the lower part of the formation, designated the Fort Hays Limestone Member (fig. 18). The Fort Hays consists of massive beds of buff to light gray chalk, 0.5 to 7 feet thick (average about 2 feet), separated by 0.1 inch thick shale partings and 0.1 to 4-inch beds of shaly chalk and/or bentonite (montmorillonite clay of volcanic origin). In Kansas, the thickness of the Fort Hays varies from about 30 to 65 feet (Zeller, 1968, p. 57). The upper part of the Niobrara, the Smoky Hill Chalk Member, consists of interbedded shale and chalk as does the lower part, but the upper part is much more shaly in most places. The Niobrara outcrop belt in Kansas and Nebraska is outlined in figure 5. The Niobrara crops out in other areas to the north and west of the area shown—in eastern South Dakota,* eastern North Dakota, around the Black Hills in western South Dakota, and in parts of Wyoming, Colorado, and New Mexico. Outcrops of the Niobrara (and the Greenhorn Limestone) along the Rocky Mountain Front Range, especially near Lyons, Colorado, provide raw material for cement manufacturing (Chronic and Chronic, 1972, p. 101). Kottlowski (1962) describes in detail the deposits of limestones of the Niobrara and other limestone formations in New Mexico.

The Fort Hays is quarried by the Ideal Cement Company in Kansas, near Superior, Nebraska, and by Hopper Brothers of Weeping Water, Nebraska, from a deposit near Nelson, Nebraska. It was previously quarried for use in construction of the Cedar Bluff Reservoir dam near Trego Center, Kansas, and for small quantities of road rock from scattered pits within the area of its outcroppings in Kansas. A detailed study of the occurrence and properties of the Fort Hays in Kansas can be found in Runnels and Dubins (1949).

Samples of the Fort Hays were taken from localities designated 7208, 7209, 7212, 7213, and 7214 (fig. 5 and app. 2).

Greenhorn Limestone

The Greenhorn Limestone contains a considerable thickness of soft and chalky limestones that were deemed to have value for inclusion in this study. The Greenhorn occurs below the shale and sandstone that underlies the Fort Hays (fig. 18), and it crops out along a band east of the Fort Hays in Kansas and elsewhere in the Great Plains states (Hattin, 1971). Chalky limestone beds in

*D. H. Vice, Burlington Northern, Billings, Montana, reports (personal communication) that more than 80 feet of chalk is exposed near Yankton, South Dakota; it averages approximately 86 percent $CaCO_3$.

the Greenhorn are 2 to 10 inches thick and are interbedded with shaly and chalky limestone beds of similar thicknesses. Some beds have a nodular structure. Their color is either buff or gray, depending on the degree of oxidation of the small amount of organic matter in the rock.

The Greenhorn was sampled at two producing quarries (loc. 7210 and 7211, fig. 5 and app. 2).

Austin Chalk

The Austin Chalk crops out in a band roughly 5 miles wide that runs almost continuously southwest to northeast through central Texas (fig. 5) and consists predominantly of chalk and some chalky and calcareous claystones. In the Austin-Waco, Texas area, it is about 360 feet thick (Pessagno, 1969, p. 69), and thick and relatively pure beds of chalk occur, especially near the base. According to Pessagno (1969), the Austin Chalk near Austin, Texas is divided into, from the bottom upwards, the Atco Chalk Member, the "Vinson Chalk" Member, the "Jonah Chalk" Member, the Dessau Chalk Member, the Burditt Marl Member, and the "Big House Chalk" Member (fig. 18). The Gober Chalk (Fisher, 1965, p. 63), also called the Gober Tongue of the Austin Chalk (Stephenson, 1937), occurs in northeastern central Texas. The exact relation between the Gober Chalk and the Dessau Chalk and Burditt Marl Members is not known, and the position of the Gober shown in figure 18 is indicative only of its occurrence in the upper part of the Austin Chalk in northeastern Texas. With the exception of the Gober, the correlation between the Texas and Arkansas rock units shown in figure 18 is that of Pessagno (1969). Only the Atco, "Jonah," and Dessau Chalk Members and the Gober Chalk of the Austin were sampled for this study.

The Atco Chalk Member, as exposed at the sampled localities (7221 near Waco, Texas, and 7222 about 18 miles southwest of Dallas), comprises 40 to 50 feet of buff (upper part) and gray (lower part) chalk, uniformly fine grained, in massive beds averaging about 1 to 2 feet in thickness separated by paper-thin breaks of up to 3 inches of thinly laminated chalk. The basal 1 to 2 feet of the chalk contains black phosphatic nodules, 1 to 10 mm across, that consist of the mineral apatite.

Chalky and nodular limestone beds of the "Jonah Chalk" (Pessagno, 1969) were sampled over a 9-foot exposure (7220, near Austin, Texas). Nodules are abundant in these beds. They consist of rather dense and hard limestone, and they are surrounded by soft chalk. The nodules average about 2 by 4 inches in size.

The Dessau Chalk Member was sampled at one locality (7219, near Austin, Texas), where it consisted of very fossiliferous (especially bivalve types) chalk in beds 2 to 2 1/2 feet thick, separated by 0.5- to 1-foot beds of shaly chalk. Some chert nodules and a few nodules of pyrite were observed in the beds sampled.

The Gober Chalk was not well exposed at the sampled locality near Paris, Texas (7224), a quarry (app. 2) in uniformly fine-grained buff and gray chalk. The Gober varies in thickness, and in the area sampled it is thought to be more than 100 feet thick (Stephenson, 1937).

Other Chalk Strata in Texas

Certain chalk beds in the Pecan Gap Chalk of the Taylor Group (Upper Cretaceous) that overlie the Austin Chalk in northeastern Texas (fig. 18) have been quarried for local agricultural and road rock uses (Fisher, 1965, p. 399). The upper 2.5 feet of chalk from beds in the Pecan Gap was sampled from an abandoned quarry at Clarksville, Texas (loc. 7225).

The Comanche Peak Limestone (Lower Cretaceous) occurs in central Texas (fig. 18) and contains chalky limestone strata. A sample was obtained (loc. 7223) for comparison with samples of the Austin. The exposure sampled in the Comanche Peak contained nodular limestone and a small amount of chalk disseminated around the nodules.

Annona Chalk

The Annona Chalk (Upper Cretaceous) occurs in the vicinity of Clarksville, Texas (Barnes, 1966), and near Foreman and Okay, Arkansas (Dane, 1929, pl. 1). The areas of outcrop are too small to show in figure 5. In the localities sampled, the Annona is 30 to 45 feet thick and consists of uniformly fine grained chalk in beds 1 to 10 feet thick. The fine texture of the chalk is interrupted only by an occasional large fossil shell. The beds of chalk are separated by thin partings of very slightly laminated chalk. Samples of Annona Chalk were obtained from freshly exposed faces at two operating quarries (locations 7226 and 7227).

Saratoga Chalk

The Saratoga Chalk (Upper Cretaceous) crops out in a rather narrow and discontinuous band in southwestern Arkansas from near Saratoga to Arkadelphia (Dane, 1929, pl. 1). This chalk ranges in thickness from 20 to 60 feet (Dane, 1929, p. 98) and includes some sandy and glauconitic (green clay) chalk and other beds that are clayey chalk. At the outcrop sampled (loc. 7228), it consisted of gray chalk with blocky fracture, uniformly fine grained except for widely scattered fossil shells, and it was 20 feet thick. Underlying the Saratoga beds sampled were 1 to 2 feet of sandy, glauconitic, and phosphatic chalk, and below this was a considerable thickness of calcareous clay of the Marlbrook Marl.

Selma Group

Chalks of the Selma Group (Upper Cretaceous) are recognized in northeastern Mississippi and northern and central Alabama (fig. 5). According to

Copeland (1968), this group of rock units is comprised of (in ascending order): the Mooreville Chalk, including the Arcola Limestone Member; the Demopolis Chalk, including the Bluffport Marl Member at the top of the Demopolis; the Ripley Formation; and the Prairie Bluff Chalk (fig. 18). Chalk outcrops of the Selma Group merge eastward and northwestward into clays and sands that are classified by other formation names.

In Alabama the Mooreville Chalk consists of about 300 feet of compact, very calcareous, locally glauconitic clay and clayey chalk (Copeland, 1972, p. 2-12). Because the rocks of the Selma Group dip southward, the outcrop of the Mooreville lies in the northern part of the outcrop belt (fig. 5). The Arcola Limestone Member averages about 10 feet in thickness and consists of 2 to 4 beds of light gray, hard, and fossiliferous limestones, each 6 to 12 inches thick, interbedded with soft chalk (Copeland, 1972, p. 2-12). A sample of the chalky beds was obtained for study (7204). The lower part of the Mooreville was not sampled.

Most of the purer chalk outcrops of the Selma Group (fig. 5) from central Alabama to the Tennessee line occur in the Demopolis Chalk. The outcropping chalk is light gray, even textured, and fine grained. The thickness of the Demopolis Chalk ranges from 420 to 495 feet (Copeland, 1972, p. 2-14). In general, the lower part contains thin beds of clayey chalk, while the middle part most consistently contains the purer chalk beds. According to Copeland, the purer chalk in western Alabama grades upward into 50 to 65 feet of calcareous clays classified as the Bluffport Marl Member. Samples 7202 and 7205, both from Alabama, and sample 7230 from Mississippi were obtained from operating quarries in the Demopolis Chalk.

The Ripley Formation, which was not sampled, consists predominantly of sand, sandstone, and calcareous clay.

The Prairie Bluff Chalk is the youngest formation of the Selma Group, and according to Copeland (1972, p. 2-20), it generally consists of sandy and micaceous chalk; however, he states that the lower 40 feet contains a high percentage of calcium carbonate in Montgomery County, Alabama. The Prairie Bluff was sampled at two outcrops near Braggs in Lowndes County, Alabama, where the chalk is rather typically sandy and has a thickness of 80 feet (locs. 7206 and 7207).

Tertiary Formations Containing Chalk and Chalky Limestone

The Tertiary System, the next youngest to the Cretaceous, contains limestone units important for this study, especially in the southeastern states. Porous and chalky limestones of the Vicksburg Group (Oligocene) crop out across central Mississippi (Bicker, 1969), extending eastward into parts of southern Alabama (Copeland, 1968), and in northern and central Florida (Cooke, 1945). The porous limestones in the Vicksburg Group are in the lower part of the Byram Formation and in the Marianna Limestone. These formations are quarried for a

variety of uses at a number of locations in southern Mississippi (Bicker, 1970, p. 20), at St. Stephens, Alabama (Copeland, 1968), and in Jackson County, Florida (Reves, 1961, and Maxwell, 1970).

The outcrop areas of the principal Tertiary limestones in the southeast are shown in figure 5. The area outlined in Mississippi was taken from Bicker (1969) and includes the Chickasawhay Limestone (Oligocene), which generally is composed of dense limestone strata that overlie the Byram. The outcrop area shown for the Tertiary limestones in Alabama includes the Chickasawhay, the Vicksburg Group, and the Jackson Group (Copeland, 1968, pl. 1), which includes the Ocala Limestone. In Georgia, only the Ocala Limestone outcrop areas are shown (Georgia Division of Mines, Mining and Geology, 1939). In Florida, the outcrop area shown includes the Ocala Group, the Avon Limestone of Eocene age, and the Oligocene Series (Vernon and Puri, 1965).

The Vicksburg Group comprises a number of formations and members, depending on the region. The principal units of interest are the lowermost beds of the Byram Formation, called the Glendon Limestone Member, and the Marianna Limestone. Samples of the lower limestone beds of the Byram were taken from an outcrop on the north side of Vicksburg (loc. 7229). The Marianna Limestone underlies the Byram in Alabama (Copeland, 1968), where in outcrops it usually consists of a thick white to cream-colored chalk. According to Toulmin and others (1966), lower beds in the Marianna include glauconitic limestone and calcareous sand in western Alabama. A sample of chalk from the Marianna was obtained for study from the St. Stephens, Alabama, quarry of the Lone Star Industries, Inc. (loc. 7201).

The Ocala Group (Eocene in age) in Florida consists of soft, cream to white, porous limestones, generally of high calcium content (Puri, 1957). It comprises the Crystal River, Williston, and Inglis Formations, which crop out extensively in Florida—in the northwestern part of the peninsula and also in the north part of the panhandle in Jackson and Holmes Counties. In Georgia and Alabama, porous limestone strata of Eocene age are classified as Ocala Limestone. They crop out in southwestern Georgia along an outcrop belt extending from near Perry (in central Georgia) to the junction of the borders of Georgia-Alabama and Florida. The Ocala is quarried by a number of companies along its outcrop belt in Georgia (Georgia Division of Mines, Mining and Geology, 1939; Georgia Department of Mines, Mining and Geology, 1968). The porous limestones of the Ocala also extend into southern Alabama from the tri-state junction northwestward to as far as the Tombigbee River (Cooke, 1926).

A sample of the Crystal River Formation in central Florida was collected for study (loc. 7120).

Characterization of Chalk and Chalky Limestone Samples

Petrographic Description

Although the chalk samples are made up primarily of very fine grains of calcite, some coarse grains do occur and it is useful to classify these

types of calcite by name. Micrite is very fine grained calcite, of roughly equidimensional grains ranging in size from about 0.5μ to 4μ in diameter. In thin sections, micrite is dark brown and is the abundant matrix shown in the micrographs (pl. 6). Coarse-grained and clear calcite is called sparite or sparry calcite. This type of calcite is nearly transparent (more like Iceland spar) and occurs as crystallites and irregularly shaped grains greater than 10μ in size, and when several grains are clustered together, they are tightly interlocked and have relatively straight grain boundaries. The light or clear areas in the micrographs shown in plate 6 are sparite. Petrographic analyses by optical and electron microscopy were made of thin sections and other specimens of the samples. Observations are listed in table 9. Transmitted light micrographs of thin sections of representative chalks at low magnifications are shown in plate 6. Scanning electron micrographs of the very fine grained material in the chalks at high magnifications are shown in plate 7. Numerous fragments of disc-shaped coccoliths occur in the micritic calcite in the chalk samples (pl. 7). The quantitative determination of the amount of sparry calcite in the chalk samples was determined by image analysis using a Quantimet (Harvey and Steinmetz, 1971); and the mean percentages determined from 40 or more microscopic fields of view are listed in table 9. The percentage of micrite in each sample is about 100 minus the sparite percentage; however, clay constituents and other impurities also occur in the micrite, and the Quantimet cannot distinguish these from micrite.

The proportion of sparry calcite in fairly pure chalks varies from 5 to 21 percent (averages 10%). The sample from the Mooreville Chalk (7204) is unique in that it contains an unusually large number of calcispheres (pl. 6B). The proportion of sparry calcite in the chalky limestones (table 9) is higher than in the chalks and accounts for one of the principal petrographic differences between the two types.

The average grain size of the samples was measured from exceptionally thin (approximately 10μ), polished thin sections of about 200 particles of crushed sample, each about 1 mm in size (16x18 mesh). The individual crystallite grains were detected by the Quantimet in cross-polarized light, and more than 80 microscopic fields of view were analyzed in each of two thin sections of each sample. The mean ratio of the measured values of area to boundary projection yields the mean grain chord length for the sample ($\bar{C}$, table 9). $\bar{C}$ reflects the predominance of the micritic component of the samples, and for the chalks it ranges from 2μ to 3.4μ (average 2.7μ). The samples classified as chalky limestones have a mean chord length from 3μ to 7.5μ (average 4.1μ).

Bulk Density and Crushing Characteristics

Bulk density measurements were made on specimen blocks (3x2x1 cm) from each of the samples. Most samples were homogeneous and one block sufficed; however, several samples were somewhat inhomogeneous, and from these two or three blocks were prepared. The blocks were oven dried, weighed, coated with paraffin, and again weighed both in air and immersed in water. The bulk density was computed

A. 7202. Demopolis Chalk (x 200)

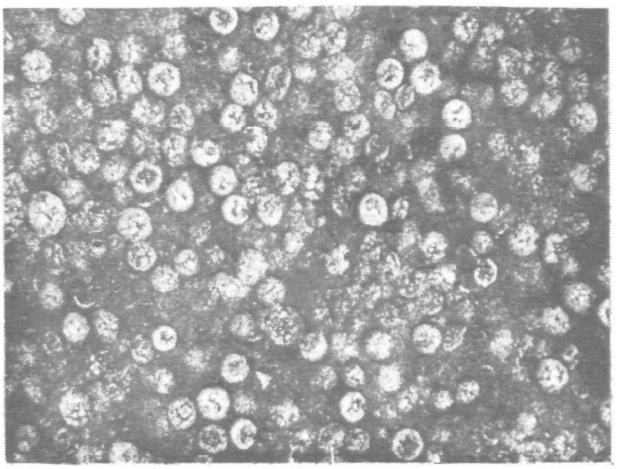

B. 7204. Calcispheres in Arcola Limestone Member (x 100)

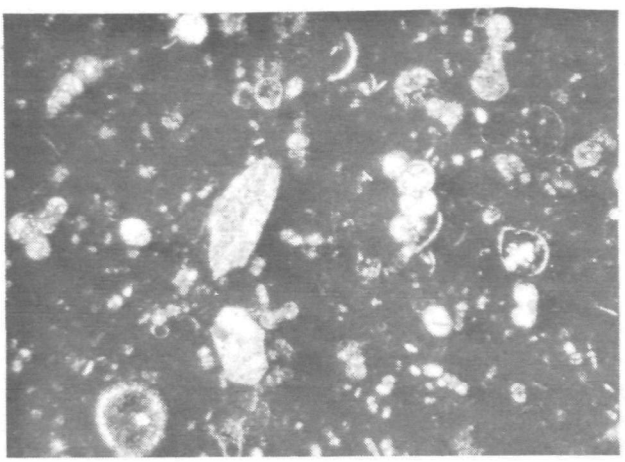

C. 7212A. Niobrara Chalk (x 50)

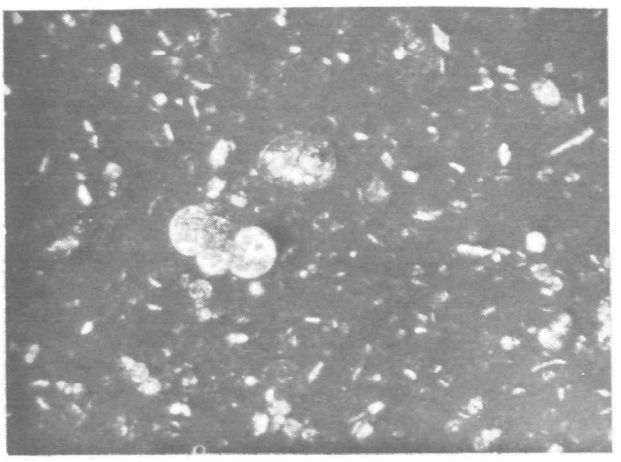

D. 7222A. Austin Chalk (x 50)

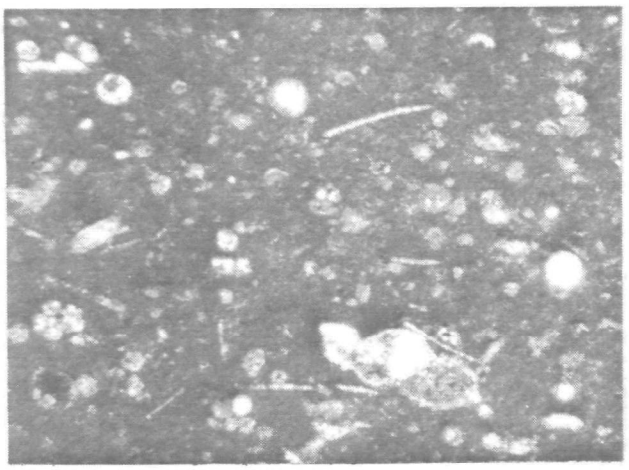

E. 7227B. Annona Chalk (x 50)

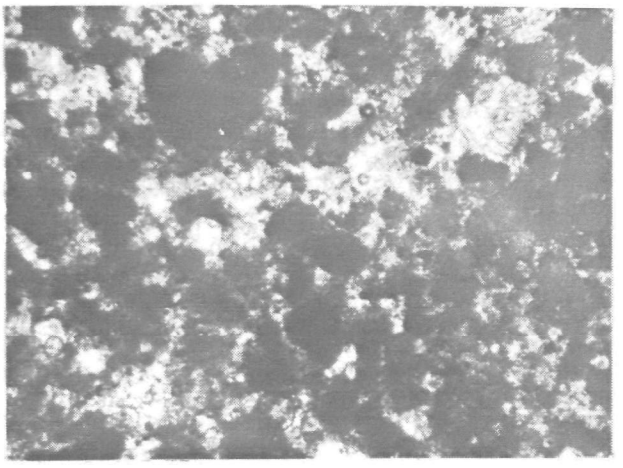

F. 7210A. Pellets (dark) in Greenhorn Limestone (x 50)

Plate 6 - Texture of chalk and a chalky limestone (F), coarse sparite in micrite.

TABLE 9 — PETROGRAPHY AND BULK DENSITIES OF SAMPLES

Geologic formation and sample number	Main type of calcite	Sparry calcite* (%)	Constituents and their distribution	Mean grain chord length, $\bar{C}$ (μ)	Bulk density (g/cc)
CHALKS					
Marianna Limestone					
7201	Micrite	8	Foraminifera tests and other coarse crystalline sparry fossil fragments moderately packed in porous micrite. Iron oxide grains (20μ) and other mineral grains scattered throughout Clay distributed throughout the porous micrite.	2.9	1.86
Demopolis Chalk					
7202	Micrite	7	Foraminifera tests, other coarsely crystalline sparry fossil fragments, and single crystal blades abundantly scattered throughout. Also scattered grains of quartz (20μ-60μ), glauconite pellets, and iron oxide (8μ-40μ dia.). Clay is scattered throughout the micrite; some of it is faintly and irregularly laminated along bedding planes.	2.1	1.95
7205	Micrite	6		2.1	1.79
7230	Micrite	5		2.2	1.88
Mooreville Chalk					
7204	Micrite	30	Spheres of sparry calcite (calcispheres), mostly 50μ dia., abundantly and irregularly scattered in dense micrite.	3.4	2.36
Prairie Bluff Chalk					
7206	Micrite	29**	Bladed mica and calcite crystals (200μ x 10μ) and a few much larger crystals (some fibrous shells) of calcite scattered in micrite. Also scattered grains (80μ) of quartz, and scattered pellets (100μ) of glauconite, many of them enclosing iron oxide grains.	2.7	1.91
7207	Micrite	16**		2.8	1.92
Niobrara Chalk					
7208B	Micrite	6	Foraminifera tests and spheres (calcispheres), composed of coarsely crystalline sparry calcite, mostly 50μ to 150μ across, scattered throughout micrite. Scattered grains of quartz (most less than 40μ) and chert (all samples except 7214A). Opaque iron oxide grains (10μ dia.) scattered in micrite and transparent iron oxide stringers occur in patches and in irregular lenses. The chalk is microscopically laminated along irregular planes more or less parallel to bedding. Clay flakes occur, mainly along certain bedding planes and, to a lesser extent, scattered in micrite.	—	—
7208C	Micrite	7		2.6	1.83
7209	Micrite	14		2.0	1.68
7212A	Micrite	13		2.6	2.02
7213	Micrite	10		3.4	2.10
7214A	Micrite	6		2.8	—
7214B	Micrite	9		2.9	2.07
7214C	Micrite	11		3.0	1.87
Austin Chalk					
7221A	Micrite	13	Foraminifera tests and other coarse sparry calcite (mostly 100μ in size); partly scattered and partly concentrated in thin beds. Rare grains (20μ) of quartz and feldspar. Iron oxide mostly in scattered grains (10μ-15μ dia.). Clay, mostly montmorillonite (except 7222B), occurs mixed with the micrite, some of which is laminated. Glauconite in 7224 occurs in pellets and altered mica flakes.	2.8	2.32
7221B	Micrite	21		2.3	2.21
7222A	Micrite	14		2.5	2.04
7222B	Micrite	20		2.4	2.25
7224	Micrite	6		2.7	2.29

Geologic formation and sample number	Main type of calcite	Sparry calcite* (%)	Constituents and their distribution	Mean grain chord length, $\bar{c}$ (μ)	Bulk density (g/cc)
Pecan Gap Chalk					
7225	Micrite	9	Spheres of sparry calcite (calcispheres, 60μ), many foraminifera tests, and a few fibrous shell fragments scattered in micrite.	2.5	2.26
Annona Chalk					
7226A	Micrite	6	Coarse sparry calcite (many calcispheres, 60μ) and foraminifera tests widely scattered throughout micrite. Clay—mainly montmorillonite, with lesser grains of quartz and iron oxide—scattered throughout.	2.6	2.25
7227B	Micrite	7		3.0	2.34
Saratoga Chalk					
7228	Micrite	23†	Coarse crystalline sparry calcite and a few shell fragments (fibrous) scattered throughout the micrite. Quartz grains, up to 150μ in dia., glauconite pellets, and iron oxide grains widely scattered. Clay, mainly montmorillonite, occurs with the micrite.	3.1	2.29
CHALKY LIMESTONES					
Crystal River					
7120	Micrite	31	Variety of coarsely crystalline fossil fragments and many coarse fibrous (shell) fragments, all closely packed in micrite. Macroscopically porous.	4.1	2.23
Caloosahatchee Marl					
7122A	Micrite	4	Abundant thin shell fragments (needle-shaped), many gastropod shells, and a few fragments of fibrous shells surrounded by macroscopically porous micrite. Most pores occur enclosed by shells and are isolated.	7.5	2.25
Greenhorn Limestone					
7210A	Micrite (pellitoidal)	33	Coarsely crystalline fossil fragments (Inoceramus shells), calcispheres (150μ to 600μ dia.), and pellets (300μ) of micrite set in sparry calcite (grains 20μ to 100μ) cement. The coarse fossil fragments most abundant in certain beds (about 1 cm thick).	3.5	2.32
7210B	Micrite (pellitoidal)	24		4.1	2.61
7211	Micrite	—		—	
Austin Chalk					
7219	Micrite	30	Coarse sparry calcite in fossil fragments including Inoceramus shells and also in irregularly shaped patches are closely packed in micrite. Rare pellets of glauconite and grains of iron oxide.	3.8	2.64
7220	Micrite	26		3.4	2.58
Commanche Peak Limestone					
7223	Micrite	14	Coarsely crystalline sparry calcite fossils, fibrous calcite shell fragments, and grains of quartz (40μ) scattered throughout micrite.	3.5	2.60
Byram					
7229A	Micrite	18	Large fragments of fibrous shells and of other sparry fossils are surrounded by micrite and very fine-grained sparry calcite (20μ). Glauconite pellets and quartz grains abundantly scattered and in part concentrated in irregular patches.	3.0	—

*Clear transparent grains of calcite 10μ diameter and larger.
**Includes some mica and quartz in addition to the sparry calcite.
†Includes some quartz in addition to the sparry calcite.

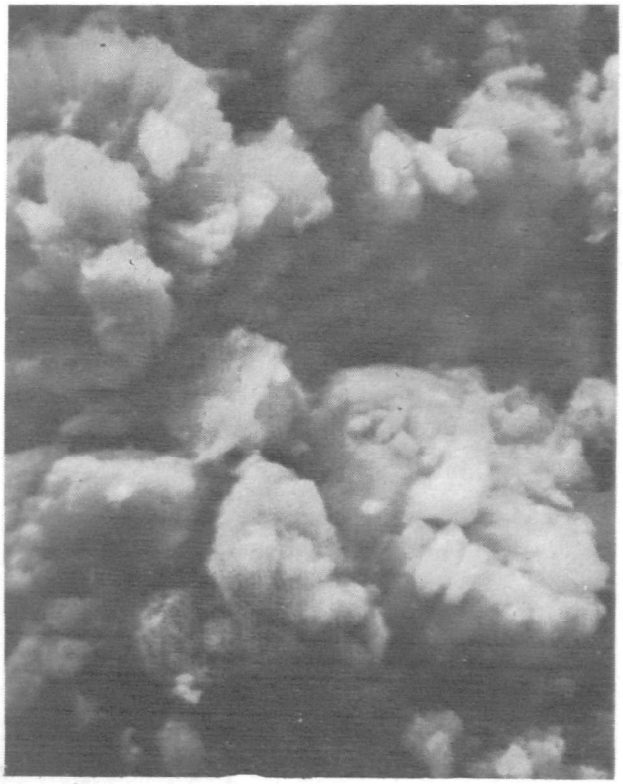

A. 7201. Marianna Chalk (x 3500)

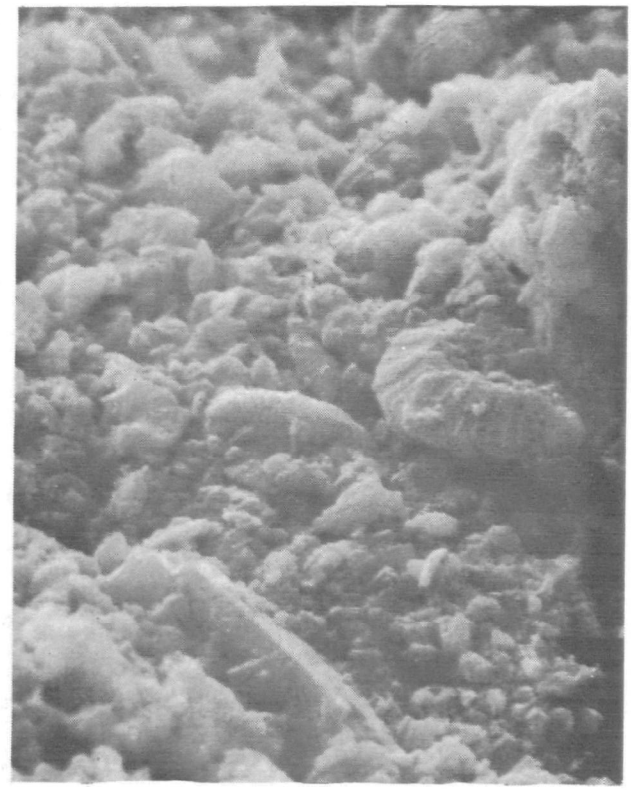

B. 7202. Demopolis Chalk (x 4100)

C. 7221A. Austin Chalk (x 3924)

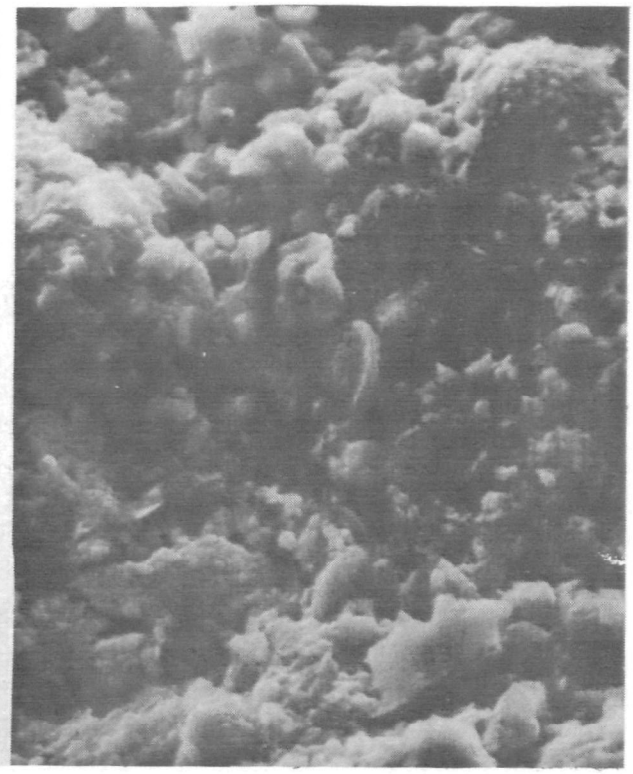

D. 7227B. Annona Chalk (x 1622)

Plate 7 - Texture of micritic calcite in chalk samples.

from these weights by using the standard formula (table 9). The mean bulk density (g/cc) of the chalk samples is 2.07, with a standard deviation of 0.21. For the chalky limestones the mean is 2.48, with a standard deviation of 0.13. The samples of the Marianna Limestone and the Demopolis and Niobrara Chalks generally are the least dense chalk (1.68 to 2.10); the samples of the Austin, Pecan Gap, Annona, and Saratoga Chalks have higher densities (2.04 to 2.34); and the chalky limestones are characterized by the highest densities (2.23 to 2.64).

An attempt was made to assess the relative ease of pulverization of the samples by crushing a portion of each with a small laboratory jaw crusher, then passing the material through a small laboratory disc pulverizer and measuring the particle-size distribution of the resultant powder. The particle-size distribution was measured by wet-sieving the greater than 53μ fraction and by standard sedimentation methods for the less than 53μ fraction of the samples. The particle-size measurements were plotted on logarithmic paper, and the median particle size was determined (table 10). It is assumed that the smaller the median particle size, the easier it is to produce a fine-grind product. The data show considerable variation and little consistency within the geologic units and with other data. Some of the samples tested between 5μ and 30μ, but most gave values near 45μ. Thus the usefulness of these particular data in terms of predicting SO_2 reactivities is questionable.

Mineral and Chemical Analyses

The samples were analyzed for their mineral composition, and the results are listed in table 11. The chalk sample from the Marianna Limestone was unusual in that a small amount (< 1%) of a very fine grained heulandite ($CaAl_2Si_7O_{18}\cdot 6H_2O$), a zeolite mineral, is present.

Quartz in grains less than 40μ and clays, mainly montmorillonite with lesser amounts of illite in the form of green pellets of glauconite, are the principal impurities in the chalks. Traces of feldspar, magnetite, pyrite grains, and mica flakes occur in most samples. These noncarbonate mineral constituents are thought to be inert with respect to absorption of SO_2.

Results of chemical analyses are shown in table 12. The two columns at the extreme right in table 12 are values calculated from loss-on-ignition data and from CaO values. The "CaO in calcine" represents the weight percentage of the CaO in the sample after being heated to 1000° C. The loss on ignition can be figured for each sample by finding the sum of the CO_2, H_2O, organic C, and SO_3 values.

Results and Discussion of Pore Structures and Surface Areas of Chalks, Chalky Limestones, and Their Calcines

The volume and size distributions of pores larger than 0.012μ in diameter and surface areas were determined on the 16x18-mesh (1 to 1.2 mm)

TABLE 10 — MEDIAN PARTICLE SIZES OF PULVERIZED SAMPLES (Pulverized under identical conditions to indicate relative ease of pulverization)

Sample	Formation	Median particle size (μ)
CHALKS		
7201	Marianna	9
7202	Demopolis	31
7230	Demopolis	7
7206	Prairie Bluff	17
7208C	Niobrara	48
7209	Niobrara	45
7212A	Niobrara	48
7213	Niobrara	45
7214A	Niobrara	50
7214B	Niobrara	21
7214C	Niobrara	9
7221A	Austin	45
7221B	Austin	45
7222A	Austin	5
7222B	Austin	30
7224	Austin	16
7225	Pecan Gap	35
7226A	Annona	25
7227B	Annona	42
7228	Saratoga	25
CHALKY LIMESTONES		
7120	Crystal River	13
7210A	Greenhorn	50
7210B	Greenhorn	48
7211	Greenhorn	48
7219	Austin	48
7220	Austin	45

particle-size fraction of the samples and their calcines. The results are given in table 13. Calcine pore volumes and surface areas were determined on calcined rock samples, but the values in table 13 were reported per gram of rock used to prepare the calcines in order that direct comparisons between the calcine and rock data could be made. The calcine data in table 13 can easily be converted from grams of rock to grams of calcine by multiplying the values given by $100/[100-(\%H_2O + \%CO_2 + \%SO_3 + \%Org.\ C)]$. The percentages are found in table 12. The theoretical pore-volume increase upon calcination of each sample, assuming no particle shrinkage and based on the $CaCO_3$ analyses (table 12), was calculated (equal to 0.20 times the $\%CaCO_3/100$) and is included in table 13.

TABLE 11 — MINERAL ANALYSES OF CHALK AND CHALKY LIMESTONES*

Sample number	Calcite (%)	Quartz	Clay**			Other minerals	HCl residue† (%)
			M	I	K		
7120‡	99	nil	nil	nil	nil	nil	nil
7122A	72	XX	nil	nil	nil	nil	27.0
7201	90	nil	XX (gl)	X	nil	heulandite-X pyrite-X mica-X	8.8
7202	73	X	XX	X (gl)	XX	feldspar-X mica-X pyrite-X	23.8
7204	95	X	XX	X	XX	mica-X garnet-X hornblende?-X	2.46
7205	72	X	XX	XX (gl)	XX	feldspar-X mica-X magnetite-X	26.12
7206	54	XXX	X	XX (gl)	XX	mica-X magnetite-X	40.4
7207	54	XX	XX	XX (gl)	XX	mica-X magnetite-X garnet-X	40.54
7208B	82	X (some chert)	XX	X	XX	feldspar-X limonite-X pyrite-X	16.29
7208C	90	X (some chert)	X	X	X	feldspar-X pyrite-X limonite-X	7.25
7209	90	X (chert)	X	X	X	feldspar-X pyrite-X limonite-X	9.72
7210A‡	93	X	X	X	X	feldspar-X biotite-X magnetite-X	5.50
7210B‡	91	X	XX	X	X	feldspar-X	7.68
7211	86	X	XX	X	X	feldspar-X	12.3
7212A	93	X (chert)	nil	X	X	feldspar-X limonite-X magnetite-X mica-X	5.36
7212B	45	XX (chert)	X	X	XX	——	49.3
7213	94	X (chert)	X	X	X	feldspar-X limonite-X	5.85
7214A	96	X	X	X	X	feldspar-X limonite-X mica-X magnetite-X	2.13
7214B	95	X (chert)	nil	X	X	feldspar-X limonite-X magnetite-X	3.48

*Relative abundance: XXX equals > 20%; XX equals 1% to 20%; X equals < 1%; —— indicates not determined.

**Clay mineral species present: M - montmorillonite; I - illite and/or muscovite-type mica, gl - part of the illite is glauconite type; K - kaolinite.

†Consists of quartz and clay plus organic matter, feldspar, mica pyrite, and/or other silicates, if present.

‡Designates chalky limestones.

(Table continued on p. 58)

TABLE 11 — Continued

Sample number	Calcite (%)	Quartz	Clay** M	Clay** I	Clay** K	Other minerals	HCl residue† (%)
7214C	92	X	nil	X	XX	feldspar-X pyrite-X limonite-X	6.17
7219	92	X (some chert)	XX	X (gl)	nil	feldspar-X limonite-X magnetite-X	6.88
7220‡	94	X	XX	X (gl)	nil	magnetite-X limonite-X	5.13
7221A	86	X	XX	X	nil	feldspar-X limonite-X	12.0
7221B	86	nil	XX	nil	nil	feldspar-X magnetite-X	11.97
7222A	87	X (chert)	XX	X	X	feldspar-X limonite-X	12.39
7222B	86	X (some chert)	nil	X (gl)	X	feldspar-X magnetite-X	13.30
7223‡	91	X (some chert)	X	nil	X	limonite-X	7.87
7224	85	X (some chert)	XX	X (gl)	X	magnetite-X limonite-X mica-X	11.79
7225	75	XX	X	X (gl)	X	feldspar-XX magnetite-X limonite-X	22.01
7226A	82	X	XX	X	X	feldspar-X	14.68
7227B	89	X	XX (gl)	X	X	feldspar-X limonite-X mica-X pyrite-X	9.43
7228	71	XX	XX	XX (gl)	X	feldspar-X magnetite-X limonite-X	24.76
7229A‡	83	XX	—	—	—	—	—
7229C‡	90	X	XX	X (gl)	X	pyrite-X feldspar-X magnetite-X	10.5
7229D‡	68	X	XX	X (gl)	X	aragonite(?)-X mica-X	29.2
7229E‡	90	X	XX	X (gl)	X	pyrite-X feldspar-X mica-X	7.9
7229F‡	50	XXX	—	—	—	aragonite-X	—
7230	80	X (some chert)	X	X (gl)	X	feldspar-X mica-X limonite-X magnetite-X	18.38

*Relative abundance: XXX equals > 20%; XX equals 1% to 20%; X equals < 1%; — indicates not determined.

**Clay mineral species present: M - montmorillonite; I - illite and/or muscovite-type mica, gl - part of the illite is glauconite type; K - kaolinite.

†Consists of quartz and clay plus organic matter, feldspar, mica pyrite, and/or other silicates, if present.

‡Designates chalky limestones.

TABLE 12 — CHEMICAL ANALYSES OF CHALKS AND CHALKY LIMESTONES
(Analyses by Analytical Chemistry Section, Illinois State Geological Survey)

Sample number	SiO_2	Al_2O_3	Fe_2O_3	MgO	CaO	Na_2O	K_2O	H_2O	CO_2	SO_3	Organic carbon	CaO in calcine	$CaCO_3$
7120*	nil	nil	0.42	0.01	55.5	0.01	0.09	0.08	43.61	0.01	nil	98.6	99.1
7122A*	0.77	nil	0.40	0.91	53.0	0.08	0.02	0.86	42.44	0.09	0.14	93.7	94.6
7201	6.48	1.79	0.74	2.04	47.30	0.08	0.17	0.69	39.47	0.33	nil	79.0	84.5
7202	14.2	5.26	1.98	0.82	39.63	0.14	0.67	1.22	31.97	1.62	0.67	59.2	70.8
7204	1.93	0.26	0.30	0.14	53.45	0.03	0.08	0.36	41.97	nil	0.17	92.7	95.4
7205	14.2	5.34	2.44	0.46	40.38	0.14	0.63	1.71	30.80	0.74	0.77	60.4	72.1
7206	17.6	7.19	3.26	1.00	29.52	0.15	1.36	1.91	23.96	1.28	0.43	40.1	52.7
7207	25.9	7.35	3.61	0.81	29.71	0.15	1.36	2.20	23.89	1.23	0.47	40.6	53.0
7208C	4.83	1.94	0.98	0.16	50.35	0.07	0.29	0.66	39.59	nil	nil	84.3	89.9
7209	5.26	1.27	1.32	0.23	50.54	0.05	0.31	0.72	38.92	nil	0.10	83.7	90.2
7210A*	3.61	0.56	0.34	0.08	52.23	0.13	0.17	0.59	40.93	0.03	0.09	89.4	93.3
7210B*	3.42	1.42	0.37	0.12	50.37	0.10	0.13	0.68	39.96	0.82	1.75	87.4	89.9
7211	6.35	1.53	0.68	0.15	47.95	0.11	0.29	1.11	37.65	nil	0.19	78.6	85.6
7212A	3.00	0.54	0.66	0.16	52.28	0.06	0.23	0.36	41.15	nil	0.05	89.8	93.4
7213	1.93	1.19	0.41	0.27	51.90	0.05	0.34	0.55	41.23	nil	0.07	88.6	92.7
7214A	0.88	0.03	0.37	nil	53.91	0.03	0.15	0.33	41.10	nil	0.41	93.6	96.3
7214B	2.44	0.06	0.79	0.33	52.58	0.05	0.16	0.31	41.79	nil	0.04	90.6	93.9
7214C	3.78	1.14	1.07	0.61	50.79	0.08	0.24	0.44	40.50	0.08	0.04	86.0	90.7
7219*	3.81	0.54	0.59	0.22	51.84	0.07	0.33	0.75	40.27	0.14	0.07	87.5	92.6
7220*	2.94	1.00	0.50	0.57	51.82	0.06	0.15	0.72	41.15	0.11	nil	88.1	92.5
7221A	7.63	1.42	0.86	0.23	48.20	0.06	0.24	1.64	37.78	nil	0.09	78.6	86.1
7221B	6.63	1.29	1.02	0.33	48.20	0.09	0.34	1.06	38.22	1.03	0.39	78.7	86.1
7222A	6.01	2.61	1.03	0.06	48.41	0.07	0.49	1.03	38.12	nil	0.12	79.4	86.4
7222B	6.62	1.71	1.27	0.31	47.93	0.09	0.53	0.82	37.95	1.19	0.20	77.9	85.6
7223*	7.40	1.05	0.44	0.44	49.21	0.03	0.11	0.53	40.20	nil	0.03	83.1	87.9
7224	7.69	2.27	1.26	0.02	47.84	0.06	0.33	1.04	37.58	0.14	0.11	78.0	85.4
7225	18.1	2.43	0.76	0.17	41.83	0.12	0.76	1.16	32.98	0.26	0.27	63.4	74.7
7226A	9.83	2.85	0.83	0.27	45.64	0.08	0.56	1.64	36.04	0.31	0.26	62.4	81.5
7227B	5.46	1.37	0.62	0.23	49.01	0.07	0.31	0.92	39.08	0.18	0.18	81.2	87.5
7228	19.6	2.42	1.16	0.60	39.22	0.14	0.66	1.34	31.22	0.11	0.20	58.1	70.0
7230	9.95	4.04	1.28	0.46	44.85	0.11	0.73	1.44	34.21	0.64	0.43	69.5	80.1

*Designates chalky limestones.

TABLE 13 — PORE STRUCTURES AND SURFACE AREAS OF CHALKS, CHALKY LIMESTONES, AND THEIR CALCINES

Geologic formation and sample number	ROCK			CALCINE			
	Pore volume (cc/g rock)	Mean pore size (μ)	Surface area (m^2/g rock)	Pore volume (cc/g rock)	Observed pore-volume increase* (cc/g rock)	Theoretical pore-volume increase** (cc/g rock)	Surface area (m^2/g rock)
CHALKS							
Marianna Limestone							
7201	0.302	0.76	8.8	0.428	0.126	0.169	14.1
Demopolis Chalk							
7202	0.212	0.15	17.6	0.352	0.140	0.142	8.7
7205	0.232	0.13	—	0.353	0.121	0.144	9.4
7230	0.179	0.15	20.1	0.329	0.150	0.160	7.4
Mooreville Chalk							
7204	0.115	0.43	3.1	0.295	0.180	0.181	11.3
Prairie Bluff Chalk							
7206	0.145	0.17	18.7	0.238	0.093	0.105	8.5
7207	0.163	0.18	—	0.238	0.075	0.106	6.3
Niobrara Chalk							
7208B	0.202	0.25	—	0.345	0.143	0.164	9.9
7208C	0.216	0.35	7.0	0.355	0.139	0.180	9.2
7209	0.242	0.40	7.6	0.388	0.146	0.180	9.7
7212A	0.217	0.39	—	0.373	0.156	0.187	8.8
7213	0.183	0.47	4.7	0.399	0.216	0.185	9.6
7214A	0.186	0.49	3.2	0.365	0.179	0.193	6.6
7214B	0.192	0.47	4.4	0.362	0.170	0.188	9.2
7214C	0.224	0.40	—	0.398	0.158	0.181	7.7
Austin Chalk							
7221A	0.132	0.20	10.8	0.292	0.160	0.172	10.3
7221B	0.131	0.18	—	0.295	0.164	0.172	8.6
7222A	0.143	0.18	10.4	0.302	0.159	0.173	8.0
7222B	0.152	0.18	—	0.305	0.153	0.171	6.9
7224	0.133	0.18	9.6	0.301	0.168	0.171	7.0
Pecan Gap Chalk							
7225	0.118	0.12	11.1	0.272	0.154	0.149	6.7
Annona Chalk							
7226A	0.118	0.12	12.8	0.283	0.165	0.163	7.6
7227B	0.121	0.20	8.0	0.299	0.178	0.175	6.4
Saratoga Chalk							
7228	0.111	0.18	16.0	0.242	0.131	0.140	10.0
CHALKY LIMESTONES							
Crystal River Limestone							
7120	0.086	0.50	0.5	0.259	0.173	0.200	14.9
Calcoosahatchee Marl							
7122A	0.043	0.21	—	0.258	0.215	0.189	2.9
Greenhorn Limestone							
7210A	0.092	0.51	—	0.292	0.200	0.186	10.1
7210B	0.107	0.24	4.4	0.297	0.190	0.180	10.2
7211	0.115	0.37	—	0.305	0.190	0.171	8.8
Austin Chalk							
7219	0.064	0.31	—	0.254	0.190	0.185	8.2
7220	0.062	0.18	5.2	0.244	0.182	0.185	9.3
Comanche Peak Limestone							
7223	0.171	0.15	5.7	0.252	0.181	0.176	9.1

*Pore volume of calcine minus that of the rock. **Based on $CaCO_3$ content of sample, assuming no shrinkage of $CaCO_3$ grains during calcination.

Characteristic textural features of calcined micritic type of calcite in selected chalk samples are shown in plate 8. Upon calcination (conditions specified above), the sparry calcite grains in Inoceramus shells retain their original coarse fibrous shape (pl. 9A), but the lime grains are partly sintered to give a spongy texture (pl. 9B). In the main, the calcination of micritic calcite grains yields porous clusters of lime grains (A in pl. 9C). However, the calcination of coccoliths, observed in several specimens, appears to produce a less porous lime (pl. 9D).

Comparison of the surface areas of the rocks and their calcines shows that some rocks gained surface area and others lost surface area on calcination. If the calcination process only enlarged existing rock pores, the surface area of the calcine would be lower than the surface area of the rock. The size of the existing pores and the amount that they are enlarged will determine the amount of surface area lost. New pores created in the rock by calcination will add surface area to the calcine. The size of the new pores will determine how much surface area will be added to the calcine. The opening of closed pores in the rock on calcination will also add surface area to the calcine. Therefore, a large loss of surface area on calcination shows that enlargement of pores predominates over creation of new pores and conversely, a large surface area gain on calcination shows that creation of very fine pores predominates over enlargement of existing pores. However, for many rock samples, both pore enlargement and the creation of new pores occur on calcination, and it is impossible to separate their contributions to the total calcine surface area.

Calcine pore-volume curves usually exhibit two steps, as seen in figures 19-24. The first step results from unaltered and enlarged pores; and the second step results from new pores, but it could include enlarged pores if they were in the same size range as the new pores.

Chalks

Comparison of the pore volumes and other properties of the chalks permits the following general observations: For the chalks that contain more than 70 percent $CaCO_3$, a good correlation (linear correlation coefficient of 0.88) was observed between the bulk density and the total pore volume as measured by mercury porosimetry. This correlation is indicative of a high degree of permeability, a characteristic that is important in gas-solid interactions. Upon calcination at 850° C under dynamic gas flow conditions, a significant correlation was observed of increasing pore volume of calcined chalk with increasing pore volume of the original chalk (linear correlation coefficient of 0.953). With few exceptions, chalks showed a slightly less than theoretical increase in pore volumes after the calcination process was complete. No correlation was observed between the mean pore sizes and the pore volumes of the chalks.

The sample of chalk from the Marianna Limestone, 7201, has the largest pore volume (0.302 cc/g) and the largest mean pore diameter (0.76μ) of all the

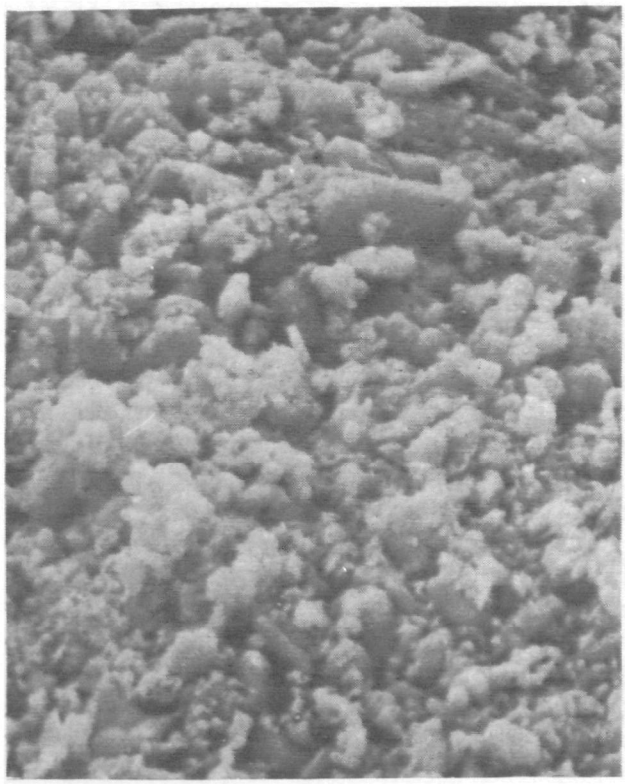

A. 7201. Calcine (x 2809)

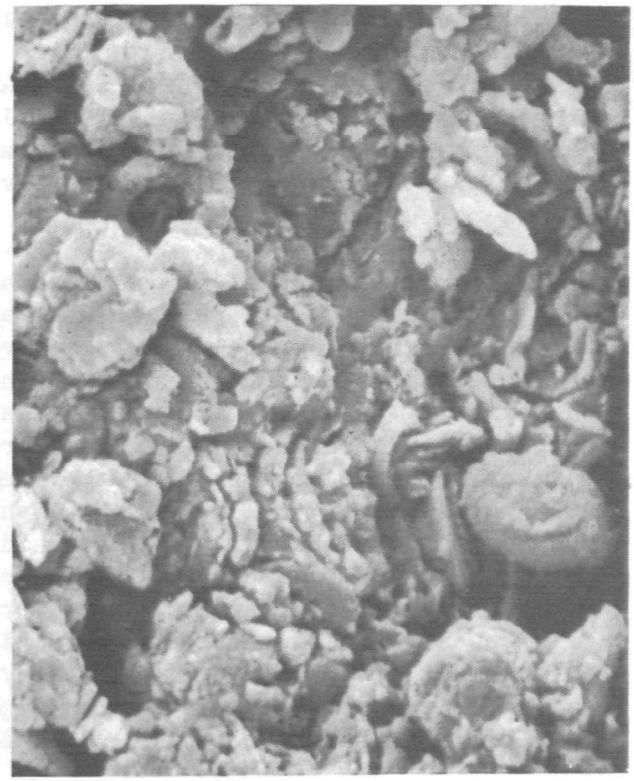

B. 7202. Calcine (x 3270)

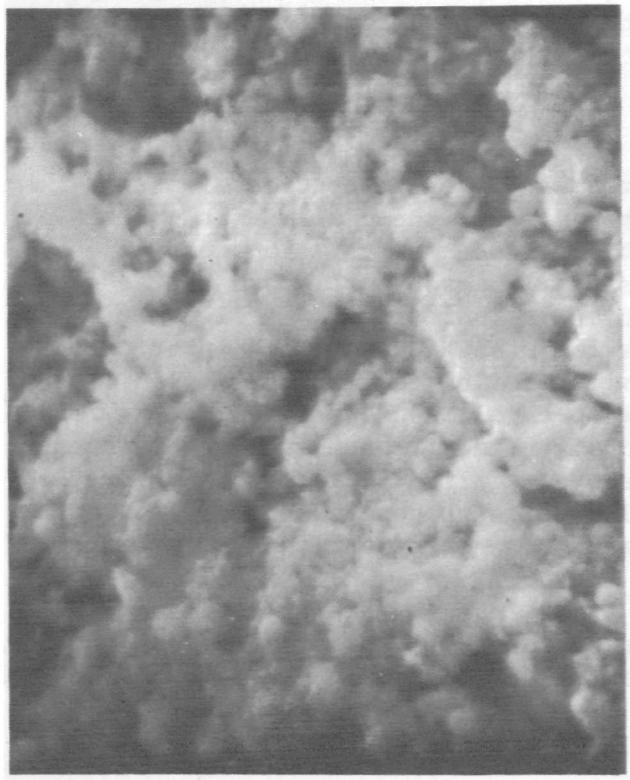

C. 7221A. Calcine (x 17,340)

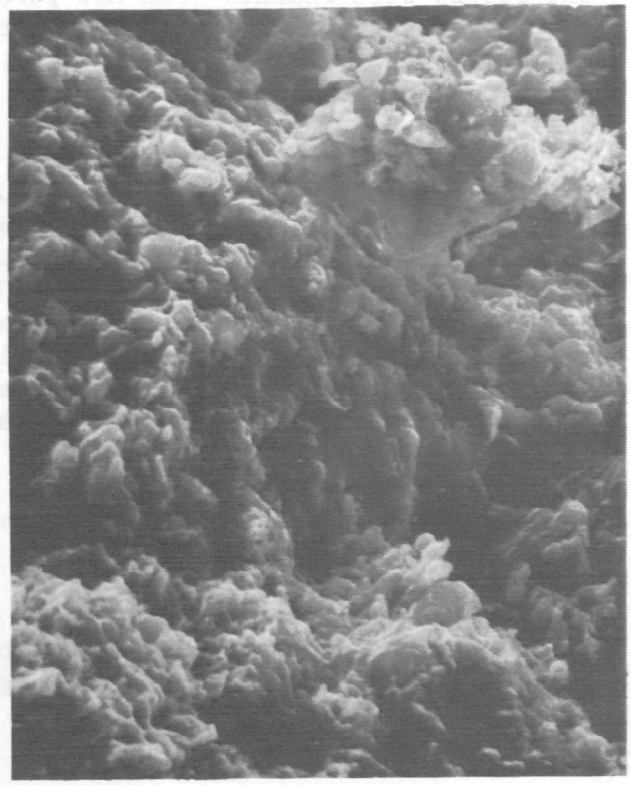

D. 7227B. Calcine (x 1912)

Plate 8 - Texture of calcined (lime) samples of chalks shown in plate 7.

A. 7220. Calcine of sparry calcite (x 510)

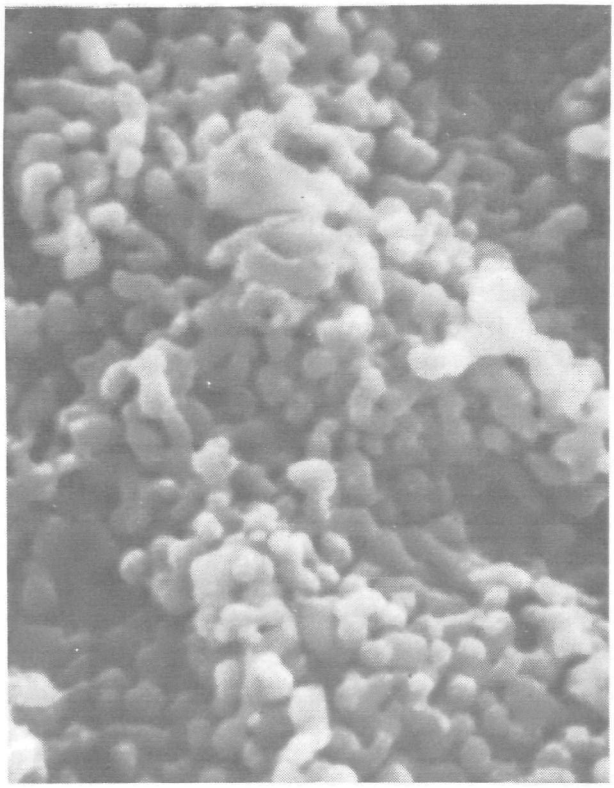

B. 7220. Close up of (A) (x 10,670)

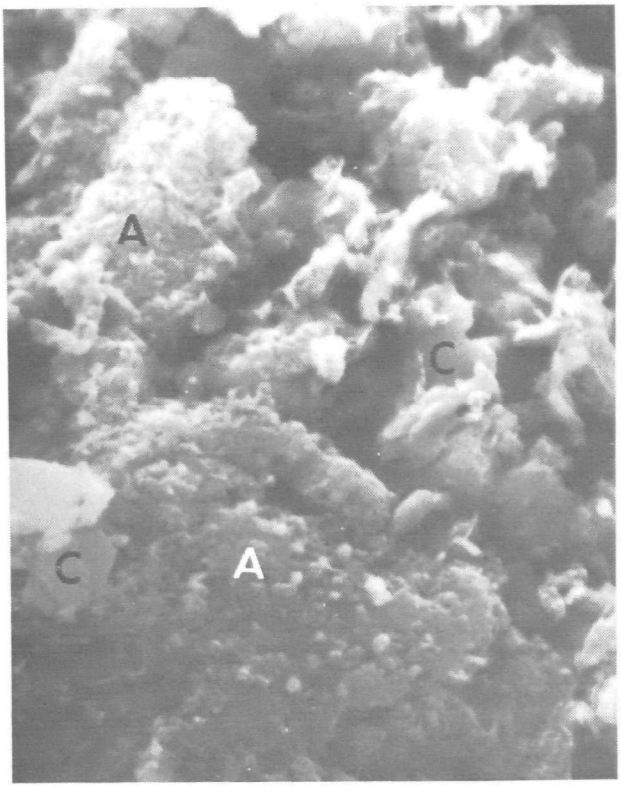

C. 7208C. Porous aggregate (A) and clay (C) (x 8200)

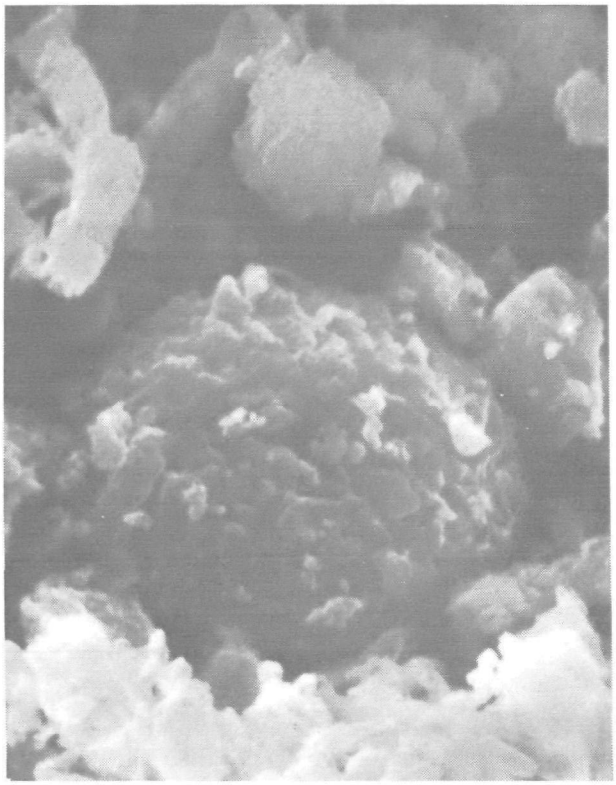

D. 7208C. Calcine of coccolith (x 8230)

Plate 9 - Texture of the calcine (lime) from three types of calcite in chalks.

chalks tested. The pore-volume curves for 7201 and its calcine are shown in figure 19. Although this sample is not of high purity (84.5% $CaCO_3$), the uniformly fine pores created during calcination (mean size of 0.035μ, fig. 19) and the corresponding large surface area (14.1 m^2/g rock) suggest that this material should be highly reactive and absorptive for SO_2.

In table 5, distinct differences can be seen among the samples studied from the three chalk formations within the Selma Group (Demopolis, Mooreville, and Prairie Bluff). The large surface areas of the samples of the Demopolis and Prairie Bluff strongly indicate the presence of abundant pores less than 0.012μ in diameter. These extremely small pores are not measurable with a 15,000 psi mercury porosimeter and are not resolved on the electron micrograph of the chalk shown in plate 2B. Pore-volume curves typical for the Selma Group samples and their calcines are shown in figure 20. On calcination, the Demopolis and Prairie Bluff samples lose considerable surface area. Therefore, the calcination process must have enlarged many of the very fine pores existing in the chalks in addition to creating some new pores within the original calcite grains. Pore enlargement is seen in figure 20 (samples 7206 and 7230) as a leftward shift of the calcine pore-volume curves. The second step (< 0.1μ pore diameter) in the calcine pore-volume curves for samples 7206 and 7230 (fig. 20) is probably due to the creation of new pores during calcination. The Mooreville sample (7204) is quite different petrographically from the Demopolis and Prairie Bluff chalks (table 9), and this difference is reflected in its pore-volume curves (fig. 20). On calcination, the surface area of sample 7204 increases from

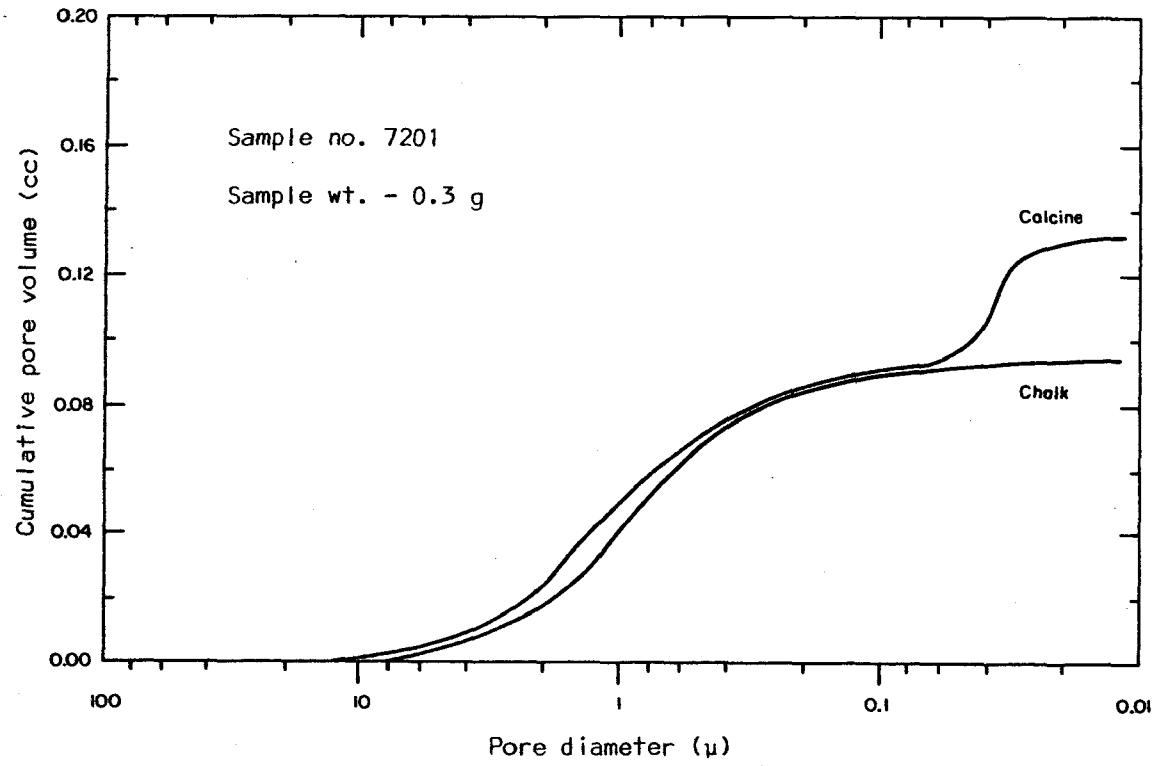

Fig. 19 - Pore-volume curves for sample of chalk of the Marianna Limestone (7201) and its calcine.

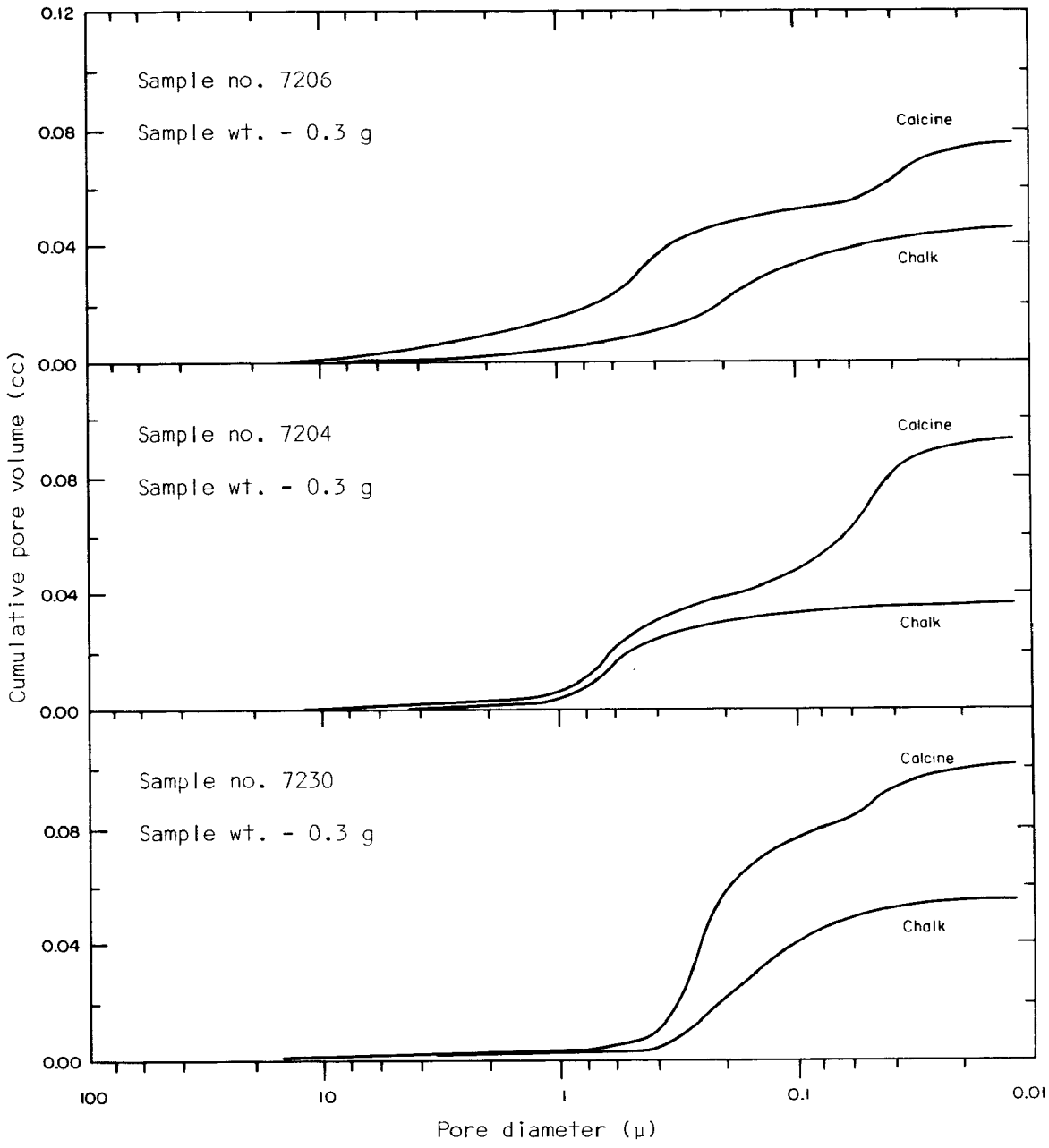

Fig. 20 - Pore-volume curves for samples of the Selma Group and their calcines: Prairie Bluff Chalk (7206), Arcola Limestone Member of the Mooreville Chalk (7204), Demopolis Chalk (7230).

3.1 to 11.3 m^2/g. Therefore, most of the porosity created by calcination must have resulted from the formation of new pores rather than from the enlargement of existing pores. This is inferred from the pore-volume curves for 7204 shown in figure 20.

The average pore volume for all the samples of the Niobrara is 0.21 cc/g, and their average mean pure size is 0.40μ. The surface areas of all the Niobrara samples increased on calcination. The pore-volume curves for samples 7209 and 7214A and their calcines (fig. 21) are typical of those obtained from most of the Niobrara samples. They show that in addition to the creation of many new pores within the micrite and sparite grains some enlargement of existing pores occurs on calcination. The pore-volume curves for sample 7213 and its calcine also are shown in figure 21. The pore-volume increase on calcination of sample 7213 is 0.216 cc/g rock whereas the theoretical pore-volume increase is 0.185 cc/g rock. This difference indicates that closed pores existed in the chalk and were opened up on calcination. This opening occurred in addition to the enlargement of existing pores and the creation of new pores. The opening up of previously closed pores is shown by the vertical displacement of the calcine pore-volume curve for sample 7213 in figure 21. The pore-volume curves for sample 7208C and its calcine (fig. 21) are distinctive in that no detectable enlargement of existing pores appeared after calcination.

The average pore volume of the chalk samples from the Austin is 0.14 cc/g, and their average mean pore size is 0.184μ. Both values are measurably smaller than those of the Niobrara samples. The surface areas of the Austin chalks are intermediate between those of the Demopolis and the Niobrara. Pore-volume curves for Austin samples 7221A and 7222B and their calcines are shown in figure 22. The surface areas of the calcines are lower than those of the chalks (table 5), and hence, on calcination, enlargement of existing pores predominates over the creation of new pores in these chalks. The fine pore structure of calcined 7221A is shown in plate 8C.

The pore-volume curves for sample 7225 (Pecan Gap) and its calcine are shown in figure 22. The calcine of this sample has the smallest mean pore size of all the calcined samples and there is no dominant mode of pore size below 0.1μ.

The pore-volume curves for Annona samples 7226A and 7227B, Saratoga sample 7228, and their calcines are shown in figure 23. All of these samples lost surface area on calcination. The pore-volume curves show that both enlargement of existing pores and creation of new pores occurred on calcination.

Chalky Limestones

Samples classified as chalky limestones (table 9) are those that have low porosity (bulk density > 2.20 g/cc or pore volume < 0.10 cc/g [table 5]) or have porosities slightly higher than these criteria but in combination with a large average grain size (mean chord length > 3μ). We include the results of tests of these samples even though they are not true chalks, because several possess properties very similar to those of chalks and may have high potential use for SO_2 control in certain areas of the country.

The results of pore-volume tests of these samples and their calcines are given in table 13. Two of the samples of the Greenhorn Limestone and the sample of the Comanche Peak Limestone have relatively high pore volumes. In nearly every case, the observed increase in pore volume on calcination is greater than the theoretical increase, an indication that these samples, as opposed to most of the chalks, have some completely closed pores or pore openings smaller

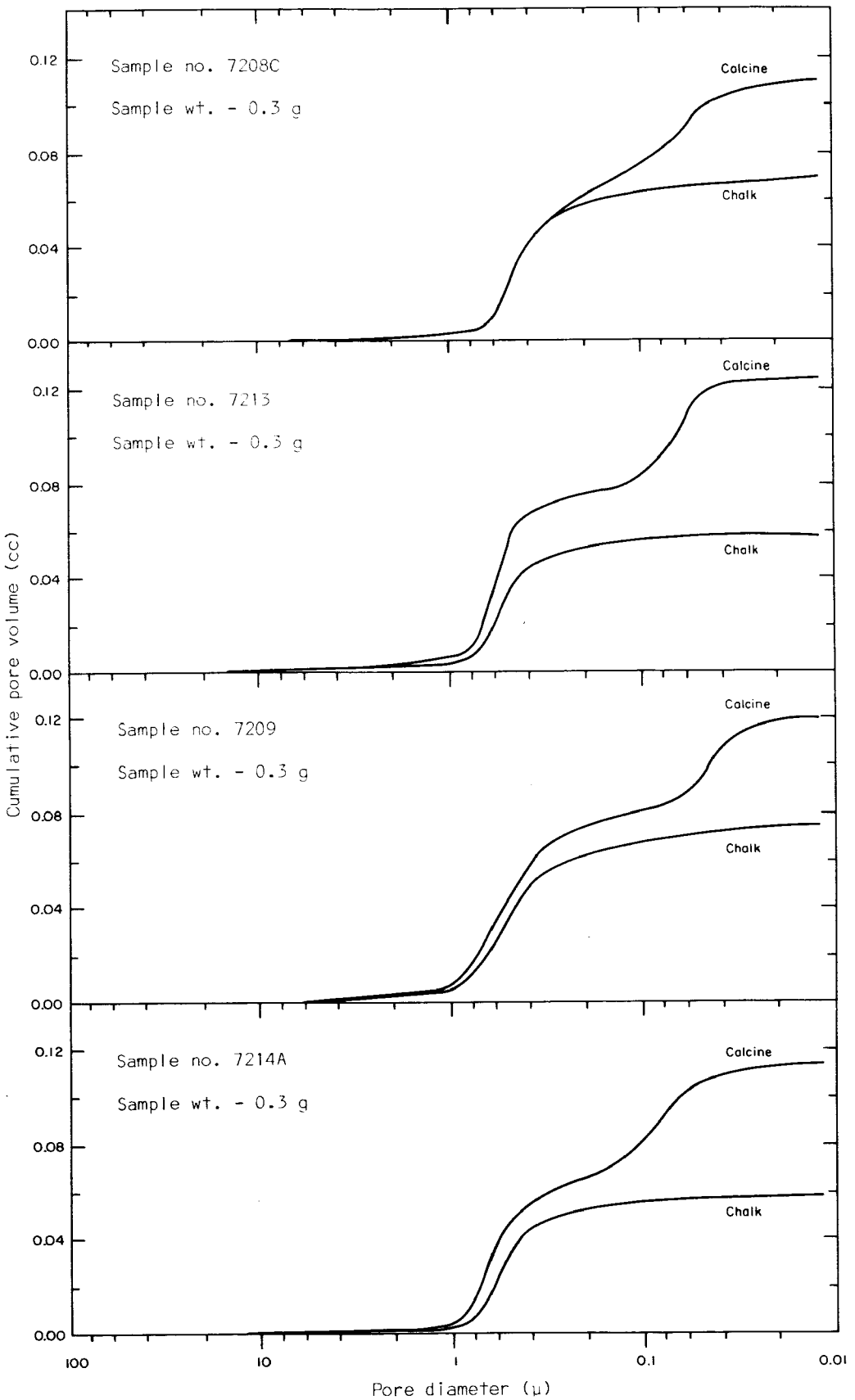

Fig. 21 - Pore-volume curves for samples of the Ft. Hays Limestone Member of the Niobrara Chalk and their calcines.

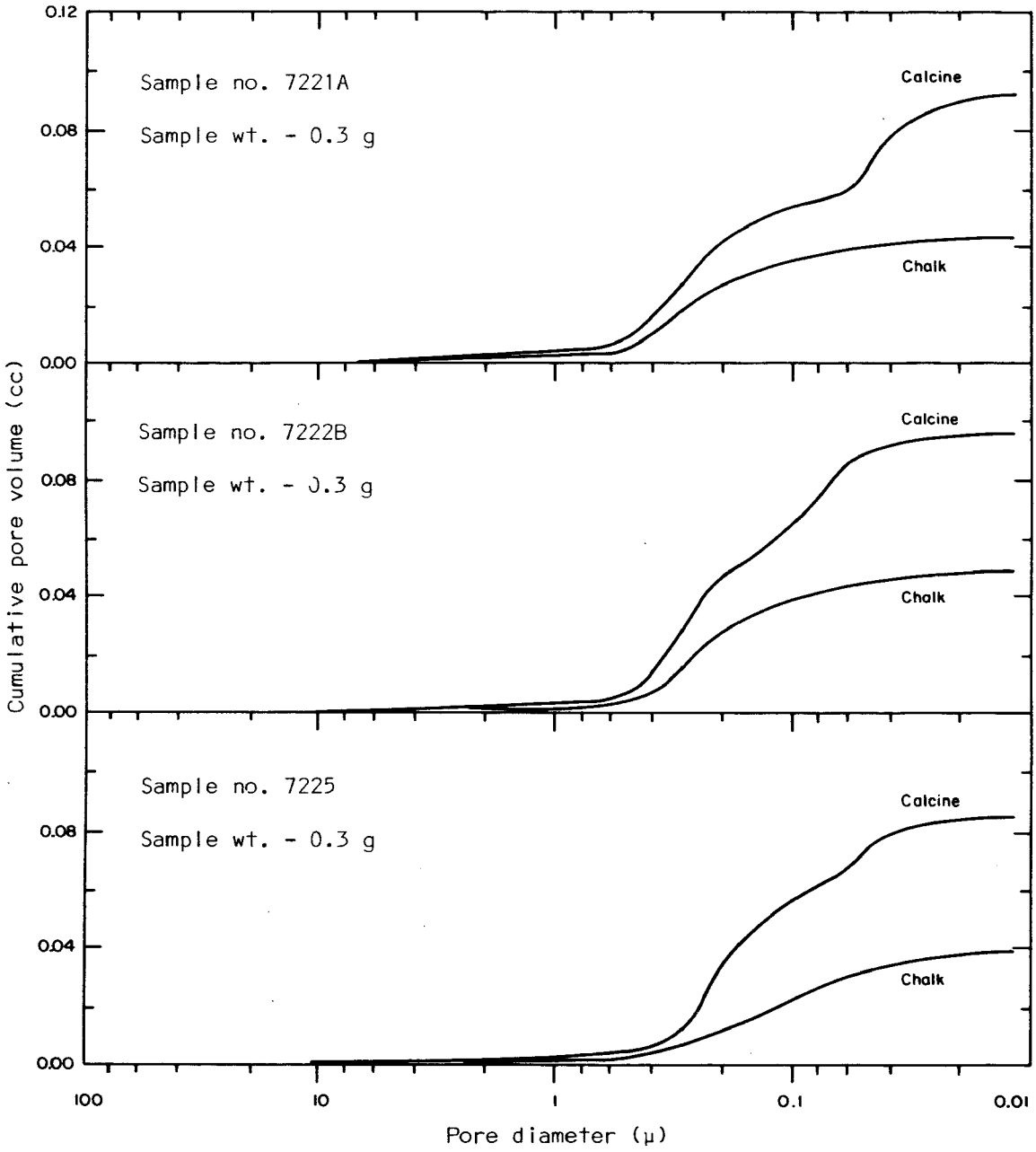

Fig. 22 - Pore-volume curves for samples of the Austin Chalk (7221A and 7222B), the Pecan Gap Chalk (7225), and their calcines.

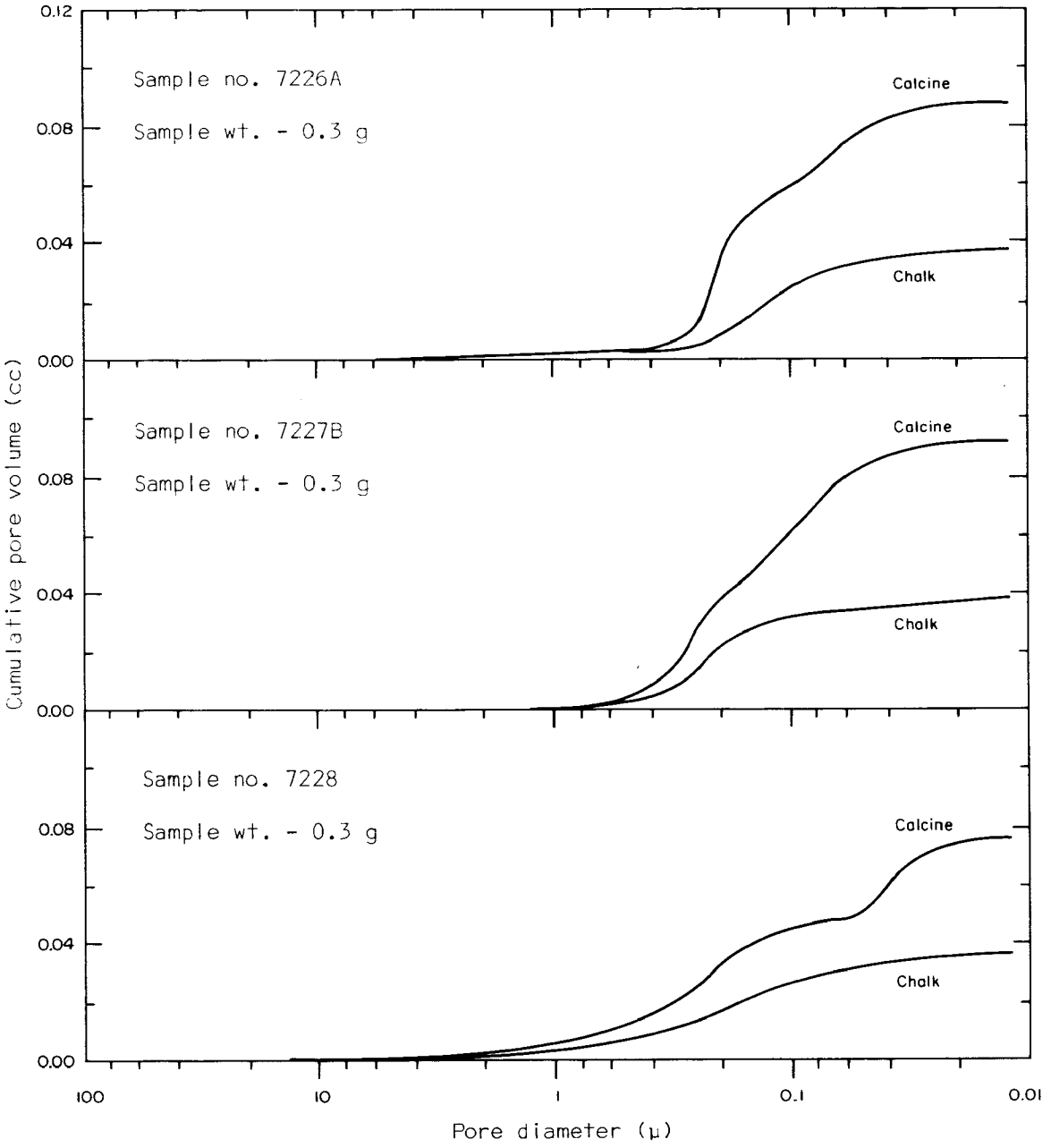

Fig. 23 - Pore-volume curves for samples of the Annona Chalk (7226A and 7227B), the Saratoga Chalk (7228), and their calcines.

than 0.012μ that are opened up during calcination. The surface areas of the chalky limestones are less than 6 m^2/g for those tested.

The pore-volume curves shown on figure 24 for typical chalky limestones and their calcines are similar to those obtained for chalks and their calcines.

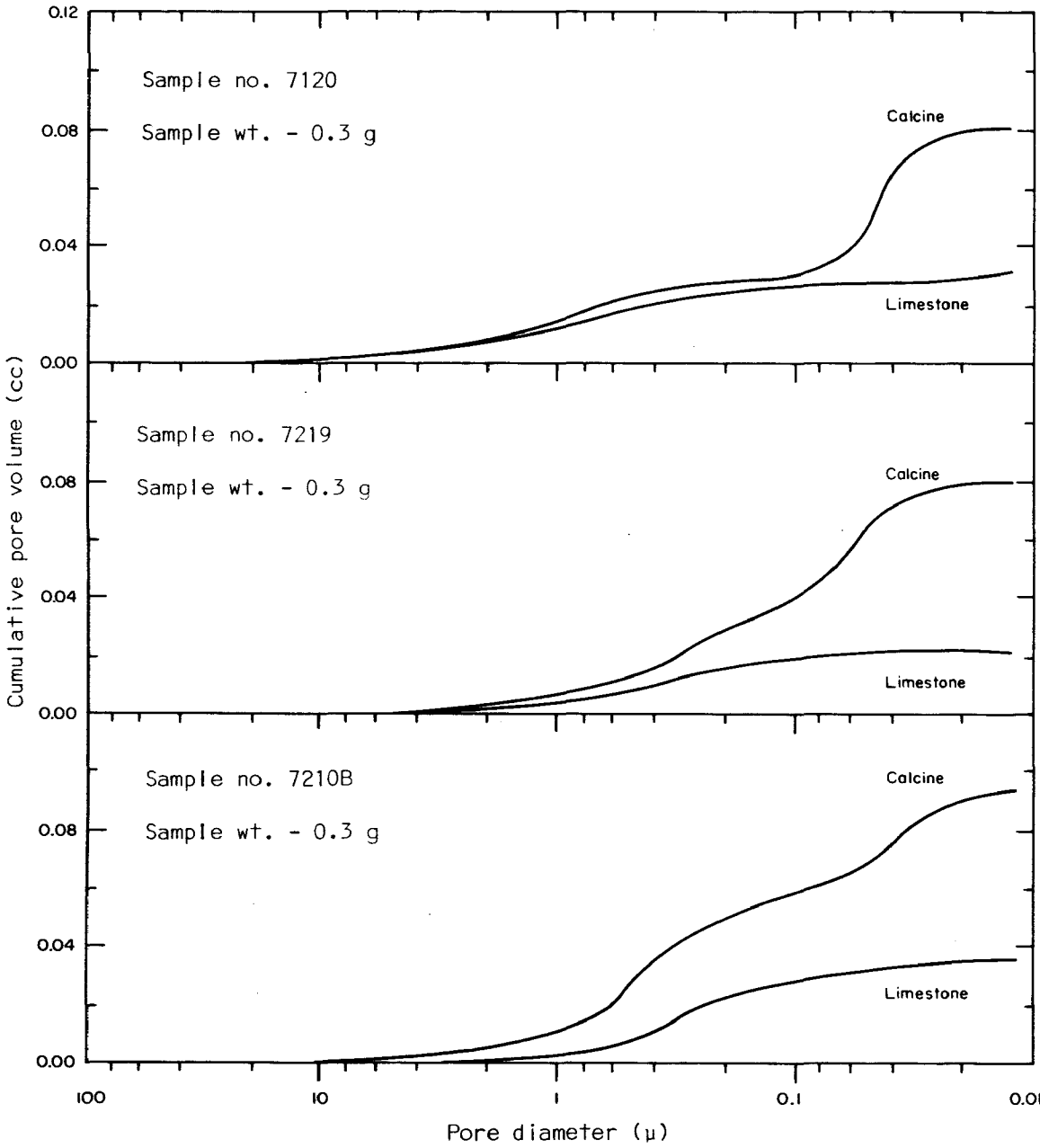

Fig. 24 - Pore-volume curves for samples of chalky limestones and their calcines: Crystal River Formation (7120), Dessau Member, Austin Chalk (7219), Greenhorn Limestone (7210B).

The calcine of sample 7120 has pores predominantly in the size range of 0.04μ to 0.06μ. Little enlargement of pores previously existing in the stone was observed. The other type of calcine pore structure is that shown by sample 7210B (fig. 24). In this sample, a bimodal pore-size distribution in the calcine is observed—a large number of pores have a diameter of about 0.04μ and a second

pore-size mode occurs at about 0.6μ. In this sample, a considerable enlargement of limestone pores, together with the opening up of isolated limestone pores, occurred in the size range from 0.1μ to 1μ. The pore structure and behavior of sample 7219 is intermediate between that of the other two samples illustrated in figure 24.

The surface areas of the calcines of chalky limestones have a wide range, 2.9 to 14.9 m^2/g rock. In each sample measured, a large increase in surface area was observed on calcination. This increase also reflects the existence of isolated or closed pores in the limestone material.

SHELL, COQUINA, CALICHE, AND SLUDGE INVESTIGATIONS

Sources of Samples

The Anastasia Formation (Pleistocene) consists predominantly of sea shells and coquina and occurs extensively along the east and west coasts of Florida (DuBar, 1958, p. 38-39). This formation was sampled on an offshore bar near Turtle Beach, Florida (7121). Sample 7121A represents the surface shells and 7121B the underlying shells, which contain some sand. Only the upper 4 feet of the Anastasia at Turtle Beach was sampled.

Certain carbonate rocks occurring in Pleistocene strata of southern Florida are coquinas (shells partly cemented together) such as those that occur in the Caloosahatchee Marl (DuBar, 1958). Two samples of this formation were collected from the pit of J. Cochran, just west of La Belle, Florida (7122). In this pit, the lower 5 feet of the quarried stone is coquina that consists of soft, incoherent carbonate shells partly cemented with fine powdery calcite (sample 7122B). The upper 2 feet quarried is a fairly hard chalky limestone bed containing large pores and small gastropods (sample 7122A). Other formations in Florida contain similar carbonate rocks (Vernon, 1943).

Another formation that contains abundant shell material, partly cemented, is the coquina facies of the Yorktown Formation in eastern Virginia (Coch, 1968). Fifteen feet of coquina exposed above the water level in the Lone Star Industries pit at Chuckatuck was sampled in three units and combined in the laboratory into a composite sample (7203). Lone Star Industries processes the coquina to produce a concentrate of shells for use in the manufacture of cement. Sample 7203D was taken from the stockpile of washed and otherwise processed coquina.

Shells are dredged from shallow waters at various locations along the Atlantic and Gulf Coasts. Two examples of such shell deposits were obtained from the Radcliff Materials, Inc. of Mobile, Alabama—one of clam shells from Lake Pontchartrain, Louisiana (7124), and one of oyster shells from Mobile Bay, Alabama (7125).

Caliche is another type of fine-grained carbonate rock type that is found in the Ogallala Formation in Kansas, New Mexico, and Texas (Frye and Leonard, 1959). Caliche was sampled at two localities. In Kansas, caliche was collected from an outcrop just south of the Cedar Bluff Reservoir dam (7215); and in Texas, a sample was obtained from an operating quarry (7218) producing road rock. Kottlowski (1962) describes occurrences of other types of high-calcium limestone deposits in New Mexico.

A very fine grained carbonate (calcite) sludge is a waste product from the Kraft paper manufacturing process. The Edwards Paper Company, Port Edwards, Wisconsin, uses this process, and a sample (7153) was taken from its sludge pile for inclusion in this study.

Characterization of Samples and Their Calcines

Samples classified as shell are from localities 7121, 7124, 7125, and 7203 (app. 2); these deposits are located along the coast of the Gulf of Mexico in Florida, Alabama, and Louisiana and on the east coast of Virginia (fig. 5). Chemical and mineral analyses of the samples are given in table 14. More than 70 percent (by weight) of the shells in 7121A are bivalves of Chione cancellata (family Veneridae). A few bivalve shells belonging to other families also occur. Less than two percent of the sample consists of gastropod shells. The shells in this sample consist mainly of the mineral aragonite. Sample 7121B, augered from below 7121A, has types of shells identical to those in 7121A but differs in that a considerable amount of quartz sand is present. These samples were obtained from an offshore bar, and similar shells occur all along this bar. According to H. S. Puri (1971, personal communication), they are from the Anastasia Formation (Pleistocene in age), which is a source of commercial shells elsewhere in Florida.

Sample 7124 contains shells of clams (Rangia), 3/4 inch to 1 1/4 inches across, gray, and consisting of aragonite. Sample 7125 contains gray shells of oysters (Ostrea) about 4 inches long and 2 inches wide and composed of calcite. Both of these samples are from shell beds that are commercially dredged and processed.

Microscopic examination reveals that the shells in each of these samples consist of fibrous crystallites of aragonite or calcite (pl. 10). In the clam shells, the fibers are laminated in two or more directions (pl. 10A) and the fibers in each lamella are nearly parallel to each other. In Chione, pores 0.1μ to 0.5μ across occur intermittently along the boundaries of the fibers (pl. 10B), and in the oyster shells, larger pore channels occur (pl. 10C). Shells observed in transmitted polarized light are birefringent, and each fiber has a slightly different orientation from that of neighboring fibers.

Samples 7122B (coquina) and 7123 (sandstone) are from the Caloosahatchee Marl (Pleistocene) and contain abundant gastropods up to 4 inches long, numerous bivalves, irregular and cylindrical "worm tubes," and a few other types of calcareous fossils and fossil fragments. Fine-grained calcite and quartz silt occur

TABLE 14 — CHEMICAL AND MINERAL ANALYSES OF SHELL AND OTHER CARBONATE SAMPLES
(Analyses by Analytical Chemistry Section, Illinois State Geological Survey)

Sample	7121A	7121B	7122B	7124	7125	7203	7203D	7215	7218	7153
ROCK TYPE	Shell	Shell	Coquina	Shell	Shell	Coquina	Coquina	Caliche	Caliche	Waste sludge
CHEMICAL ANALYSES (%)										
SiO_2	1.36	34.3	22.6	0.88	0.37	—	7.31	33.3	38.4	nil
Al_2O_3	0.05	nil	0.70	nil	0.34	—	nil	1.73	2.32	0.02
Fe_2O_3	0.06	0.11	0.36	0.12	0.49	—	1.55	0.42	0.57	0.19
MgO	0.13	nil	0.73	0.10	0.06	—	0.15	0.85	1.28	0.52
CaO	53.4	35.4	40.5	54.0	53.9	—	49.1	33.6	29.2	53.8
Na_2O	0.60	0.49	0.25	0.34	0.41	—	0.43	0.30	0.24	0.85
K_2O	0.09	nil	0.08	0.03	0.04	—	0.07	0.92	0.85	nil
H_2O	0.87	nil	1.33	0.92	0.96	—	0.62	0.60	1.65	1.76
CO_2	41.96	28.78	32.53	42.71	42.50	—	38.78	22.99	23.70	41.47
SO_3	0.07	0.11	0.09	nil	0.09	—	0.59	0.03	0.04	0.14
MINERAL ANALYSES (%)*										
Calcite	XX (95)†	XX (63)†	XXX (72)†	nil	XXX(96)	XXX	XXX	XXX(61)	XXX(54)	XXX(96)
Aragonite	XXX	XXX	XX	XXX(96)	nil	XX(81)†	XX(88)†	nil	nil	nil
Quartz	nil	XX	XX	nil	X	XX	X	XXX	XXX (cherty)	nil
Clay	nil	nil	nil	X	X	XX (glauconite)	nil	nil	X (illite)	nil
Other	nil	nil	nil	nil	Mica-X	Magnetite-X Mica-X	nil	nil	Feldspar-X Opal-X Magnetite-X	Organic-X

*Relative abundance: XXX = > 20%, XX = 1% to 20%, X = < 1%.
†Value is the sum of the percentages of calcite and aragonite.

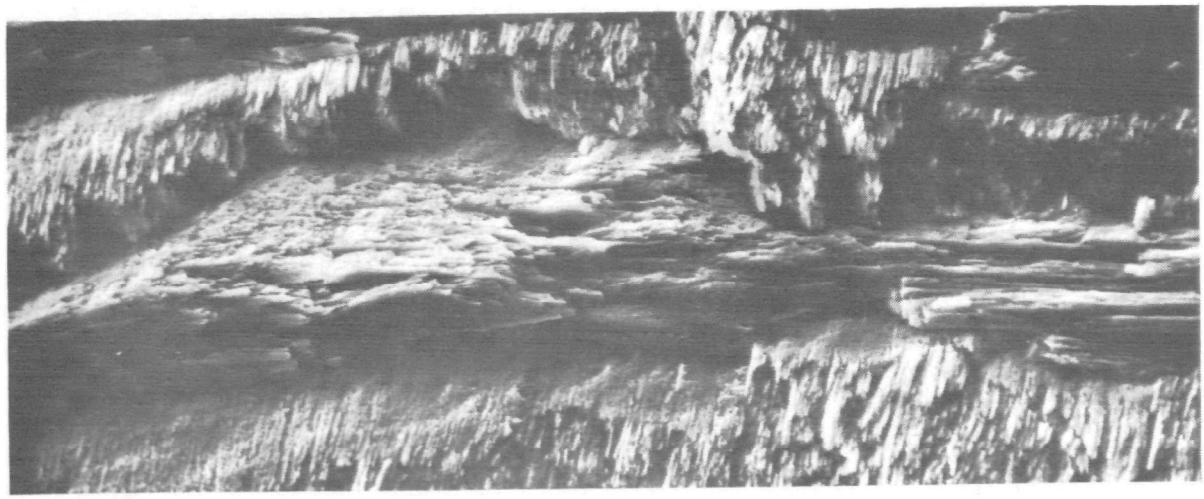

A. Clam shell from 7124 ⌊ 20μ ⌋ (x 930)

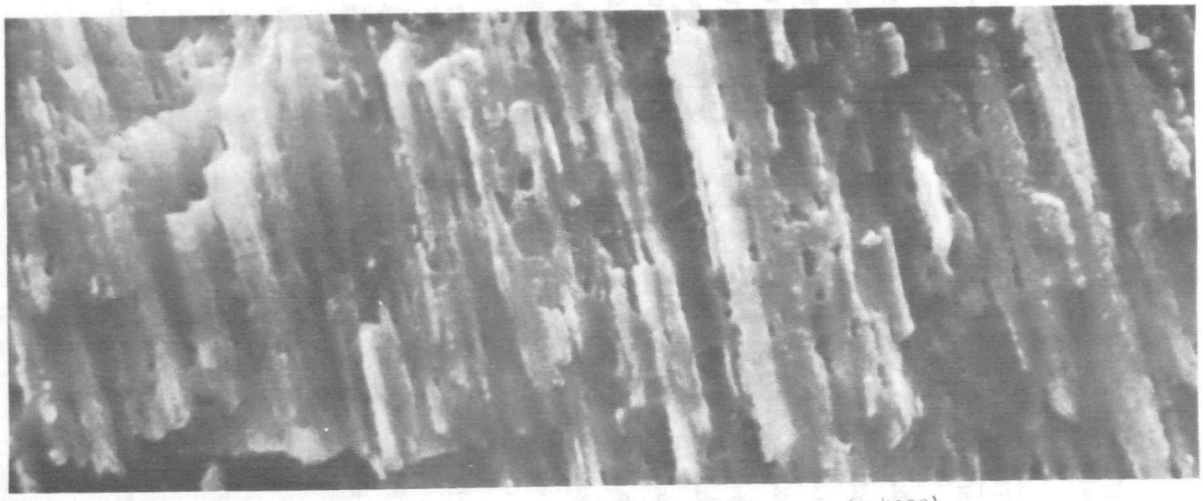

B. Chione from 7121A ⌊ 5μ ⌋ (x 4120)

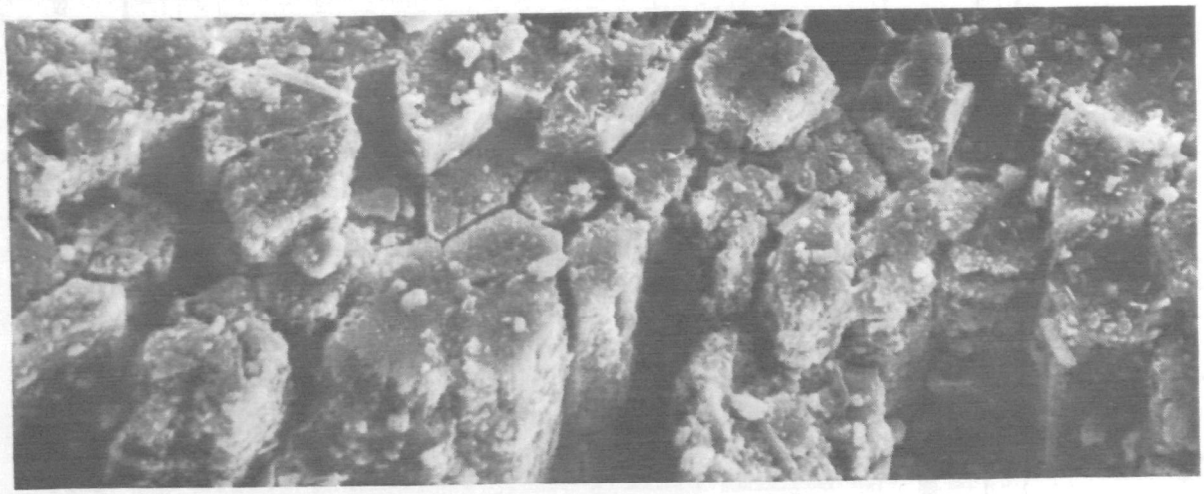

C. Oyster shell from 7125 ⌊ 20μ ⌋ (x 1100)

Plate 10 - Characteristic textural features of shells.

between the shells. Less than 3 miles to the northeast (loc. 7123), the beds sampled at 7122 grade laterally into more impure coquina and into quartz-rich sands containing only a few shells.

Pore structures and surface areas of the shell and other samples of the group and their calcines are listed in table 15. The total pore volumes of shell samples are characteristically very low; these data show an average of 0.014 cc/g. The pore-volume curves for shell 7124 and its calcine shown in figure 25 are similar to those for other shells and their calcines. The pore-volume curve of the calcined shell 7124 shows a rather narrow distribution of pore sizes (fig. 25). Mean pore sizes of shell calcines are large; they range from 1.5μ to 2.3μ (table 15).

The coquina and shell samples increased in pore volume on calcination at 850° C from 0.156 to 0.215 cc/g rock. Electron micrographs of shell calcines confirm the absence of small-diameter pores in the calcines, as shown by plate 11A. The CaO grains, about 1μ to 4μ in diameter, are rounded and partly fused together.

A sample of caliche, 7218 (table 15), has a low pore volume and its calcine has a very low pore volume in comparison with the calcines of other carbonate rock types because it contains high quantities of quartz sand impurity, typical of caliche. The pore structure of sample 7215 was not determined.

Sample 7153, a carbonate sludge from a paper manufacturing plant, is of special interest because it is a waste product. The sludge consists of precipitated calcite (table 14) with about 4 percent organic matter as the only impurity. The sludge consists of particles that are in large measure composed of single grains, 0.5μ to 2.0μ across, with only slight grain-to-grain interlock. The pore volume (170x200-mesh) for the sample tested was 0.27 cc/g, which probably included a moderate fraction of intergranular void space. The sludge had a mean pore size of 1.5μ. Pore-structure data for the sludge and its calcine are listed in table 15. The sample was calcined at 800° C and at 850° C; the penetration-volume curves for the uncalcined sample and the calcines are shown in figure 26. The calcined sludge resembles calcined shell in its granular texture. The CaO grains, about 0.3μ to 2.0μ in diameter, are spherical and smooth (pl. 11B). Since the pore volumes of the 850° C calcine and the sludge material are nearly identical, the pores that were formed within single calcite grains during the early stages of calcination (800° C) were very rapidly eliminated by fusion of the lime to form grains about 1μ across.

TABLE 15 — PORE STRUCTURES OF SHELL AND OTHER CARBONATE SAMPLES AND THEIR CALCINES (16x18 MESH PARTICLES)

Sample number	ROCK			CALCINE (850° C)				
	Type	Pore volume (cc/g)	Mean pore size (μ)	Pore volume (cc/g rock)	Mean pore size (μ)	Observed pore-volume increase (cc/g rock)	Theoretical pore-volume increase (cc/g rock)	Surface area (m^2/g rock)
7121A	shell	0.006	0.30	0.207	2.3	0.201	0.171	1.1
7121B	shell	0.013	0.30	—	—	—	—	—
7124	shell	0.014	0.15	0.221	1.5	0.207	0.165	0.3
7125	shell	0.023	0.15	0.240	1.8	0.217	0.192	0.3
7122B	coquina	0.106	0.41	0.262	0.7	0.156	0.145	2.1
7203D	coquina	0.039	0.56	0.235	1.5	0.196	0.168	0.5
7218	caliche	0.039	0.25	0.157	—	0.118	0.176	7.2
7153(1)*	sludge	0.270	0.15	0.270	—	—	0.192	0.5
7153(2)*,†	sludge	0.270	—	0.415	—	0.145	0.192	—

*The particle size of samples 7153(1) and 7153(2) tested was 170x200 mesh.
†Calcined at 800° C.

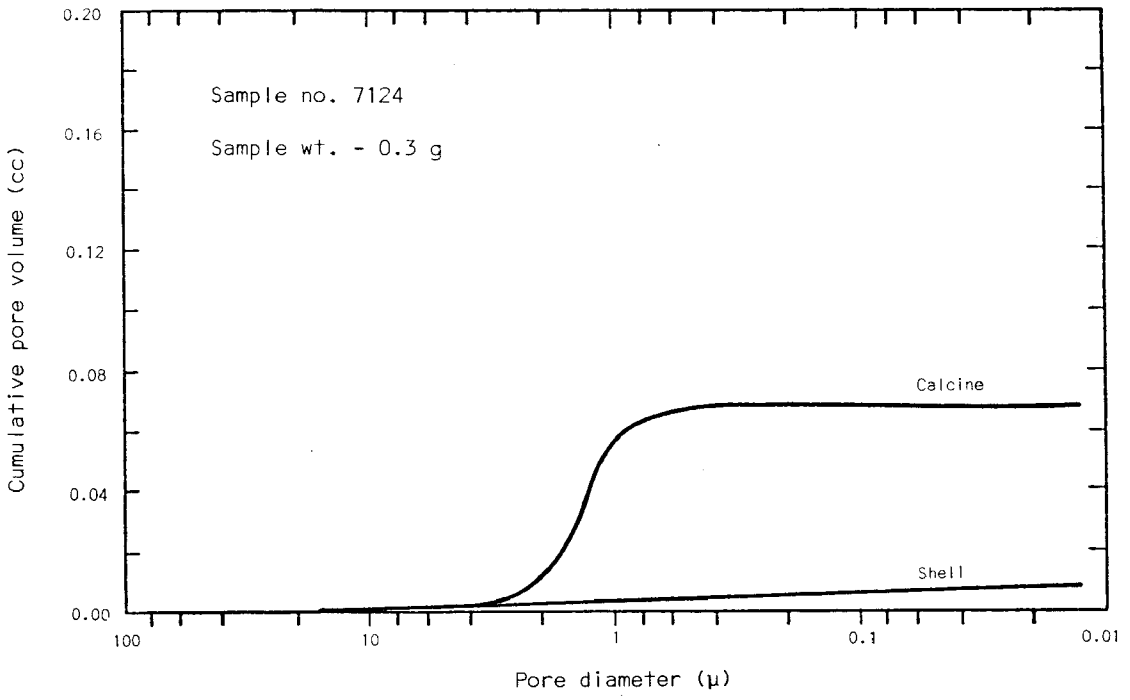

Fig. 25 - Pore-volume curves for 16x18 mesh particles of clam shell 7124 and its calcine.

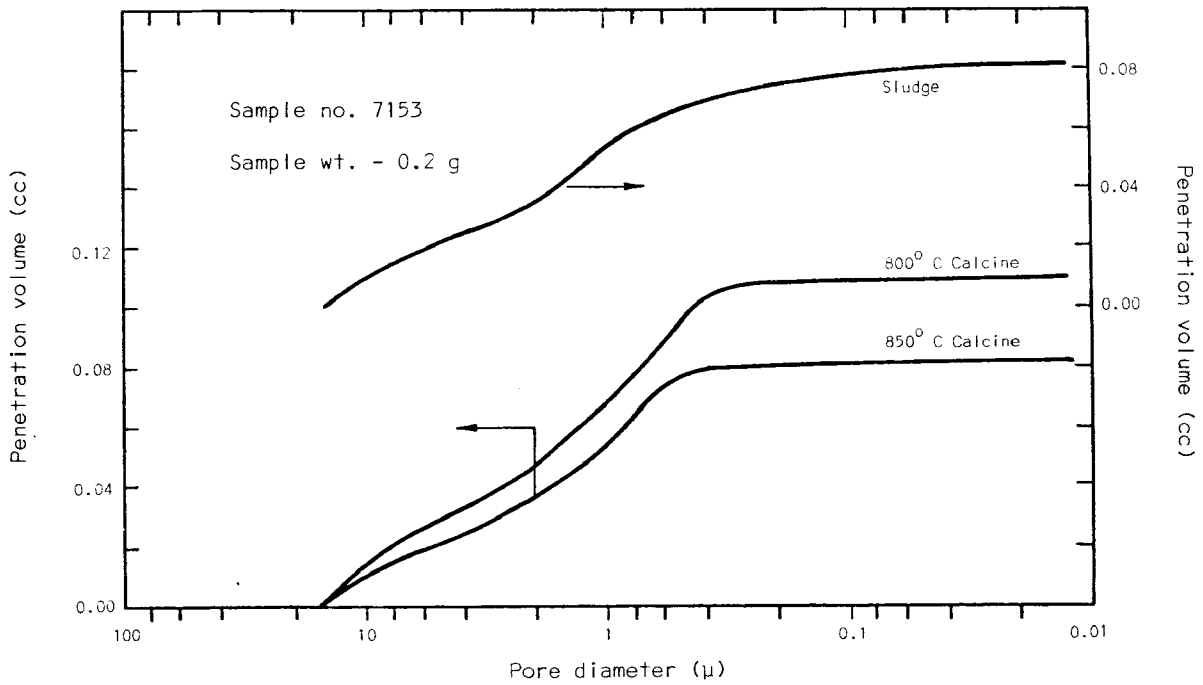

Fig. 26 - Penetration-volume curves for 170x200 mesh particles of carbonate sludge 7153 and its calcines.

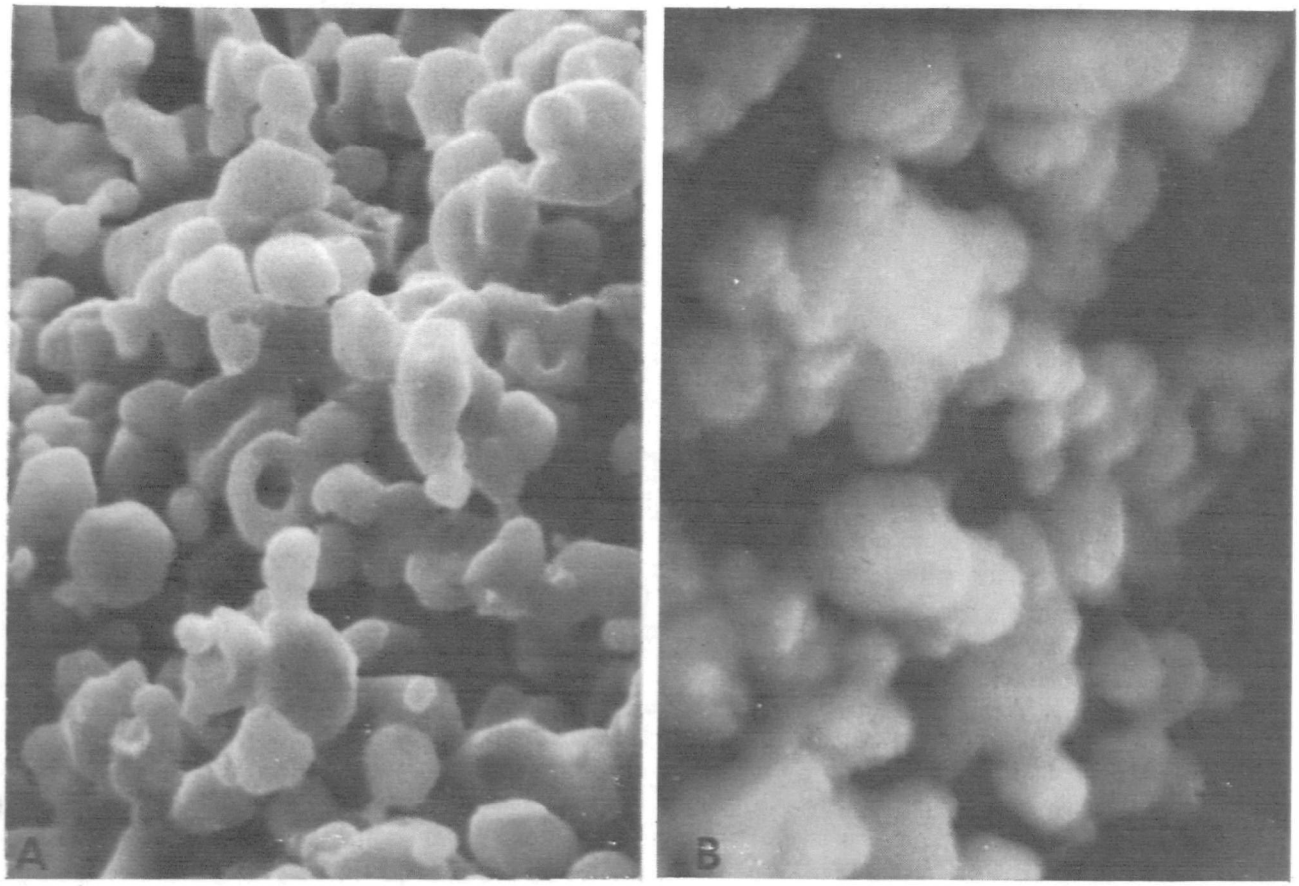

Plate 11 - A. Relatively smooth and coarse grains of lime in calcined shell material, 7124 (x 4500); B. Relatively smooth and fine grains of lime in calcined sludge, 7153 (x 14,250).

INVESTIGATION OF CARBONATE ROCKS RELATED TO PREVIOUS FLUIDIZED BED DESULFURIZATION TESTS

Certain carbonate rocks have been used in pilot plant tests of fluidized bed desulfurization of flue gases. In these tests, crushed limestone or dolomite has been added to the combustion chamber to react with the SO_2 that is produced therein from the fuel. A number of advantages are associated with this process and the experiments are described in detail in reports to the U.S. Environmental Protection Agency (Robison et al., 1970; Jonke et al., 1971; Hammons and Skopp, 1971; and Craig et al., 1971). Two advantages of this process are the recovery of calcined additive composed of lime and the recovery of SO_2 in a form suitable for conversion to elemental sulfur or sulfuric acid. Favorable results were obtained from these pilot plant tests.

Problems experienced in these tests associated with the carbonate rock additives were excessive attrition of particles of certain samples by decrepitation or breakage during high temperature treatment and excessive agglomeration of one sample (sample no. 1690, described below) during the lime regeneration cycle. It was deemed useful to conduct petrographic studies of certain samples tested in the fluidized bed process to assess possible causes for the high decrepitation and agglomeration that occurred.

Samples and Their Relative Decrepitation

The samples selected for study were supplied by Dr. Dennis Drehmel, Control Systems Laboratory, U. . Environmental Protection Agency. The samples are listed in table 16 and their sources noted by footnote. Fluidized bed tests

TABLE 16 — PETROGRAPHY, PORE STRUCTURES, AND DECREPITATION TEST RESULTS

SAMPLE NUMBER	1690[a]	2231[b]	1691[c]	2257[d]
ROCK TYPE	dolomite, sandy and calcitic	dolomite	limestone, dolomitic	limestone, fossiliferous
TYPES OF CALCITE (%)	micrite (6) sparite (5)	None	micrite (90) sparite (10)*	micrite (52) sparite (48)
MEAN GRAIN CHORD, $\bar{c}$ (μ)	47	19	4	10
GRAIN DEFECTS[†]				
Point	1678	987	407	659
Line	129	30	15	62
PORE VOLUME (cc/g)	0.0084	0.0250	0.0056	0.020
CALCINE				
Pore volume (cc/g)	0.150	0.210	0.192	0.200
Mean pore size (μ)	0.039	0.051	0.110	0.060
Pore-volume increase (cc/g rock)	0.142	0.185	0.186	0.180
Theoretical increase (cc/g rock)	0.145	0.182	0.174	0.182
Surface area (m^2/g rock)	13.8	13.9	4.9	13.9
DECREPITATION (%)	3.67	0.23	0.0	3.68

*Includes dolomite grains > 10μ diameter.
[a]McConville, Inc., Ogdensburg, New York
[b]C. E. Duff & Sons, Huntsville, Ohio (Tymochtee Dolomite).
[c]Warren Bros. Road Construction, Syracuse, New York.
[d]Denbighshire, Northern Wales, United Kingdom.
[†]Number in 100 carbonate grains that are > 50μ diameter times percentage of > 50μ grains in sample.

of samples 1690 and 2257 gave relatively high attrition rates, whereas sample 1691 produced a low attrition rate (Craig et al., 1971). In addition, the tests of Craig showed excessive agglomeration of sample 1690. The relative rate of attrition of sample 2231 in fluid bed tests is not known at this time.

As the attrition by decrepitation of limestone particles is routinely evaluated by glass manufacturers, the samples were tested using the same procedure (Bitner,* personal communication). The test measures the relative amount of crushed sample that explodes over the sides of a sample container (long, thin boat) during exposure to 1100° C. Results of our tests on the samples studied are given in table 16. These results are in agreement with the results of relative attrition in fluidized bed tests (Craig et al., 1971).

Characterization of Samples

The samples received were of a crushed product from a commercial source. Representative splits of the samples were prepared and analyzed as described in the first section of this report. As these samples consist of a variety of types of particles, it is interpreted that the types were derived from different beds or strata within the commercial quarry. The most typical granular texture of each sample is shown photographically in plate 12. Measurable petrographic parameters, including relative frequency of line and point types of grain defects observed optically within the carbonate grains and the pore-volume data for the samples and their calcines, are listed in table 16. The pore-volume curves for the rocks are very much the same and show little porosity. The mean pore sizes of the calcines range from 0.039μ to 0.110μ (table 16). The pore-volume curves for the calcines are shown in figure 27.

Mineral and chemical analyses are given in table 17.

Sample 1690 is a sandy dolomite. It has an inequigranular mosaic texture (pl. 12A). About 89 percent of the particles (or beds) contain rounded grains of quartz and feldspar sand, 80μ to 100μ across, that are abundantly scattered among rhombic and irregular grains (50μ to 500μ) of dolomite. The dolomite grains are generally tightly interlocked. Some particles consist of micritic type of calcite with scattered dolomite rhombs. Other particles consist almost entirely of quartz and feldspar grains. Others (5 percent of the particles) consist of coarse sparry calcite. Several particles contain clay.

Sample 2231 is a medium-grained dolomite. It has an equigranular mosaic texture (pl. 12B). Grain shapes are commonly equidimensional with v-points which make a tight grain-to-grain interlock. In most particles the size of the grains is fairly constant, mostly around 40μ in diameter; other particles have grains mostly 20μ in diameter. Some particles are porous and contain rhombic dolomite grains. Impurities are rare iron-stained grains of quartz and feldspar, mostly 50μ in diameter, and clay, which are especially concentrated in parallel bands in certain particles.

---

* Jay Bitner, Assistant Plant Manager, Ball Corporation, Mundelein, IL.

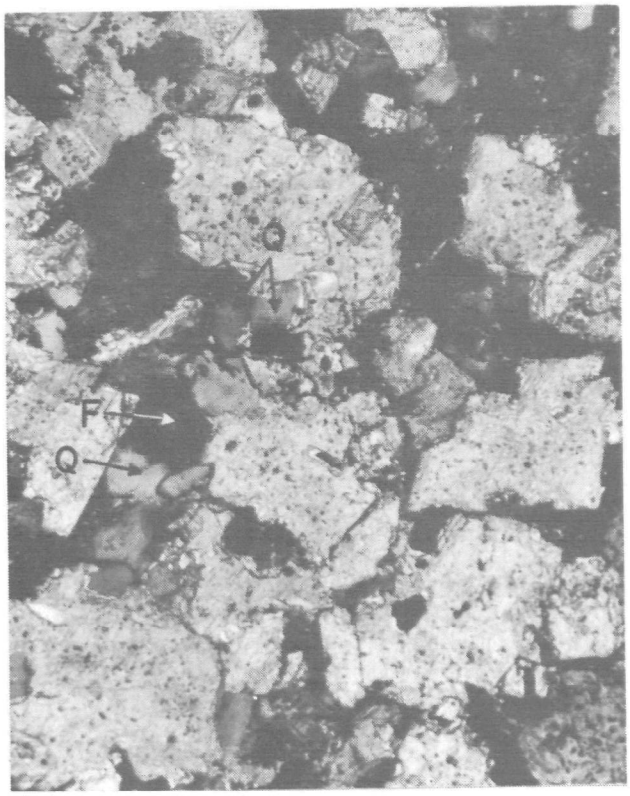

A. 1690. Quartz (Q), feldspar (F), and clay around dolomite grains.

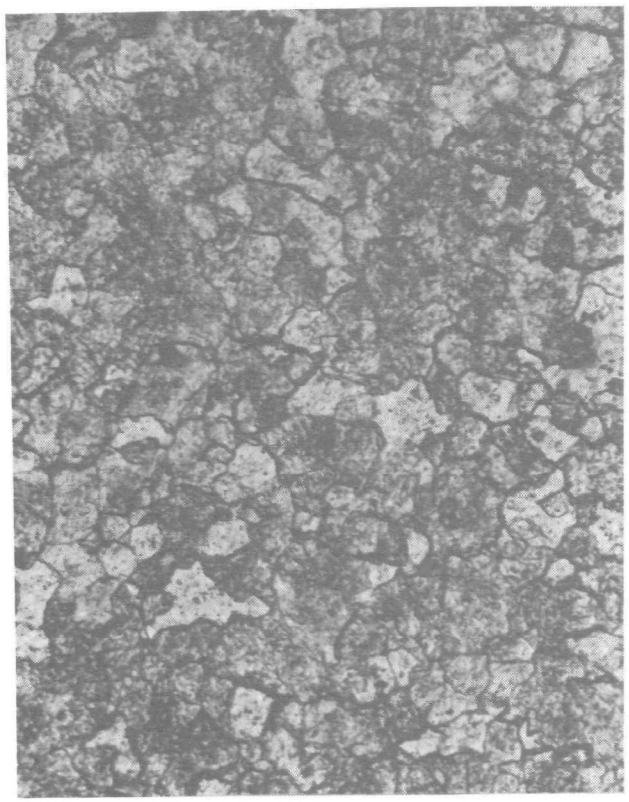

B. 2231. Equigranular and interlocking dolomite

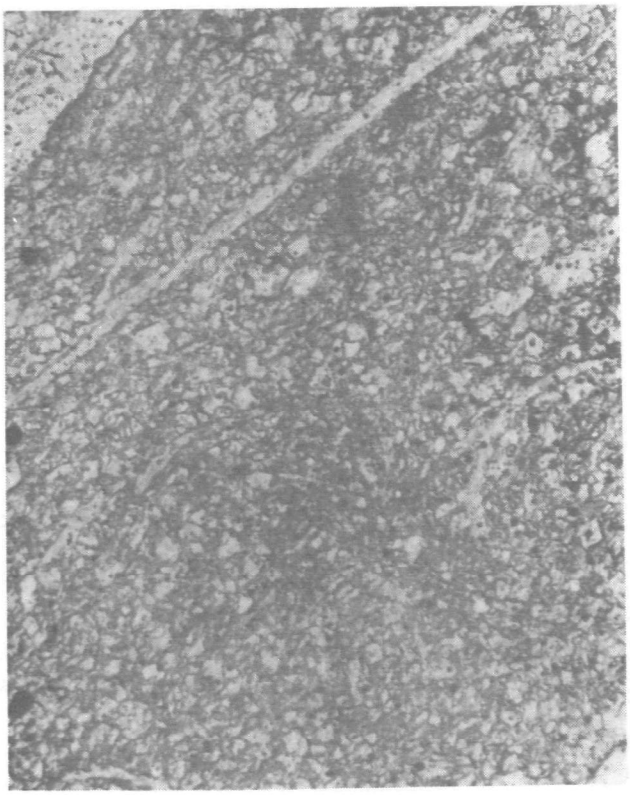

C. 1691. Dolomite (clear) in micritic calcite; pyrite (black)

D. 2257. Inequigranular limestone: sparry and micritic (dark) calcite

Plate 12 - Typical textural characteristics of samples studied related to fluidized bed desulfurization. Micrograph A taken in crossed polarized light and the others in plane polarized light; all magnified x 165.

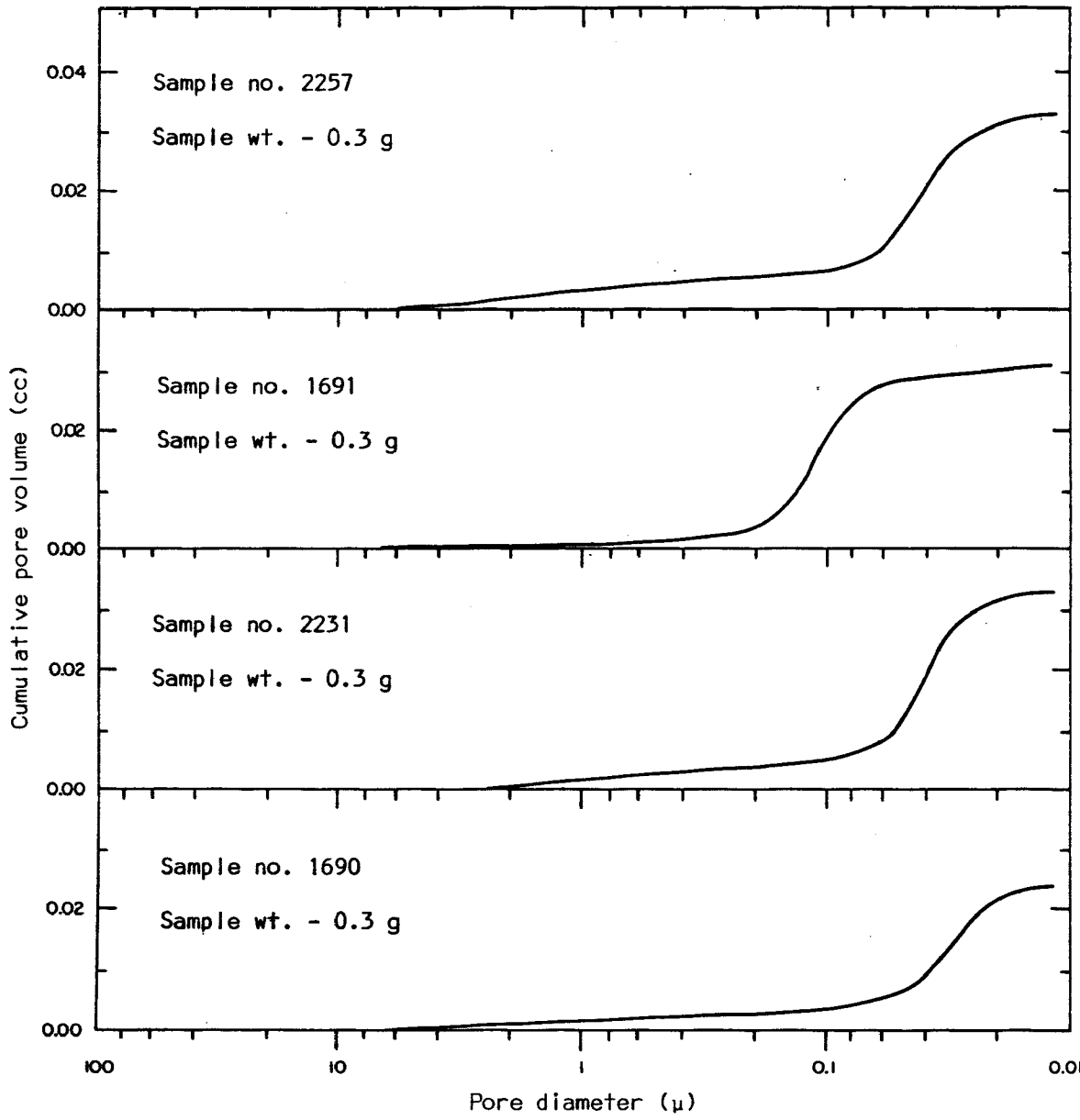

Fig. 27 - Calcine pore-volume curves for samples studied related to fluidized bed desulfurization.

Sample 1691 is a fine-grained dolomitic limestone. It has an inequigranular texture with scattered needle-shaped sparite (fossil shell and crinoid fragments) and dolomite rhombs (mostly 25μ across) densely scattered through micritic calcite (pl. 12C). Some particles contain sparitic calcite in grains up to 100μ across. Impurities of magnetite and pyrite grains (10μ in diameter, and in larger agglomerates) occur scattered throughout the sample. Other impurities of chert (SiO_2) and clay are restricted to certain particles.

TABLE 17 — CHEMICAL AND MINERAL ANALYSES

Sample	1690	2231	1691	2257
CHEMICAL ANALYSES (%)				
SiO_2	21.4	2.12	9.0	0.34
Al_2O_3	0.96	0.67	0.56	0.14
Fe_2O_3	0.58	0.54	0.33	0.04
MgO	14.5	19.9	0.71	nil
CaO	23.4	27.7	45.3	53.4
Na_2O	0.04	0.06	0.04	0.01
K_2O	0.95	0.32	0.27	nil
H_2O^+	0.62	1.19	0.75	0.41
CO_2	34.59	43.52	38.16	43.48
S	1.07	0.73	0.60	0.03
MINERAL ANALYSES*(%)				
Calcite	X (7)	nil	XXX (82)	XXX (99)
Dolomite	XXX (66)	XXX (92)	X (5)	nil
Quartz	XX	X	XX	X
Feldspar	XX	nil	nil	X
Clay	X	XX	X	X
Other (All X)	Magnetite Pyrite	Magnetite	Magnetite Pyrite Mica	nil
HCl residue	26.0	7.1	12.6	0.74

*Relative abundance: XXX = > 20%, XX = 1% to 20%, X = < 1%

Sample 2257 is a fossiliferous limestone. It has an inequigranular texture (pl. 12D). Very coarse fossil fragments and calcispheres, both consisting of sparitic calcite in grains up to 120μ across, occur mixed with micritic calcite. The sparry calcite content of the particles varies considerably (10% to 75%, average 48%), and micritic calcite makes up the remaining fraction of the particles. Very few impurities occur; these are rounded grains, 30μ to 60μ in diameter, of quartz and feldspar, widely scattered flakes of clay, and 10μ grains of magnetite and/or pyrite.

Discussion of Results

The mineral, chemical, and petrographic properties of the four samples vary widely. Impurities are mainly siliceous quartz, clay, and feldspar—the latter especially abundant in sample 1690. The occurrence of abundant feldspar in 1690 accounts for the agglomeration of regenerated calcine particles of the dolomite observed by Craig et al. (1971). The feldspar in the sample has a (220) d-spacing of 3.244 Å, which is characteristic of potassium-bearing feldspar (microcline, ideally $KalSi_3O_8$). Normally, some sodium and calcium substitute for potassium in the microcline feldspar structure. Feldspar begins to fuse at 1100° C. It is used as a flux in the ceramic industry to reduce the eutectic temperature of silicate mixes in the manufacture of glass (Searle, 1933). During the process of regeneration of the calcine, Craig heated the sulfated calcine particles to 1100° C, and it is at this point that the feldspar, especially the finer grained feldspar, partly fused and caused the undesirable agglomeration.

The relative abundance of defects within the carbonate grains (table 16) appears to correlate well with the observed decrepitation. The defects in the two dolomites and the dolomitic limestone (1690, 2231, and 1691) are mainly point defects. Increases in point defects in these samples correspond to increasing decrepitation. Also, the mean chord length (table 16), which corresponds to grain size, increases as decrepitation increases. The relatively high decrepitation observed in limestone 2257 appears to be related to the abundance of line defects in the sparry calcite, an abundant component in the limestone (table 16). The presence of line defects (cleavage and lamellar twin planes) within the sparry calcite grains also contributes to fracture propagation through the rock, thereby reducing the hardness and decreasing the resistance of the rock to attrition within fluidized bed systems.

SUMMARY AND CONCLUSIONS

Marl

Many rocks described in geologic literature as marls are not carbonate rocks, and some have only a very low carbonate content, which would make them unsuitable for use in SO_2 control processes. This is especially true of many

so-called marls of marine origin, which contain some carbonate constituents, mainly shells and shell fragments, but consist mostly of quartz and clay minerals.

Most deposits of marl (the term marl being restricted to incoherent carbonate-rich sediments of fresh-water origin) have $CaCO_3$ contents between 80 and 90 percent; a few have more than 90 percent. The main impurities are quartz silt and organic matter. The grain (crystallite) size of marls is mostly less than 4μ; however, grains 10μ to 25μ, especially in tufaceous marls, occur scattered throughout the marl material. Dispersion of marls in water yields particles (polygranular) whose median size varies from 6μ to 38μ. These particle sizes are less than half of those of three pulverized (2 1/2 hours in a ball mill) limestones tested.

The pore volume in marl samples with 85 percent or more calcite varies from 0.2 to 0.9 cc/g (average 0.5). Although not as significant as expected, a correlation was observed of decreasing optimum density (Harvard miniature compaction test) with increasing pore volume ($r^* = 0.52$). Upon calcination (at 850° C, for 5 to 10 minutes, and under a high gas flow rate), the pore volume increased about 0.2 cc/g to an average of 0.7 cc/g of rock. The marl pore structure is retained and the fine pores created are, for the most part, less than 0.1μ in diameter. The surface areas of the calcines of marls are generally between 11 and 17 m^2/g of marl. Increasing the calcination temperature to 950° C has little effect on the calcine pore structure but causes a decrease in the surface areas of the calcines. However, calcination at 950° C under a 10 percent carbon dioxide-90 percent nitrogen gas stream and/or for a calcination time of 60 minutes generally results in an enlargement of the fine pores. Under these conditions, a major reduction in the surface areas of the calcines is observed.

The large pore volumes and fine grain sizes of marls and their calcines indicate that the marls and their calcines would have high reactivities with SO_2. In addition, because of the ease of production (no blasting or crushing) of marl, together with its high degree of disaggregation when mixed with water (no grinding), this carbonate material should be given important consideration for use in limestone scrubbing of flue gases at power plants in areas near marl deposits.

Chalk and Chalky Limestone

Chalk, being a very porous and very fine grained variety of limestone, occurs mainly in Upper Cretaceous formations in three different areas in the central and eastern part of the United States: the Nebraska-Kansas-Colorado area, along a southwest-northeast belt across central Texas and extending into southwestern Arkansas, and along a broad belt across Mississippi and Alabama. Certain Tertiary formations in the southeastern states also contain chalk and chalky limestones. On the basis of laboratory studies and tests of 37 samples collected from the principal chalk occurrences, the following conclusions can be drawn.

---

* Linear correlation coefficient.

The $CaCO_3$ content of chalks, with certain exceptions, is 85 to 95 percent. The principal mineral components, other than calcite, are montmorillonite and illite (glauconite) types of clay, quartz silt, and traces of magnetite. Each mineral component is mainly microscopic in grain size.

Petrographically, the chalks consist of 5 to 30 percent relatively coarse-grained sparry type calcite that occurs in microscopic fossils 50μ to 200μ across, which are scattered throughout a matrix of micritic calcite in grains 0.5μ to 4μ across. Of this very fine grained calcite, about 10 to 20 percent is recognizable as fragments of coccoliths, and the rest consists of more or less equal dimensional grains that have relatively few grain-to-grain contacts.

The bulk density of the chalks tested ranges from 1.68 to 2.36 g/cc and averages 2.09 g/cc, corresponding to an average porosity of about 23 percent. Bulk density measurements can be used with moderate success to predict the total pore volume of the purer chalks ($r = 0.88$).

Standarized pulverization of the chalks and chalky limestone samples yields different particle-size distributions. The median particle sizes for some samples was between 5μ and 30μ, but for most samples, it was near 45μ. No apparent relationship exists between the median particle sizes and the volume or size of the pores in the samples. However, the smaller the median particle size, the less coherent is the sample. The particle-size distribution in a pulverized sample is theoretically as important as the volume and size of its pores in determining the sample reactivity in SO_2 scrubbing processes.

The pore volumes of the samples range from 0.043 to 0.302 cc/g, and the mean pore sizes range from 0.12μ to 0.76μ. Chalk samples from the Marianna Limestone in Alabama, the Demopolis Chalk in Alabama and Mississippi, and the Niobrara Chalk in Kansas and Nebraska are, in general, more porous than those from other chalk formations. The surface areas of the chalks range from 3.1 to 20.1 m^2/g, and of chalky limestones from 0.56 to 8.8 m^2/g. However, they vary most from one formation to another.

On the basis of the weight of chalk, calcines (850° C under dynamic gas flow conditions) of samples of the Demopolis, the Prairie Bluff, the Austin, and the Annona Chalks have lower surface areas than do the original chalk materials. Both the enlargement of existing chalk pores and the creation of new pores (<0.1μ) within the calcite grains were observed in the calcines. Calcination of six of the eight chalky limestones apparently opened enclosed pores in the samples, in addition to enlarging existing pores and creating new pores. Chalks, with few exceptions, showed slightly less than theoretical increase in pore volume after the calcination process was complete.

Shell, Coquina, Caliche, and Waste Sludge

The pore volumes in shell and coquina, which consists mainly of shell, range from 0.006 to 0.106 cc/g. Unweathered shell material averages 0.014 cc/g.

As a group, shells have the lowest pore volume. There is no significant difference in pore volume between calcitic and aragonitic shells. As a consequence of the low pore volumes of shell, its calcines have low pore volumes (0.21 to 0.26 cc/g rock). The surface areas of shells and coquinas are very low as are those of their calcines (0.3 to 2.1 m^2/g rock). Therefore, shell material is considered to have low reactivity with SO_2, whether used in the calcined form or as pulverized in a wet scrubbing process.

Caliche is not recommended for use in desulfurization processes, as deposits are of low purity—less than 65 percent $CaCO_3$.

Carbonate waste sludge resembles natural marl in many ways and is potentially very reactive with SO_2, especially in a wet scrubbing process. However, calcined sludge undergoes more shrinkage than marl and the grains of lime that are formed have little or no internal porosity.

Conclusions Regarding Carbonates Studied in Relation to Fluidized Bed Desulfurization

The feldspar grains present in sample 1690 partly fused during heating to 1100° C in the generation cycle of the fluidized bed tests of Craig et al. (1971). The number of intragranular optical defects, both point and line types, was high in samples that showed high attrition rates in fluidized bed tests. These samples also showed a high percentage of decrepitation. The attrition rate and relative decrepitation also increased in carbonate rock with the coarseness of their mean grain size.

REFERENCES

Attig, R. C., and P. Sedor, 1970, Additive injection for sulfur dioxide control, a pilot plant study (Research Center Rept. 5460 - Contract PH 86-67-127): Alliance, OH, Babcock & Wilcox Co., 59 p. + 7 app.

Barnes, V. E. [proj. director], 1966, Geologic atlas of Texas, Texarkana sheet: Univ. Texas Bur. of Econ. Geology, Austin.

Bicker, A. R., Jr. [compiler], 1969, Geologic map of Mississippi: Mississippi Geol. Survey, Jackson.

Bicker, A. R., Jr., 1970, Economic minerals of Mississippi: Mississippi Geol., Econ., and Topog. Survey Bull. 112, 80 p., 2 pls.

Borgwardt, R. H., 1970, Isothermal reactivity of selected calcined limestones with SO_2, in Natl. Air Pollution Control Agency Limestone Injection Process Symposium Proc.: Gilbertsville, KY, June 22-26.

Boswell, E. H., G. K. Moore, L. M. MacCary, and others, 1965, Cretaceous aquifers in the Mississippi Embayment: U. S. Geol. Survey Prof. Paper 448-C, 37 p., 8 pls.

Brunauer, S., P. H. Emmett, and E. Teller, 1938, Adsorption of gases in multimolecular layers: Jour. Am. Chem. Soc., v. 60, p. 309-319.

Burchett, R. R. [compiler], 1969, Geologic bedrock map of Nebraska: Conservation and Survey Division, Univ. Nebraska, Lincoln, NB.

Chronic, John, and Halka Chronic, 1972, Prairie peak and plateau: Colorado Geol. Survey Bull. 32, 136 p.

Coch, N. K., 1968, Geology of the Benns Church, Smithfield, Windsor, and Chuckatuck Quadrangles, Virginia: Virginia Div. of Mineral Resources Rept. Inv. 17, 39 p., 5 pls.

Cooke, C. W., 1945, Geology of Florida: Florida Geol. Survey Bull. 29, 339 p., 1 pl.

Cooke, Wythe, 1926, The Cenozoic formations, in Geology of Alabama: Geol. Survey of Alabama Spec. Rept. 14, p. 251-297.

Copeland, C. W. [ed.], 1968, Geology of the Alabama coastal plain, a guidebook: Geol. Survey of Alabama Circ. 47, 97 p.

Copeland, C. W., 1972, Upper Cretaceous series in central Alabama, in Tolson, J. S. [ed.], Guide to Alabama geology; guidebook for mtg., Southeastern Sec. Geol. Soc. America: Alabama Geol. Soc., University, AL, p. 2-1, 2-45.

Coutant, R. W., et al., 1971, Investigation of the reactivity of limestone and dolomite for capturing SO_2 from flue gas (Final Report - Contract CPA 70-111): Columbus, OH, Battelle, 54 p. + 4 app.

Craig, J. W. T., G. L. Johnes, G. Moss, and J. H. Taylor, 1971, Study of chemically active fluid bed gasifier for reduction of sulfur oxide emissions: Esso Research Centre (Abingdon, Berkshire, UK, Interim Rept. June 22 to Feb. 22, 1971, Contract CPA 70-46 (with the U.S. National Air Pollution Control Adm.), 57 p.

Dane, C. H., 1929, Upper Cretaceous formations of southwestern Arkansas: Arkansas Geol. Survey Bull. 1, 215 p., 3 pls.

Davis, C. A., 1901, A second contribution to the natural history of marl: Jour. Geology, v. 9, no. 6, p. 491-506.

Deboo, P. B., 1965, Biostratigraphic correlation of the type Shubuta Member of the Yazoo Clay and Red Bluff Clay with their equivalents in southwestern Alabama: Alabama Geol. Survey Bull. 80, 84 p.

Dibbs, H. P., 1971, Methods for the removal of sulfur dioxide from waste gases: Canada Dept. Energy Mines and Resources Mines Branch Inf. Circ. IC 272, Ottawa, 174 p.

Drehmel, D. C., 1971, Limestone types for flue gas scrubbing, in Second Int. Lime/Limestone Wet Scrubbing Symposium Proc., sponsored by Office of Air Programs, Environmental Protection Agency, New Orleans, LA, Nov. 8-12.

DuBar, J. R., 1958, Stratigraphy and paleontology of the last Neogene strata of the Caloosahatchee River area of southern Florida: Florida Geol. Survey Bull. 40, 267 p., 4 pls.

Fisher, W. L., 1965, Rock and mineral resources of east Texas: Univ. Texas Bur. of Econ. Geol. Rept. Inv. 54, 439 p.

Folk, R. L., 1958, Petrology of sedimentary rocks, second ed.: Austin, TX: Hemphill's, p. 47-49.

Frye, J. C., and A. B. Leonard, 1959, Correlation of the Ogallala Formation (Neogene) in western Texas with type localities in Nebraska: Univ. Texas Bur. of Econ. Geol. Rept. Inv. 39, 46 p.

Georgia Department of Mines, Mining and Geology, 1968, Directory of Georgia mineral producers: The Geol. Survey Circ. 2, 44 p.

Georgia Division of Mines, Mining and Geology, 1939, Geologic map of Georgia: Georgia Div. Mines, Mining and Geology, Atlanta.

Hammons, G. A., and A. Skopp, 1971, A regenerative limestone process for fluidized bed combustion and desulfurization: Esso Research and Engineering Company (Linden, NJ), Final Rept., Contract CPA 70-19 (with the U.S. Air Pollution Control Office), 115 p.

Harvey, R. D., and J. C. Steinmetz, 1971, Petrographic properties of carbonate rocks related to their sorption of sulfur dioxide: Illinois Geol. Survey Environmental Geology Note 50, 37 p.

Hattin, D. E., 1971, Widespread, synchronously deposited, burrow-mottled limestone beds in Greenhorn Limestone (Upper Cretaceous) of Kansas and southeastern Colorado: Am. Assoc. Petroleum Geologists Bull., v. 55, no. 3, p. 412-431.

Jonke, A. A., G. J. Vogel, L. J. Anstasia, R. L. Jarry, D. Ramaswami, M. Haas, C. B. Schoffstoll, J. R. Pavlik, G. N. Vargo, and R. Green, 1971, Reduction of atmospheric pollution by the application of fluidized bed combustion: Argonne National Laboratory (Argonne, IL) Annual Report ANL/ES-CEN-1004, 112 p.

Kansas Geological Survey, 1964, Geologic map of Kansas: Kansas Geol. Survey Map M-1

Kottlowski, F. E., 1962, Reconnaissance of commercial high-calcium limestones in New Mexico: New Mexico Bureau of Mines and Mineral Resources Circ. 60, 77 p.

Maxwell, E. L., 1970, Mineral producers in Florida: Florida Bur. of Geology Inf. Circ. 66, 40 p.

Nelsen, F. M., and F. T. Eggertsen, 1958, Determination of surface area: Anal. Chem., v. 30, p. 1387-1390.

Oetking, P. F. [compiler], 1959, Geological highway map of Texas: Dallas Geol. Soc., Dallas, TX.

Pessagno, E. A., Jr., 1969, Upper Cretaceous stratigraphy of the western Gulf Coast area of Mexico, Texas, and Arkansas: Geol. Soc. America Mem. 111, 139 p.

Purdue University Cooperative Extension Service, 1971, Sources and analyses of liming materials: Agronomy Dept. Rept. 64, Lafayette, IN, 25 p.

Puri, H. S., 1957, Stratigraphy and zonation of the Ocala Group: Florida Geol. Survey Bull. 38, 248 p., 4 pls.

Raben, I. A., 1973, Status of technology of commercially offered lime and limestone flue gas desulfurization systems, in Flue Gas Desulfurization Symposium Proc., Sponsored by Control Systems Laboratory, Environmental Protection Agency, New Orleans, LA, May 14-17.

Reeside, J. B., Jr., 1932, Stratigraphic nomenclature in the United States: Internat. Geol. Cong. XVI, Guidebook 29: Washington, DC: U.S. Govt. Printing Office, 7 p., 10 pls.

Reves, W. D., 1961, The limestone resources of Washington, Holmes and Jackson Counties, Florida: Florida Geol. Survey Bull. 42, 121 p.

Robison, E. B., A. H. Bagnulo, J. W. Bishop, and S. Ehrlich, 1970, Characterization and control of gaseous emissions from coal-fired fluidized-bed boilers: Pope, Evans and Robbins, Div. Perathon Incorporated (Alexandria, VA), Interim Report to U.S. National Air Pollution Control Administration, Oct., 1970, 133 p.

Rochelle, G. T., 1973, Economics of flue gas desulfurization, in Flue Gas Desulfurization Symposium Proc., sponsored by Control Systems Laboratory, Environmental Protection Agency, New Orleans, LA, May 14-17.

Runnels, R. T., and I. M. Dubins, 1949, Chemical and petrographic studies of the Fort Hays Chalk in Kansas: Kansas Geol. Survey Bull. 82, pt. 1, p. 1-36.

Searle, A. B., 1933, The chemistry and physics of clays and other ceramic materials, second ed.: London: Ernest Benn Limited, p. 538.

Segall, R. T., 1972, Michigan mineral producers, 1971: Michigan Geol. Survey Ann. Directory 5, p. 13.

Stephenson, L. W., 1937, Stratigraphic relations of the Austin, Taylor, and equivalent formations in Texas: U.S. Geol. Survey Prof. Paper 186-G, p. 133-146.

Terlecky, P. M., Jr., in press, The origin of a late Pleistocene and Holocene marl deposit: Jour. Sed. Petrology.

Thiel, G. A., 1930, A correlation of marl beds with types of glacial deposits: Jour. Geology, v. 38, p. 717-728.

Thomas, Josephus, Jr., and R. R. Frost, 1971, Versatile apparatus for studying reactions involving gas adsorption or evolution: Illinois Acad. Sci. Trans., v. 64, no. 3, p. 248-253.

Toulmin, L. D., and others, 1966, Summary of the Tertiary stratigraphy of south-central and southwest Alabama, in Copeland, C. W. [ed.], Facies changes in the Alabama Tertiary: Alabama Geol. Soc. Guidebook 4, University, AL, p. 3-10.

U.S. Bureau of Mines, 1969, Minerals yearbook - 1968, vols. I-II: Washington, DC: U.S. Govt. Printing Office, p. 1046.

U.S. Bureau of Mines, 1971, Minerals yearbook - 1969, vols. I-II: Washington, DC: U.S. Govt. Printing Office, p. 1038.

Valentine, G. M., 1960, Inventory of Washington minerals, pt. I, Nonmetallic minerals, second ed. (revised by M. T. Huntting): Washington State Division of Mines and Geology Bull. 37, 175 p.

Vernon, R. O., 1943, Florida mineral industry: Florida Geol. Survey Bull. 24, 207 p.

Vernon, R. O., and H. S. Puri [compilers], 1965, Geologic map of Florida: Florida Div. of Geology Map Series 18.

Wayland, J. R., and W. E. Ham, 1955, General and economic geology of the Baum Limestone, Ravia-Mannsville area, Oklahoma: Oklahoma Geol. Survey Circ. 33, 44 p.

Wayne, W. J., 1971, Marl resources of Indiana: Indiana Dept. Nat. Resources, Geol. Survey Bull. 42-G, 16 p.

Wilson, S. D., 1970, Suggested method of test for moisture-density relations of soils using Harvard compaction apparatus, in American Society for Testing Materials, Special procedures for testing soil and rock for engineering purposes: ASTM Spec. Tech. Pub. 479, p. 101-103.

Zeller, D. E. [ed.], 1968, The stratigraphic succession in Kansas: Kansas Geol. Survey Bull. 189, p. 1-81.

APPENDIX 1

ANNOTATED BIBLIOGRAPHY ON MARLS
IN THE NORTHEASTERN QUARTER OF THE UNITED STATES

This bibliography includes works on fresh-water marls that have formed in lakes and bogs in the northeastern quarter of the United States. In the United States such marls occur as commercial deposits only within this area. Deposits of so-called marine marls from the Atlantic Coast have been excluded.

CONNECTICUT

Perry, J. B., 1873, Hints toward the post-Tertiary history of New England from personal study of rocks, with strictures on Dana's "Geology of the New Haven region": Boston Soc. Nat. Hist. Proc., v. 15, p. 48-148.

Discussion of the marl and peat periods of post-Pliocene time.

ILLINOIS

Athy, L. F., 1928, Geology and mineral resources of the Herscher Quadrangle: Illinois Geol. Survey Bull. 55, 120 p.

Marl described (p. 108-109).

Baker, F. C., 1912, Postglacial life of Wilmette Bay, glacial Lake Chicago: Illinois Acad. Sci. Trans. (1911), v. 4, p. 108-116.

Describes a marl bed about 5 inches thick (p. 109, 111-112).

Baker, F. C., 1918, Postglacial Mollusca from the marls of Central Illinois: Jour. Geol., v. 26, no. 7, p. 659-671.

Describes 8- to 12-inch thick marl bed on campus of University of Illinois, Urbana (p. 660). Refers to marls from Maine (p. 661-663, 665).

Decker, C. E., 1912, A tufa deposit near Danville, Illinois: Illinois Acad. Sci. Trans., v. 5, p. 109-111.

An unsuccessful search was made for this deposit in July 1971.

Lamar, J. E., 1938, Unexploited or little known industrial minerals of Illinois: Illinois Geol. Survey Circ. 23, p. 213-232.

Describes shell marl localities in Illinois (p. 220-221).

Lamar, J. E., 1965, Industrial minerals and metals of Illinois: Illinois Geol. Survey Ed. Ser. 8, 48 p.

Brief account of deposits of marl, tufa, and travertine in Illinois. Includes names of counties in which some deposits have been worked (p. 46).

Mosier, J. G., S. V. Holt, F. A. Fisher, E. E. DeTurk, H. J. Snider, and L. H. Smith, 1923, Livingston County soils: Univ. of Illinois Agr. Exp. Sta. Soil Rept. 25, 55 p.

Reports muck on marl in SE¼ Sec. 32, T. 30 N., R. 7 E. (p. 27).

Powers, W. E., 1936, Geological setting of the Aurora mastodon remains: Illinois Acad. Sci. Trans. (1935), v. 28, no. 2, p. 193-194.

Reports occurrence of 30 feet of marl (p. 193).

Rubey, W. W., 1952, Geology and mineral resources of the Hardin and Brussels Quadrangles (Illinois): U. S. Geol. Survey Prof. Paper 218, 179 p.

Describes calcareous tufa deposits (p. 97-98).

INDIANA

Blatchley, W. S., and G. H. Ashley, 1901, The lakes of northern Indiana and their associated marl deposits: in W. S. Blatchley, Indiana Dept. Geol. and Nat. Resources, 25th Ann. Rept. (1900), p. 31-321.

McGregor, D. J., 1958, Cement raw materials in Indiana: Indiana Geol. Survey Bull. 15, 88 p.

Use of marls in cement in Indiana (p. 14). Discussion of marl (p. 45, 49); analyses of marls (p. 50).

Wayne, W. J., 1963, Pleistocene formations in Indiana: Indiana Geol. Survey Bull. 25, 85 p.

Martinsville Formation defined to include a paludal facies with calcareous marl (p. 28-31). Refers to sections of Martinsville Formation that contain marl (p. 80).

Wayne, W. J., 1971, Marl resources of Indiana: Indiana Geol. Survey Bull. 42-G, 16 p.

Distribution, production, and analyses of marl deposits in Indiana.

MAINE

Dodge, J. R., 1868, On the limestone and pond-marls of Maine: U. S. Agricultural Rept., p. 370-371.

Description of formations and localities with analyses; special reference to fertilizing qualities.

MASSACHUSETTS

Hitchcock, Edward, 1833, Report on the geology, mineralogy, botany, and zoology of Massachusetts: Amherst: J. S. and C. Adams, xii p., 692 p.

Marl occurrences (p. 38, 120).

Hitchcock, Edward, 1841, Geology of Massachusetts, v. 1: Amherst: J. S. and C. Adams, 299 p.

Discussion of marl with locations (p. 67-75); analyses of marls (p. 70). Discussion of green sand (marl) with analyses (p. 91-95).

MICHIGAN

Cook, C. W., 1912, Michigan cement: Michigan Geol. and Biol. Survey Pub. 8, Geol. Ser. 6, p. 337-354.

Discussion of marls (p. 338-342) and analyses of marls (p. 341). Use of marl by plants (p. 344-350).

Davis, C. A., 1900, A contribution to the natural history of marl: Jour. Geol., v. 8, no. 6, p. 485-497.

Davis, C. A., 1900, A remarkable marl lake: Jour. Geol., v. 8, no. 6, p. 498-503.

Davis, C. A., 1901, A second contribution to the natural history of marl: Jour. Geol., v. 9, no. 6, p. 491-506.

Three papers by Davis describe marl that occurs in certain lakes in Michigan (Montcalm, Branch, and Isabella Counties) and discuss the origin of the marl derived from chemical processes of plants, especially Chara that grows on the bottoms of the lakes.

Hale, D. J., and others, 1903, Marl (bog lime) and its application to the manufacture of portland cement: Michigan Geol. Survey, v. 8, pt. 3, 399 p.

Klyce, D. F., and R. J. Bishop, 1971, Mineral industry of Michigan 1969: Michigan Geol. Survey Ann. Statistical Summ. 13, 18 p.

Agricultural production of marl (p. 8). Quantity and value of marl production for 1968 and 1969 (p. 9). Principal marl producers listed (p. 18).

Segall, R. T., 1972, Michigan mineral producers 1971: Michigan Geol. Survey Ann. Directory 4, 52 p.

List of marl producers (p. 13).

MINNESOTA

Armstrong, L. C., 1927, The geologic conditions favorable for the accumulation of marl, with special reference to east central Minnesota: Univ. of Minnesota, Minneapolis, E. M. thesis.

Emmons, W. H., and F. F. Grout, eds., 1943, Mineral resources of Minnesota: Minnesota Geol. Survey Bull. 30, 149 p.

Section on marls (p. 101-105, 108); includes map of distribution and number of deposits per county.

Kirk, R. E., 1926, The manufacture of portland cement from marl: Univ. of Minnesota Eng. Expt. Sta. Bull. 4.

Roepke, H. H., 1958, The Nisswa Lake marl deposit, Crow Wing County, Minnesota: Univ. of Minnesota, Minneapolis, M.S. thesis.

See G. M. Schwartz below.

Schwartz, G. M., et al., 1959, Investigation of the commercial possibilities of marl in Minnesota: St. Paul: Office of Iron Range Resources and Rehabilitation (in coop. with the Minnesota Geol. Survey and Univ. of Minnesota, Minneapolis), xiii p., 99 p.

Among other subjects related to production and uses of marl, this book contains chapters on methods of chemical analyses of marl, investigation of marl deposits, and experiments on drying marl. Chapter IV is a reprint of H. H. Roepke's thesis on the Nisswa Lake marl deposit.

Appendix A is a reprint of C. R. Stauffer and G. A. Thiel's paper, 1933, "The limestones and marls of Minnesota": Minnesota Geol. Survey Bull. 23, pt. II (p. 79-190).

Minnesota Geological Survey. Marl: Minnesota Geol. Survey Misc. Rept. 8, 3 p.

Defines marl and lists five large marl deposits in Minnesota. Counties having large marl tonnages include Crow Wing, Wright, and Stearn. Lists uses of limestone and marls.

Stauffer, C. R., and G. A. Thiel, 1933, The limestones and marls of Minnesota: Minnesota Geol. Survey Bull. 23, 193 p.

Uses of marl (p. 1-8). Part II, "The marls of Minnesota" (p. 79-190) has been reprinted as Appendix A in G. M. Schwartz et al., 1959.

Thiel, G. A., 1930, A correlation of marl beds with types of glacial deposits: Jour. Geol., v. 38, no. 8, November-December, p. 717-728.

Thiel, G. A., 1946, Marl: Conservation Volunteer, v. 9, no. 51, March-April, p. 13-15.

Zumberge, J. H., 1952, The lakes of Minnesota, their origin and classification: Minnesota Geol. Survey Bull. 35, xiii p., 99 p.

Discussion of marls in lakes (p. 69, 71-72).

NEW HAMPSHIRE

Hitchcock, C. H., 1874, The geology of New Hampshire: Part I. Physical geography: Concord, NH: Edward A. Jenks, xi p., 667 p.

Information on marl localities (p. 549).

Hitchcock, C. H., 1878, The geology of New Hampshire: Part V. Economic geology: Concord, NH: Edward A. Jenks, 103 p.

Gives marl localities (p. 95).

NEW JERSEY

Cook, G. H., 1868, Geology of New Jersey: Newark, xxiv p., 899 p.

Discussion of shell-marl, calcareous sinter, calcareous tufa, and travertine (p. 170-172).

Kummel, H. B., 1901, Report on the portland cement industry: New Jersey Geol. Survey Ann. Rept. of the State Geologist for the year 1900, pt. 2, p. 9-101.

Numerous and very small lake deposits of marl are described (p. 98-101); analyses (p. 98).

NEW YORK

Graham, J. A., 1955, The mineral industries of New York State 1949-1959: New York State Mus. and Science Service Circ. 41, 76 p.

Report of one marl producer in Livingston County in 1949 giving quantity and value of production (p. 30).

Hartnagel, C. A., 1927, The mining and quarry industries of New York from 1919 to 1924 including lists of operators: New York State Mus. Bull. 273, 102 p.

Marl discussed (p. 52-54). Dunkirk operator reporting production in 1924.

Hartnagel, C. A., and J. G. Broughton, 1951, The mining and quarry industries of New York State, 1937 to 1948: New York State Mus. Bull. 343, 130 p.

Use of marl in portland cement (p. 23-24).

Luedke, E. M., C. T. Wrucke, and J. A. Graham, 1959, Mineral occurrences of New York State with selected references to each locality: U. S. Geol. Survey Bull. 1072-F, p. iii, p. 385-444.

Marl occurrences (p. 420-421).

Newland, D. H., 1912, The mining and quarry industry of New York State: Report of operations and production during 1911: New York State Mus. Bull. 161, 114 p.

Marl discussed (p. 80-81).

Newland, D. H., 1921, The mineral resources of the state of New York: New York State Mus. Bull. 223, 224 (1919), 315 p.

Marl discussed (p. 145-149); chemical analyses (p. 147).

Newland, D. H., and C. A. Hartnagel, 1936, The mining and quarry industries of New York State for 1930 to 1933: New York State Mus. Bull. 305, 95 p.

Discussion of marl (p. 48-52). Little marl now being produced (p. 51-52).

Ries, Heinrich, and E. C. Eckel, 1901, Lime and cement industries of New York: New York State Mus. Bull., v. 8, no. 44, 968 p.

Terlecky, P. M., Jr., 1972, The origin, stratigraphy and post-depositional history of a late Pleistocene marl deposit, Rochester, N.Y. area (abstract), in Northeastern Section, Geological Society America Program, 7th Ann. Mtg., March 9-11, p. 9-11.

Report of a study at locality 7133.

OHIO

Kefauver, Hazel, ed., 1960, Annual coal and nonmetallic mineral report with directories of reporting firms for 1960: Ohio Dept. Indus. Relations, 290 p.

One marl producer listed (p. 244).

Stout, Wilber, 1940, Marl, tufa rock, travertine, and bog ore in Ohio: Ohio Geol. Survey Bull. 41, 56 p.

PENNSYLVANIA

Dickey, J. B. R., 1923, Calcareous marl in Pennsylvania south of the terminal moraine: Pennsylvania Geol. Survey Bull. 76, 10 p.

Miller, B. L., 1934, Limestones of Pennsylvania: Pennsylvania Geol. Survey Bull. M 20, 729 p.

Marl deposit in Crawford County described (p. 332-335); analyses (p. 335). General discussion of marls (p. 54-56). Repeats descriptions of marls from Dickey (1923) (p. 167, 292, 345-346, 388, 394, 423, 499, and 700). Describes concretions (p. 475-477). Reports marl locations (p. 387 and 714).

VERMONT

Hitchcock, Edward, Edward Hitchcock, Jr., A. D. Hager, and C. M. Hitchcock, 1861, Report on the geology of Vermont: descriptive, theoretical, economical, and scenographical, Vols. I and II: Claremont Manufacturing Company, Claremont, NH, 988 p.

Marls discussed (p. 167-171, 725-726, and 805-806); analyses (p. 168, 697-698, and 805).

VIRGINIA

LeVan, D. C., 1971, Directory of the mineral industry in Virginia—1971: Virginia Div. of Mineral Resources, 46 p.

Lists four marl producers (p. 27-28), one fresh-water marl producer (J. C. Digges), and three producers of marine shell marls.
marls

McGill, W. M., 1936, Outline of the mineral resources of Virginia: Virginia Geol. Survey Bull. 47, Ed. Ser. No. 3, 81 p.

Calcareous (shell) marl and travertine discussed (p. 36).

WEST VIRGINIA

Davies, W. E., 1949, Caverns of West Virginia: West Virginia Geol. Survey, v. 19, x p., 353 p.

Marl deposits (p. 5). Shelter caves present in marl bed at Williamsport (p. 60).

Gillespie, W. H., and J. A. Clendening, 1964, An interesting marl deposit in Hardy County, West Virginia: West Virginia Acad. Sci. Proc., v. 36, p. 147-151.

Grimsley, G. P., 1906, Clays, limestones, and cements: West Virginia Geol. Survey, v. 3 (1905), xviii p., 565 p.

Marl reported with analysis (p. 515-516).

Grimsley, G. P., 1916, Jefferson, Berkeley, and Morgan Counties: West Virginia Geol. Survey County Repts., xxvi p., 644 p.

Marl deposits discussed (p. 393-396); analyses (p. 394-396).

McCue, J. B., J. B. Lucke, and H. P. Woodward, 1939, Limestones of West Virginia: West Virginia Geol. Survey, v. 12, xiv p., 560 p.

Marl locations mentioned (p. 98, 102, 115, 153, 204, 211-213, 455, 483-484); analyses of marls (p. 111, 160, 216, 396, 428).

Price, P. H., R. C. Tucker, and O. L. Haught, 1938, Geology and natural resources of West Virginia: West Virginia Geol. Survey, v. 10, xi p., 462 p.

Calcareous tufa, travertine, and calcareous marl described as minor cement materials. Refers to use by only two plants at Charles Town (p. 302, 305).

Reger, D. B., and R. C. Tucker, 1924, Mineral and Grant Counties: West Virginia Geol. Survey County Repts., xxiv p., 866 p.

Discusses marl deposits (p. 675-676); analyses (p. 678); and locations (p. 680).

Tilton, J. L., W. F. Prouty, and P. H. Price, 1927, Pendleton County: West Virginia Geol. Survey County Repts., xviii p., 384 p.

Marls discussed with one location given (p. 289); photograph of outcrop (p. 288).

Tilton, J. L., W. F. Prouty, R. C. Tucker, and P. H. Price, 1927, Hampshire and and Hardy Counties: West Virginia Geol. Survey County Repts., xxii p., 624 p.

Travertine locations given (p. 18 and 138). Photograph of marl deposit (p. 140). Marl analyses (p. 274, 308, 554). Marl deposits discussed (p. 274, 308).

Woodward, H. P., 1951, Ordovician System of West Virginia: West Virginia Geol. Survey, v. 21, xi p., 627 p.

Discusses marl deposits in vicinity of Charles Town (p. 487).

WISCONSIN

Natural Resources Committee of State Agencies of Wisconsin, 1956, The natural resources of Wisconsin: Wisconsin Nat. Resources Comm. of State Agencies, 159 p.

Marl discussed (p. 109). Gives production of agricultural lime of four counties in 1952.

Ostrom, M. E., 1970, Directory of Wisconsin mineral producers. 1968: Wisconsin Geol. and Nat. History Survey Inf. Circ. 12, 68 p.

One marl producer listed (p. 57).

Steidtmann, Edward, 1924, Limestones and marls of Wisconsin: Wisconsin Geol. and Nat. History Survey Bull. 66, 208 p.

Origin of marls (p. 6); the marls of Wisconsin (p. 128-153); uses of marl (p. 98, 111-116).

Appendix 2 begins on page 102.

APPENDIX 2

SOURCES OF SAMPLES AND REMARKS ON THE DEPOSITS

Location and sample number	Thickness represented (ft)	Type	Source and location (quadrangle map in parentheses)	Remarks on the deposit and geologic unit sampled
7120	35	Limestone, chalky (coquina)	Houdaille-Duval-Wright Co. quarry, 5 mi NE of Newberry, FL; SE¼ Sec. 23, 9S-17E (Newberry Quad., FL).	Extensive deposit in the Crystal River Formation (Eocene).
7121A	0.5	Shells and broken shells	Turtle Beach of Siesta Key, offshore bar, 3 mi N and 2 mi W of Osprey, FL; SE¼ Sec. 23, 37S-18E (Bird Keys Quad., FL).	Anastasia Formation (Pleistocene). No notable deposit at this locality. Samples considered typical of shells of the Anastasia, which occurs for many miles south of Turtle Beach along the Gulf Coast.
7121B	3.5+			
7122A	2	Limestone, chalky Coquina	J. Cochran pit, 4 mi W and 2 mi N (off Rt. 80) of La Belle, FL; SE¼ Sec. 13, 43S-28E (Sears Quad., FL).	Operating pit extends over about 5 acres in the Caloosahatchee Marl (Pleistocene).
7122B	5			
7123	4	Sandstone, calcareous	Outcrop on north bank of Caloosahatchee River, north side of La Belle, FL; SE¼ Sec. 32, 42S-29E (La Belle Quad., FL).	Sandy facies of Caloosahatchee Marl (Pleistocene).
7124	10+	Clam shells	Radcliff Materials, Inc., Mobile, AL. Lake Pontchartrain, LA (30°10'N, 90°05'W).	Dredging operation in Lake Pontchartrain, LA (Holocene).
7125	10+	Oyster shells	Radcliff Materials, Inc., Mobile, AL. Mobile Bay, AL (30°32'N, 88°02'W).	Dredging operation in a dead oyster reef in Mobile Bay, AL (Holocene).
7126A	15	Bog marl	Woodrow Gary, New Madison, OH. Pit location in SE¼ SW¼ Sec. 1, 10N-1E (New Madison Quad., OH).	Former operations extended over about a 5-acre bog (Pleistocene). Upper beds exposed near center of deposit.
7126B	2.5			

7127A	0.5	Tufaceous bog marl	Abandoned pit, 1.3 mi N of intersection Rt. 269 and NYC RR at Castalia, OH, and 0.65 mi W. In Resthaven Wildlife Area (Castalia Quad., OH).	Sample from plowed surface of a 10-acre field adjacent to an extensive bog deposit formerly operated by a cement company (Pleistocene).
7127B	0.8	Clayey and marly silt		0.5 to 0.8 ft below sample 7127A above.
7127C	2.5	Clayey and marly silt		0.8 to 3.8 ft below sample 7127A above.
7127D		Tufaceous bog marl		Typical of the large lumps present in deposit (Pleistocene).
7128A	1.0	Tufaceous bog marl	Abandoned pit in road embankment. 0.6 mi S of 7127 (Castalia Quad., OH).	Same deposit as 7127 0.5 ft to 1.5 ft below surface of embankment.
7128B	1.5			Same deposit as 7127 1.5 ft to 3.0 ft below surface of embankment (Pleistocene).
7129	15	Tufaceous bog marl	Abandoned pit, SE¼ SE¼ Sec. 15, 20N-15W, 1.1 mi SW of McZena, OH (Loudonville Quad., OH).	Sample from edge of old road bed used during production of marl from a moderate size bog. Probably typical of marl underlying the small lake 20 yards to the west (Pleistocene).
7130	2.5	Bog marl	Abandoned pit, 0.7 mi S of intersection Rt. 424 and Frisbee Rd. and 0.2 mi due east (Cassadaga Quad., NY).	Old portland cement plant. Sample from below 1.5 ft of muck and adjacent to water-filled pit in a moderately extensive bog (Pleistocene).
7131A	1.9	Bog marl	Jasper Robinson, 0.5 mi SW of Clarendon, NY (Holley Quad., NY).	Samples from a 10 to 15 acre area (Pleistocene).
7131B	3.5			
7131C	1.5			
				Commercial operation in a Pleistocene bog.
7132A	2.8	Bog marl	Scofield Lime Products, Fancher, NY. Pit 0.5 mi S of intersection of Rt. 19 and New York Throughway and 0.1 mi W of Rt. 19 (Churchville Quad., NY).	Sample A from upper marl, center of pit.
7132B	5.5+			Sample of marl under 7132A.
7132C	6			Sample of the upper part of the marl in the north end of the pit.
7132D	20			Sample from stockpile.

APPENDIX 2, continued

Location and sample number	Thickness represented (ft)	Type	Source and location (quadrangle map in parentheses)	Remarks on the deposit and geologic unit sampled
7133	5.5	Tufaceous bog marl	Abandoned pit of the Genesee Lime Products Co., Rochester, NY. Pit located 1.0 mi E and 0.8 mi N of Caledonia, NY (Caledonia Quad., NY).	Sample from auger hole in an extensive bog (Pleistocene).
7134A	1.5	Lake marl	Abandoned pit 0.9 mi SW (on Rt. 245) of Wayland, NY (Wayland Quad., NY).	Extensive areal deposit (Pleistocene). Sample from auger hole on edge of lake. Marl is underlain by muck and gravel at the site of the auger hole.
7135	1.0	Bog marl	John Underwood, Camillus, NY. Pit located 1 mi S and 1 mi W of Warners, NY (Camillus Quad., NY).	Abandoned portland cement pit and plant. Workings in an extensive bog (Pleistocene).
7136	2.0	Tufaceous bog marl	Outcrop under Penn. Cent. Railroad bridge over Letort Spring Run Creek in Carlisle, PA (Carlisle Quad., PA).	Very limited deposit (Pleistocene).
7137	20	Bog marl	J. C. Digges & Sons, White Post, VA. Pit and plant located $\frac{1}{4}$ mi S of Rt. 617 at point 0.65 mi E of intersection of Rts. 255 and 617, near Briggs (Boyce Quad., VA).	Commercial operations in an extensive bog deposit (Pleistocene) above water table. Sample representative of pit production.
7138	5.5	Lake marl	Sampsel & Son, R.R. 1, Rochester, IN. Pit on east side of Lake 16, 2 mi E of Athens, IN, NW$\frac{1}{4}$ SE$\frac{1}{4}$ Sec. 16, 30N-4E, Fulton Co. (Akron Quad., IN).	Discontinued operations. Sample from above water level. More than 4 ft of similar marl occurs below the beds sampled (Pleistocene).

7139	10-12	Bog marl	Stanley Custer, R.R. 1, Box 1, Milford, IN. Pit on east side of Rt. 15 on the north edge of Milford, IN, NW¼ NE¼ Sec. 8, 34N-6E, Kosciusko Co. (Milford Quad., IN).	Discontinued operation. Sample from stockpile from a 4 to 6 acre bog (Pleistocene).
7140	5.5+	Lake marl	Raymond Beezley, R.R. 4, Albion, IN. Erdly pit located on Whirledge Lake 1 3/4 mi E of Kimmell, IN, Cen. E½ NE¼ Sec. 19, 34N-9E, Noble Co. (Ligonier Quad., IN).	Commercial operations on the east side of lake. Sample from stockpile of Pleistocene marl.
7141	7+	Bog marl	Vernon Kaufman, R.R. 1, Topeka, IN. Fought pit located 3 mi E and 1 mi S of Topeka, IN, NW¼ NW¼ NW¼ Sec. 3, 35N-9E, Noble Co. (Oliver Lake Quad., IN).	Commercial operations in a Pleistocene bog. Sample from stockpile.
7142	16-18	Lake marl	Miller Marl Co., R.R. 1, Middlebury, IN. Pit on south end of Cass Lake, 3 mi E of Middlebury, NW¼ Sec. 5, 37N-8E, La Grange Co. (Middlebury Quad., IN).	Commercial operations. Sample from stockpile of Pleistocene marl.
7143A	?	Bog marl	K. Fleming, Fremont, IN. Pit on west edge of Fremont, SW¼, SE¼ Sec. 20, 38N-14E, Steuben Co. (Angola East Quad., IN).	Abandoned pit in a large Pleistocene bog. Sample from stockpile.
7144A	12-18	Lake marl	Taylor & Son, R.R. 2, Fremont, IN. Garman Pit on Warner Lake, 1½ mi E and 1 mi S of Orland, Cen. W½ Sec. 27, 38N-12E, Steuben Co. (Orland Quad., IN).	Commercial operations in a Pleistocene lake. Sample from stockpile.

APPENDIX 2, continued

Location and sample number	Thickness represented (ft)	Type	Source and location (quadrangle map in parentheses)	Remarks on the deposit and geologic unit sampled
7145A	?	Lake marl	Harlan Spoor, R.R. 1, Burlington, MI. Pit is 0.2 mi S of R Drive S Rd., 2.5 mi NW of Burlington, Cen. N½ Sec. 21, 4S-7W, Calhoun Co. (Union City Quad., MI).	Commercial operation in a Pleistocene lake. Sample from stockpile.
7146A	10-15	Lake marl	Darrell Hamilton, Nashville, MI. Pit on south side of Thornapple Lake, 4 mi W of Nashville, NE¼ NW¼ NE¼ Sec. 30, 3N-7W, Barry Co. (Nashville Quad., MI).	Commercial operation on the southeast edge of a Pleistocene lake. Sample from stockpile.
7147A	20+	Bog marl	S. K. Vorres, Fremont, MI. Pit is 5 mi N of Fremont, on the east side of Luce Rd., Cen. Sec. 6, 13N-13W, Newaygo Co. (White Cloud Quad., MI).	Location of pit from which marl (Pleistocene) was dug for full-scale tests by TVA. Sample from depleted stockpile.
7148	4+	Tufaceous marl (spring deposit)	Grant Tufa Lime Co., Grant, MI. Pit is 7 mi E of Grant, NW¼ NE¼ Sec. 29, 11N-11W, Newaygo Co. (Sand Lake Quad., MI).	Abandoned operations in a Pleistocene spring deposit.
7149A	1-4	Tufaceous bog marl	Gerald Arnsman, R.R. 1, Hopkins, MI. Belden Pit, 0.5 mi E of South Monterey, MI, SE¼ SE¼ NW¼ Sec. 34, 3N-13W, Allegan Co. (Allegan Quad., MI).	Commercial operation in a Pleistocene bog. Sample A from upper tufaceous beds in center of pit.
7149B	12+	Bog marl		Sample B from lower beds.

7150	20	Lake marl	Leon Hayward Dry Marl, R.R. 2, Vicksburg, MI. Marl is dredged from beneath the south side of Indian Lake, 3 mi NE of Vicksburg in Sec. 8, 4S-10W, Kalamazoo Co. (Leonidas Quad., MI).	Commercial operations in Pleistocene lake. Sample from stockpile.
7151A 7151B 7151C	20+	Bog marl	Poehlman & Sons, R.R. 2, Cassopolis, MI. Operations are 6 mi SW of Cassopolis, SE¼ NE¼ Sec. 13, 7S-16W, Cass Co. (Cassopolis Quad., MI).	Commercial operations in Pleistocene marl. Samples of three typical marl types from the pit.
7152	5+	Bog marl	Lime Products Co. Former dredging 3.5 mi N of Eagle, WI, in SW¼ SE¼ Sec. 34, 6N-17E, Waukesha Co. (Eagle Quad., WI).	Abandoned operation in a Pleistocene bog. Samples represent upper 4 ft of marl at three different places along former workings. Area is within Kettle Moraine State Forest.
7153	—	Sludge from paper mfg. plant	Nekoosa Edwards Paper Co., Port Edwards, WI. Sludge pond east side of river at Nekoosa, WI, SE¼ Sec. 10, 21N-5E, Wood Co. (Wisconsin Rapids Quad., WI).	Waste product from Kraft paper process, sold to area farmers as ag lime, consists of more than 95% $CaCO_3$.
7154	5-10	Bog marl	Floyd Helgeson, R.R. 1, Iola, WI. Pit 3 mi NW of Iola, SW¼ NE¼ Sec. 21, 24N-11E, Waupaca Co. (Tigerton Quad., WI).	Dredging operations have been discontinued in a Pleistocene bog. Sample from stockpile.
7155	3.5+	Lake marl	Clifford Caldwell Marl Co., Scandinavia, WI. Pit is on south side of Marl Lake, 3 mi SW of Scandinavia, W½ NW¼ Sec. 33, 23N-11E, Waupaca Co. (Waupaca Quad., WI).	Dredging operations have been discontinued in the Pleistocene lake. Sample from the upper 3.5 ft at water's edge.
7156	3.5+	Bog marl	A. E. Stelter, Bloomer, WI. Neitzel pit along O'Neal Creek, 5.5 mi E of Bloomer on Rt. 64, SW¼ SW¼ Sec. 33, 3N-8W, Chippewa Co. (Bloomer Quad., WI).	Abandoned pit in a Pleistocene bog. Sample from upper 3 to 5 ft adjacent to pond.

APPENDIX 2, continued

Location and sample number	Thickness represented (ft)	Type	Source and location (quadrangle map in parentheses)	Remarks on the deposit and geologic unit sampled
				Operations in a Pleistocene lake deposit.
7157A	15-18	Lake marl	Burnett County Highway Dept., Siren, WI. Pit located on northeast shore of Wood Lake, 8 mi W and 2 mi S of Siren, NW¼ SE¼ Sec. 27, 38N-18W, Burnett Co. (Milltown Quad., WI).	Sample A from stockpile.
7157B	2.5			Uppermost beds of marl.
7157C	3.5			2.5 to 6 ft below top of marl.
7157D	2.0			6 to 8 ft below top of marl.
7158	?	Lake marl	Sorum's Marl Service, Remer, MN. On the south shore of Birch Lake, 2 mi SE of Remer, near Cen. N½ Sec. 8, 141N-25W, Cass Co., MN (Hibbing 1:250,000 Quad., MN).	Commercial operations in a Pleistocene lake deposit. Sample from stockpile.
7159	13	Bog marl	Richard Nanik Marl, Staples, MN. Pit located along Tower Creek, 10.5 mi N of Staples, NE¼ NW¼ Sec. 13, 136N-33W, Wadena Co. (Brainerd 1:250,000 Quad., MN).	Commercial operations in a Pleistocene bog. Sample from upper beds below muck.
7160	2.5	Bog marl	Lily pond on Urbana campus, Univ. of Illinois, near Cen. Sec. 18, 19N-9E, Champaign Co. (Urbana Quad., IL).	Excavation exposure. Sampled in 1947 as NF446 (Pleistocene).
7161	1.0+	Bog marl	Along Blackberry Creek, 5 mi due west of Fox River at Aurora, IL, NE¼ NE¼ SW¼ Sec. 14, 38N-7E, Kane Co. (Geneva Quad., IL).	Outcrop of marl. Sampled in 1933 as NF153 (Pleistocene).

7162A 7162B 7162C 7162D	12+	Bog marl	Delmer Ford, Chatsworth, IL. Located 5 mi S and 2 mi W of Chatsworth along creek north side of road SE¼ SW¼ Sec. 32, 26N-8E, Livingston Co. (Sibley Quad., IL).	Discontinued operations in a Pleistocene bog. Samples from four types of marl from stockpiles. The marl occurs under various thicknesses of Grayslake Peat.
7163A	4.2+	Bog marl	Batavia Soil Builders. Located 2.5 mi W of Batavia, IL, SW¼ SW¼ Sec. 19, 39N-8E, Kane Co. (Geneva Quad., IL).	Marl occurs under 3 ft of Grayslake Peat. Currently the peat is being produced. Boring taken on the west side of bog. Sample A from lower marl beds (Pleistocene).
7163B	0.2			Sample from middle marl bed.
7163C	5.8			Sample from upper marl beds.
7163D	24			Sample from stockpile near center of north end of bog.
7201	60	Chalk	Lone Star Industries Inc. quarry, west side of Tombigbee River, 2.2 mi NE of St. Stephens, Washington Co., AL.	Marianna Limestone, Vicksburg Group (Oligocene). Large quarry.
7202	50±	Chalk	Lone Star Industries Inc. quarry, Demopolis, Marengo Co., AL.	Demopolis Chalk Formation, Selma Group (Upper Cretaceous). Large quarry.
7203	15	Coquina	Lone Star Industries Inc. pit, east side of Rt. 10, 1¼ mi N of Chuckatuck, VA.	Yorktown Formation, coquina facies (Miocene). Sample 7203 is composite of three samples taken from the upper 15 ft, exposed in pit. 7203D from stockpile after plant processing.
7203D	30-50			
7204	3-5	Chalk	Outcrop on Rt. 12, ½ mi W of Jct. with Rt. 61, 5.8 mi S of Newbern, Hale Co., AL.	Arcola Limestone Mbr. of Mooreville Chalk, Selma Gr., (Upper Cretaceous). Sample from soft chalky beds.
7205	20-25	Chalk	Outcrop north side of Rt. 80 at Faunsdale, Marengo Co., AL.	Demopolis Chalk (upper part), Selma Gr. (Upper Cretaceous).

APPENDIX 2, continued

Location and sample number	Thickness represented (ft)	Type	Source and location (quadrangle map in parentheses)	Remarks on the deposit and geologic unit sampled
7206	15	Chalk, clayey	Outcrop along Rt. 263, 0.4 mi S of Jct. with Rt. 21, near Braggs, Lowndes Co., AL.	Prairie Bluff Chalk (lower part), Selma Group (Upper Cretaceous).
7207	8	Chalk, clayey	Outcrop along Rt. 263, 2.8 mi S of Jct. Lowndes Co. Rt. 7 and Alabama Rt. 21, Southwest Braggs, Lowndes Co., AL.	Prairie Bluff Chalk, Selma Group (Upper Cretaceous). Sample taken from beds just above the phosphatic and cobbly chalk beds at base of the Prairie Bluff.
7208B	3	Chalk & calcareous shale	Ideal Cement Co., Superior, NB, quarry located 6 mi SW of Superior in Kansas, Sec. 6, 15-7W, Jewell Co., KS.	Smoky Hill Chalk Mbr. (lower 3 ft) of Niobrara Chalk (Upper Cretaceous). Chalk and chalky shale (beds 0.5" to 8" thick) interbedded. Overlies 7208C.
7208C	20	Chalk		Ft. Hays Limestone Mbr. of Niobrara Chalk. Beds 0.8 to 3 ft thick separated by 0.5" shale partings. Quarried by ripping.
7209	16-17	Chalk	Nelson Quarry of Hopper Bros., Weeping Water, NB. Located 1 mi S of Nelson, NB, on E side Rt. 14, SE¼, SE¼ Sec. 36, 3N-7W, Nuckolls Co., NB.	Ft. Hays Limestone Mbr. of Niobrara Chalk (Upper Cretaceous). Beds generally 1" to 3" thick, separated by thin shale partings.
7210A	12	Limestone, chalky and clayey	Hebron Quarry of Hooper Bros., Weeping Water, NB. Located 2.6 mi W of Gilead on Rt. 136, then 0.6 mi N, Thayer Co., NB.	Greenhorn Limestone (Upper Cretaceous). Upper, buff beds generally 2" to 4" thick; overlies 7210B.
7210B	16-17	Limestone, chalky and clayey		Lower, gray strata, in 2" to 4" beds, partly nodular and fossiliferous.

7211	3*	Limestone, chalky and clayey	Haddam Quarry of Hooper Bros., Weeping Water, NB. Located ¼ mi N of Rt. 36, 0.7 mi E of Jct. of Rts. 22 and 36, Washington Co., KS.	Greenhorn Limestone (Upper Cretaceous). Very small quarry, intermittent operations.
7212A	38	Chalk	Discontinued quarry along RR tracks, 1½ mi W of Cedar, KS, SE¼ SE¼ Sec. 35, 4S-15W, Smith Co., KS.	Ft. Hays Limestone Mbr. of Niobrara Chalk (Upper Cretaceous). In beds 0.5 to 3 ft thick.
7212B	0.5	Shale, chalky		Sample representative of the 5 shale beds (each < 2" thick) interbedded with chalk (7212A).
7213	10*	Chalk	Outcrop west side of gravel road at Utility Sta. 3½ mi N and 2 mi W of Hays, KS, cen. of E line Sec. 7, 13S-18W, Ellis Co., KS.	Ft. Hays Limestone Mbr. of Niobrara Chalk (Upper Cretaceous). In beds 1-2 ft thick interbedded with two 3" beds of chalky shale that were excluded from sample.
7214A	17	Chalk	Outcrop bluff on south side, west end of Cedar Bluff Res., Sec. 6, 15S-22W, Trego Co., KS.	Ft. Hays Limestone Mbr. of Niobrara Chalk (Upper Cretaceous). Uppermost beds (0.8 to 3 ft).
7214B	19.3	Chalk		Middle beds; sample excludes four beds (4" to 6" each) of chalky shale within this unit.
7214C	18.2	Chalk		Lower beds (the base of the Ft. Hays). Sample excludes three beds (3" to 6" thick) of calcareous shale within this unit.
7215	33	Caliche, sandy	Outcrop west side of Rt. 147, 3 mi S of dam of Cedar Bluff Res., SE¼ Sec. 14, 15S-22W, Trego Co., KS.	Ogallala Formation (Pliocene).
7216C	6-10	Siltstone, calcareous	Outcrop south side of North Fork Smoky Hill River on Garvey Ranch, 15 mi N and 5 mi E of Wallace, KS, NE½ NE¼ Sec. 11, 11S-38W, Wallace Co., KS.	Ogallala Formation (Pliocene). Small exposure.

* The beds below are inaccessible but belong to the same geologic unit and are thought to have properties similar to those of the sampled beds.

APPENDIX 2, continued

Location and sample number	Thickness represented (ft)	Type	Source and location (quadrangle map in parentheses)	Remarks on the deposit and geologic unit sampled
7217	8-12	Marl, diatomaceous	Delore Div., NL Industries quarry, south side of North Fork Smoky Hill River, 15 mi N and 4 mi E of Wallace, KS, SE¼, NW¼ Sec. 11, 11S-38W, Wallace Co., KS.	Ogallala Formation (Pliocene). Source of raw material for Delore Div. plant located in Edson, KS.
7218	35	Caliche	Texas Highway Dept. quarry, Herndon Quarry, 16 mi S of Perryton, TX, on Rt. 83, Ochiltree Co., TX.	Ogallala Formation (Pliocene). Hard and soft beds (1 to 3 ft) are crushed for use in road construction.
7219	25-30	Limestone, chalky	Outcrop in bluff along Walnut Creek ¼ mi SE of Jct. with Dessau-Austin Rd., 7.5 mi NE of Austin, Travis Co., TX.	Dessau Mbr. of Austin Chalk (Upper Cretaceous). Weathered outcrop beds of chalk, 2 to 3 ft thick, separated by 0.5 to 1 ft beds of shaley chalk.
7220	9	Limestone, chalky	Outcrop in bluff of Walnut Creek, ½ mi W of Jct. with Interstate 35, 8 mi NE of center of Austin, Travis Co., TX.	"Jonah Chalk" Mbr. of Austin Chalk (Upper Cretaceous). Moderately dense and nodular limestone beds 2 to 3 ft thick separated by chalk beds 0.6 to 1.5 ft thick. Underlies Dessau Chalk at this exposure.
7221A	15-25	Chalk (buff)	Universal Atlas Cement Co. quarry, 1.5 mi SW of Woodway, Ellis Co., TX.	Atco Chalk Mbr. of Austin Chalk (Upper Cretaceous). Buff chalk beds 1 to 3 ft thick separated by 0.5" shale partings and occasional 3" to 6" calcareous shale beds.
7221B	15-35	Chalk (gray)		Gray chalk, underlies the buff chalk (7221A). Thickness of chalk quarried is 40 to 50 ft.
7222A	40	Chalk (buff)	Gifford-Hill Portland Cement Co. quarry, located 2.5 mi N of Midlothian, TX, on old Rt. 67 and 0.5 mi W, Ellis Co., TX.	Atco Chalk Mbr. of Austin Chalk (Upper Cretaceous). Buff chalk occurs in upper beds and along vertical joints. Lower beds are gray chalk. Lowermost bed contains black phosphatic nodules, 1 - 3 mm diameter.
7222B		Chalk (gray)		

7223	5*	Limestone, chalky	Outcrop on property of Texas Lime Co., Cleburne, TX, located at base of bluff on south side of road 1 mi S of State Park and 13 mi SW of Cleburne, Johnson Co., TX.	Comanche Peak Limestone (Lower Cretaceous). Chalky limestone with 2" to 3" nodules of dense limestone abundant throughout this exposure. The base of the limestone unit is covered.
7224	4*	Chalk	Prospect pit, east side of farm road, 2 mi N and ½ mi W of Roxton, Lamar Co., TX.	Gober Chalk Mbr. of Austin Chalk (Upper Cretaceous). Sample from stockpile.
7225	2.5*	Chalk	Abandoned quarry at Jct. of Rts. 114 and 82 on east side of Clarksville, Red River Co., TX.	Pecan Gap Chalk (Upper Cretaceous). Quarry pit is filled with water. Uppermost beds sampled.
7226A	30-35	Chalk	Arkansas Cement Corp. quarry, 3 mi SW of Forman, Little River Co., AR.	Annona Chalk (Upper Cretaceous). Quarried by ripping.
7227B	40-45	Chalk	Ideal Cement Co. quarry, ½ mi NW of Okay, Howard Co., AR.	Annona Chalk (Upper Cretaceous).
7228	20	Chalk	Outcrop east side of Rt. 4, 3 mi N of Washington, Hempstead Co., AR.	Saratoga Chalk (Upper Cretaceous). Weathered buff chalk. Gray thin-bedded chalk 10 to 16 ft thick overlies the buff chalk beds sampled. Phosphatic and clayey chalk beds (1-2 ft thick) and claystone beds of the Marlbrook Marl underlie the beds sampled.

*The beds below are inaccessible but belong to the same geologic unit and are thought to have properties similar to those of the sampled beds.

APPENDIX 2, continued

Location and sample number	Thickness represented (ft)	Type	Source and location (quadrangle map in parentheses)	Remarks on the deposit and geologic unit sample
7229A	2	Limestone, chalky	Outcrop east side of Rt. 61 at Jct. with Bypass 61 on north edge of Vicksburg, Warren Co., MS	Byram Formation, Vicksburg Gr. (Oligocene). Sample A is from the uppermost bedrock strata; F is near the base of exposure. Glendon Limestone Mbr. of Byram Fm., Vicksburg Gr. Sample B underlies A, C underlies B, etc. Vicksburg Gr. limestones and marls are used for cement raw materials at nearby Redwood, MS (Miss. Valley Portland Cement Co.).
7229B	1	Siltstone		
7229C	4	Limestone, chalky		
7229D	1	Limestone, chalky		
7229E	1	Limestone, chalky		
7229F	1.3	Limestone, chalky		
7230	15-18	Chalk	Mississippi Dept. Agriculture and Commerce quarry located east side of Rt. 47, 8 mi S of Trebloc in Clay Co., MS.	Demopolis Chalk (upper part), Selma Group (Upper Cretaceous). Quarried by ripping.